

Reactions of Platinum(II) Complexes with Dioxygen: Progress Toward Alkane Functionalization

Thesis by

Vsevolod V. Rostovtsev

In Partial Fulfillment of the Requirements

For the Degree of

Doctor of Philosophy

California Institute of Technology

Pasadena, California

2001

(Defended May 29, 2001)

© 2001

Vsevolod V. Rostovtsev

All Rights Reserved

For Olga and Daniel

Acknowledgements

This part of my thesis is the hardest one to write. I am grateful to many people who have helped and supported me during the last five years. Let me start by saying thank you to all of you. The following is not going to be proof-read by anyone so I apologize for any mistakes you might find.

I want to thank Olga for her patience and support during my graduate studies (both here and in Nebraska). This thesis would not have been possible without her help and sacrifice. Spending time with Danya not only took my mind off work but also gave me a chance to read (or sleep) during his naps.

I would like to thank my chemistry teachers: my high school chemistry teachers Olga Nikolaevna Tulyakova and Alexei Dmitrievich Sobolev, who got me interested in *himiya*, and my master's degree advisor, Bob Hembre, who first taught me organometallic chemistry and showed me how to work on a Schlenk line (one of the Hembre group lines moved to 205 Noyes).

To put it simply, John Bercaw is the best advisor in the whole world. I am very grateful for an opportunity to work in his group. His knowledge and experience will always be an inspiration to me. From him, I learned many things *"...of shoes—and ships—and sealing-wax/Of cabbages—and kings/And why the sea is boiling hot/And whether pigs have wings."* Thank you, John.

I would also like to thank Jay Labinger for his help and guidance during my graduate studies. I am grateful to Harry Gray for his advice and expertise as well as for a copy of Langford and Gray.

I thank Shannon Stahl and Matt Holtcamp for helping me to get started on the platinum project. With Matt, I shared an unforgettable win in a basketball game. Dario Veghini showed me how to use swivel frits and left Olga and me

his spacious apartment. The inhabitants of 209 South made me the honorary resident of that lab for which I am very grateful. Alex "Puzo" Muci is one the best chemists I have ever met and I thank him for his advice and support. His enthusiasm for organic chemistry turned out to be contagious. He has been a great friend to me, Olga and Daniel. Papa-to-be Chris "Theory" Brandow was on my right hand side in the computer room all throughout the writing of this thesis and I wish him and Maggie the best of luck in West Virginia. Lily Ackerman will forever be remembered for her Cluckender page-turning ritual. Antek Wong-Foy single-handedly changed the way chemistry is discussed in the Bercaw Group and was an excellent colleague on the platinum project. In my eyes, Jeff Yoder has surpassed Bob Bergman in the art of double-labeling experiments. I wish him the best of luck this year. Ola Wendt was invaluable source of information about platinum, kinetics, platinum kinetics and lots of other things. Joseph Sadighi is the best labmate one could hope for and I thank him for his help and advice as well as for remembering (with the help of JosephBrainScotchTape®) one of the best quotes about Russians. I belatedly apologize to Mike Abrams for nagging him about his props. The Bercaw Group have changed a great deal during my stay here and I am very thankful to the people who made this last year one of the best: Susan "Aloha" Schofer, Sara "Man's Pants" Klamo, Endy "Mushroom" Min, Jonathan "Barney" Owen, Cliff Baar (thanks for reading my thesis) and Christoph "Toph" Balzarek (tea this Sunday?). Thank you, come visit us in San Diego.

I would also like to thank Todd Younkin for many discussions about the peculiarities of olefin complexes of platinum(II), Tom Dunn for helping me keep my sanity during my days as the GLA for AM, and later AMX, 500, Larry

Henling for his help with X-ray structure determinations and many HeavenEggs, Bill Schaefer and Dick Marsch for their help with the notorious vvr7, and Pat Anderson and Dian Buchness for keeping this place rolling. Angelo DiBilio has helped me a great deal with EPR data collection and analysis. John Eiler carried out MS analysis of dioxygen samples.

Abstract

Whereas stoichiometric activation of C–H bonds by complexes of transition metals is becoming increasingly common, selective functionalization of alkanes remains a formidable challenge in organometallic chemistry. The recent advances in catalytic alkane functionalization by transition-metal complexes are summarized in Chapter I.

The studies of the displacement of pentafluoropyridine in $[(\text{tmeda})\text{Pt}(\text{CH}_3)(\text{NC}_5\text{F}_5)][\text{BAr}_4^f]$ (**1**) with γ -tetrafluoropicoline, a very poor nucleophile, are reported in Chapter II. The ligand substitution occurs by a dissociative interchange mechanism. This result implies that dissociative loss of pentafluoropyridine is the rate-limiting step in the C–H activation reactions of **1**.

Oxidation of dimethylplatinum(II) complexes $(\text{N–N})\text{Pt}(\text{CH}_3)_2$ ($\text{N–N} = \text{tmeda}$ (**1**), α -diimines) by dioxygen is described in Chapter III. Mechanistic studies suggest a two-step mechanism. First, a hydroperoxoplatinum(IV) complex is formed in a reaction between $(\text{N–N})\text{Pt}(\text{CH}_3)_2$ and dioxygen. Next, the hydroperoxy complex reacts with a second equivalent of $(\text{N–N})\text{Pt}(\text{CH}_3)_2$ to afford the final product, $(\text{N–N})\text{Pt}(\text{OH})(\text{OCH}_3)(\text{CH}_3)_2$. The hydroperoxy intermediate, $(\text{tmeda})\text{Pt}(\text{OOH})(\text{OCH}_3)(\text{CH}_3)_2$ (**2**), was isolated and characterized. The reactivity of **2** with several dimethylplatinum(II) complexes is reported.

The studies described in Chapter IV are directed toward the development of a platinum(II)-catalyzed oxidative alkane dehydrogenation. Stoichiometric conversion of alkanes (cyclohexane, ethane) to olefins (cyclohexene, ethylene) is achieved by C–H activation with $[(\text{N–N})\text{Pt}(\text{CH}_3)(\text{CF}_3\text{CH}_2\text{OH})]\text{BF}_4$ (**1**, N–N is N,N' -bis(3,5-di-*t*-butylphenyl)-1,4-diazabutadiene) which results in the formation of olefin hydride complexes. The first step in the C–H activation reaction is formation of a platinum(II) alkyl which undergoes β -hydrogen elimination to afford the olefin hydride complex. The cationic ethylplatinum(II) intermediate can be generated *in situ* by treating diethylplatinum(II) compounds with acids. Treatment of $(\text{phen})\text{PtEt}_2$ with $[\text{H}(\text{OEt}_2)_2]\text{BAr}_4^f$ at low temperatures resulted in the formation of a mixture of $[(\text{phen})\text{PtEt}(\text{OEt}_2)]\text{BAr}_4^f$ (**8**) and $[(\text{phen})\text{Pt}(\text{C}_2\text{H}_4)\text{H}]\text{BAr}_4^f$ (**7**). The cationic olefin complexes are unreactive toward dioxygen or hydrogen peroxide. Since the success of the overall catalytic cycle depends on our ability to oxidize the olefin hydride complexes, a series of neutral olefin complexes of platinum(II) with monoanionic ligands (derivatives of pyrrole-2-carboxyaldehyde *N*-aryl imines) was prepared. Unfortunately, these are also stable to oxidation.

TABLE OF CONTENTS

Chapter I. Catalytic Alkane Functionalization	1
Mechanistic Considerations.....	2
Alkane Functionalization.....	5
Conclusions.....	13
References	15
 Chapter II. Ligand Substitution in Cationic Platinum(II) Complexes. Implications for the Mechanism of C–H Activation with Electrophilic Complexes of Platinum(II)	19
Abstract	19
Introduction	20
Results	21
Discussion	26
Conclusions.....	32
Experimental.....	33
References	36
 Chapter III. Oxidation of Dimethylplatinum(II) Complexes with Dioxygen	38
Abstract	38
Introduction	39
Results	41
Discussion	57
Conclusions.....	67
Experimental.....	69
References	79
 Chapter IV. Approaches to Catalytic Oxidative Dehydrogenation of Alkanes. Synthesis and Reactivity of Olefin Complexes of Platinum(II)	83
Abstract	83
Introduction	84

Results	85
Discussion	93
Conclusions	100
Experimental	102
References	109
Compound Nomenclature for Appendices	113
Appendix A. Structure Determination of 1	114
Crystal Data Details for 1	117
Data Collection	117
Structure Solution and Refinement	118
Programs Used	118
References	119
Refinement Details	119
Appendix B. Structure Determination of 2	123
Crystal Data Details for 2	126
Data Collection	126
Structure Solution and Refinement	127
Programs Used	127
References	128
Special Refinement Details	128
Appendix C. Structure Determination of 3	136
Data Collection	137
Structure Solution and Refinement	137
Special Refinement Details	138

LIST OF TABLES

Chapter II

Table 1. Selected ^{19}F NMR Data for Compounds **1**, **3-5**.....22

Table 2. Kinetic data for the reaction of **1** with **2** in CD_3NO_2 at 70 °C.....23

Chapter III

Table 1. Selected bond lengths (in Å) and angles (in °) for **4**.....51

Table 2. Selected bond lengths (in Å) and angles (in °) for **2**.....53

Table 3. Relative rates of oxidation for (α -diimine) $\text{Pt}(\text{CH}_3)_2$56

Chapter IV

Table 1. Selected Data from DFT Calculations91

Table 2. Selected Calculated Bond Lengths and Angles91

Table 3. Selected bond lengths (in Å) and angles (in °) for **11a**92

Table 4. Selected Bond Lengths of Platinum(II) Olefin Complexes98

Appendix A

Table 1. Atomic coordinates and equivalent isotropic displacement parameters for **1**121

Table 2. Bond lengths [Å] and angles [°] for **1**122

Appendix B

Table 1. Atomic coordinates and equivalent isotropic displacement parameters for **2**132

Table 2. Bond lengths [Å] and angles [°] for **2**133

Appendix C

Table 1. Atomic coordinates and equivalent isotropic displacement parameters for **3**.139

Table 2. Bond lengths [Å] and angles [°] for **3**140

LIST OF FIGURES

Chapter II

Figure 1. Disappearance of **1** in the reaction with pentafluorotoluene.....25

Figure 2. Eyring plot for the reaction of **1** with pentafluorotoluene.25

Chapter III

Figure 1. EPR spectrum of the frozen blue-colored solution.43

Figure 2. Room temperature EPR spectra of $[(\text{tmeda})\text{Pt}^{\text{III}}(\text{"N"}) (\text{CH}_3)_2]^+ \dots$ 43

Figure 3. Ratios of **2** to **4** at various concentrations of $(\text{tmeda})\text{Pt}(\text{CH}_3)_2$ and O_245

Figure 4. Oxidation of $(\text{teeda})\text{Pt}(\text{CH}_3)_2$ with $(\text{tmeda})\text{Pt}(\text{OOH})(\text{OCH}_3)(\text{CH}_3)_2$49

Figure 5. Labeled Diamond view of **4**, with 50% ellipsoids.....50

Figure 6. Labeled Diamond view of **2**, with 50% ellipsoids.....53

Figure 7. First-order dependence of the observed rate of oxidation of $(\text{phen})\text{Pt}(\text{CH}_3)_2$ and $(\text{CyDAB}^{\text{H}})\text{Pt}(\text{CH}_3)_2$ on $[\text{O}_2]$55

Figure 8. Kinetic trace of the oxidation of $(\text{phen})\text{Pt}(\text{CH}_3)_2$ with O_255

Figure 9. MO diagram of a square-planar platinum(II) complex.....67

Chapter IV

Figure 1. Structure of **11a**.92

Appendix A

Figure 1. Labeled Diamond view of **1**, with 50% ellipsoids..... 115

Appendix B

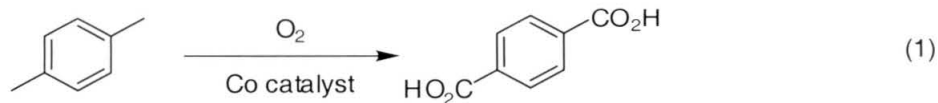
Figure 1. Unlabeled Diamond view of the molecule. 124

Figure 2. Unlabeled Diamond view of an A, B pair of molecules 125

Chapter I

CATALYTIC ALKANE FUNCTIONALIZATION

The oxidation of hydrocarbons by molecular oxygen is one of the largest commercial applications of transition-metal complexes in homogeneous catalysis (see, for example, eq. 1).¹ The oxidation follows a radical mechanism, in which the main role of the transition metal catalyst is decomposition of alkyl hydroperoxides formed by radical processes.

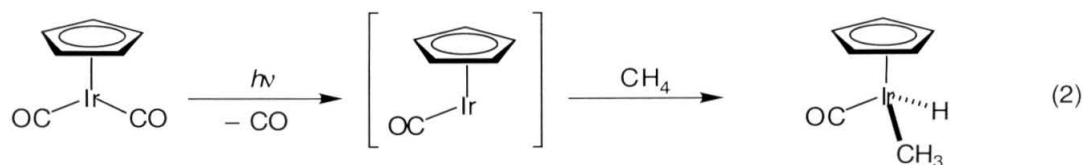


Since the rates of radical reactions are determined primarily by the bond strengths,² it is difficult to control their chemo- and regioselectivity. Due to these limitations, saturated hydrocarbons have mostly been used as fuels. Recently, considerable effort has been devoted to the studies of alternative approaches to C–H bond activation. Selective C–H bond functionalization will not only allow the use of natural gas as a primary chemical feedstock, but also enrich our arsenal of organic transformations.

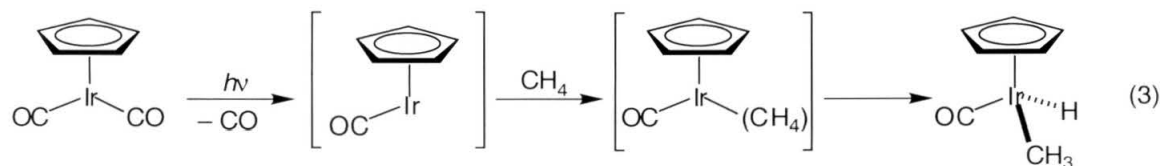
Mechanistic Considerations

During the past thirty years, a number of low-temperature alkane activation reactions using transition metal complexes have been discovered.³ From the mechanistic point of view, all cases can be arranged into five groups.^{4,5}

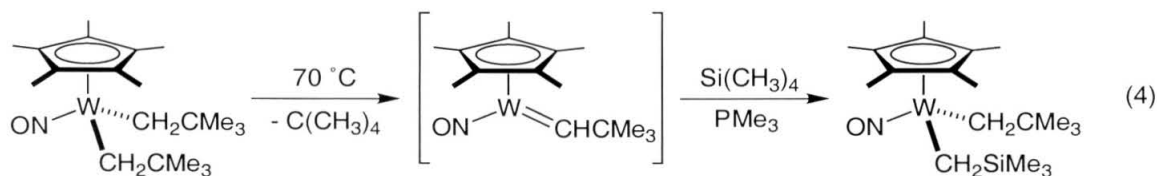
- *Oxidative addition* is most typical for low-valent and electron-rich complexes of late transition metals (eq. 2). The selectivity pattern is opposite to that observed in radical chemistry: primary C–H bonds are more reactive than secondary. Tertiary C–H bonds are essentially inert.⁵



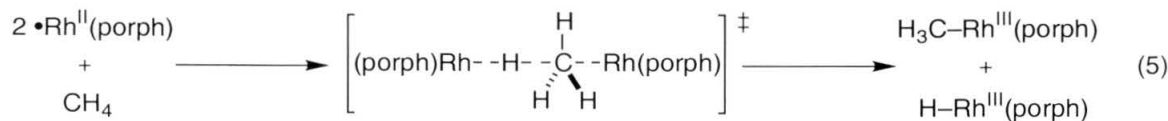
In many cases, formation of alkane σ -complexes prior to the oxidative addition step was inferred from spectroscopic studies or isotopic labeling experiments (eq. 3).⁶



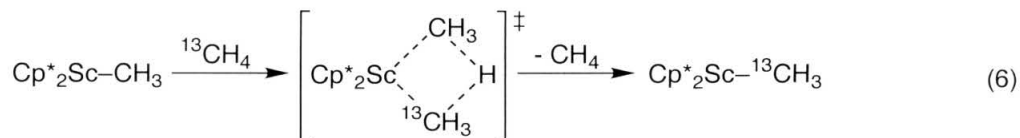
• *1,2-Addition* of alkanes to metal-imide⁷ and metal-alkylidene⁸ bonds has been identified as a way to break C–H bonds (eq. 4).



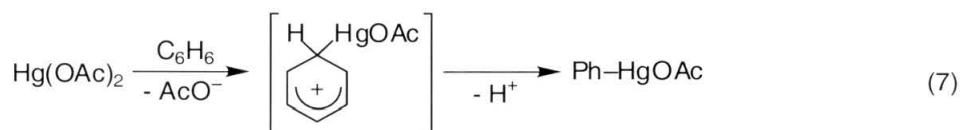
• *Metalloradical* C–H bond activation has only been observed for rhodium(II) porphyrin complexes (eq. 5).^{9,10}



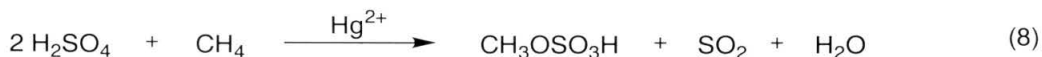
• *σ -Bond metathesis* is usually observed in reactions of early transition metal complexes in their highest oxidation state (eq. 6).¹¹ Selectivity patterns resemble those for oxidative addition.



• *Electrophilic* C–H bond activation in arenes occurs by an electrophilic aromatic substitution mechanism through a Wheland-type intermediate (eq. 7).¹² These reactions were reported for complexes of palladium(II),¹³ mercury(II)¹⁴ and thallium(III).¹⁵



Another set of electrophilic C–H bond activation reactions consists of palladium(II)¹⁶-, mercury(II)¹⁷- and cobalt(III)¹⁸-catalyzed alkane oxidations (eq. 8). These reactions are typically carried out in polar protic media such as water, acetic, trifluoroacetic and sulfuric acids.



The details of the C–H activation event are not yet clear. In analogy to aromatic electrophilic activation, deprotonation of the alkane σ -complex might be the C–H bond-breaking step.¹⁹ This chemistry needs to be studied in more detail before the exact nature of the C–H activation step is established. At present, it is not even clear whether these reactions operate by a mechanism truly different from the ones described above.

Alkane Functionalization

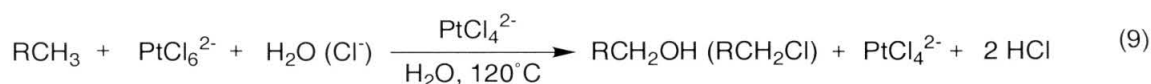
Whereas stoichiometric activation of C–H bonds by complexes of transition metals is becoming increasingly common, selective *functionalization* of alkanes remains a formidable challenge in organometallic chemistry.³ Organometallic complexes formed by C–H activation rarely act as catalytically competent intermediates in alkane functionalization. Instead, formation of kinetically inert or thermodynamically stable compounds (or both) is frequently observed. Carbon-hydrogen bonds are some of the strongest single bonds, and only a limited number of thermodynamically favorable approaches are available.²⁰ These include hydroxylation of C–H bonds, oxidative dehydrogenation, oxidative coupling and insertion of alkenes and alkynes into C–H bonds. A great deal of effort has been invested into the discovery and study of a few transition metal-catalyzed systems capable of C–H activation.

Heterogeneous alkane functionalization will not be considered here since it typically occurs by radical mechanisms, which inherently limit their selectivity.²¹ However, these selectivity constraints can sometimes be relaxed as demonstrated recently by Thomas and co-workers.²²

Alkane Hydroxylation. The best catalysts for the conversion of alkanes to alcohols using dioxygen are found in biological systems. Such enzymes as cytochrome P450²³ and methane monooxygenase²⁴ can convert a number of hydrocarbons to the corresponding alcohols with high turnover numbers at ambient conditions. The detailed mechanism of C–H bond activation in these systems is the subject of an on-going debate.²⁵ Despite intensive efforts to

develop functional models, the efficiency of these enzymes has not yet been equaled. In the majority of cases, oxidation occurred by a radical mechanism.

In 1972, Shilov and co-workers reported the first of the “electrophilic” systems for C–H bond activation. After the initial discovery of platinum(II)-catalyzed H/D exchange in alkanes,²⁶ they reported that addition of an oxidant, PtCl_6^{2-} , resulted in selective conversion of alkanes to alcohols and alkyl chlorides (eq. 9).²⁷

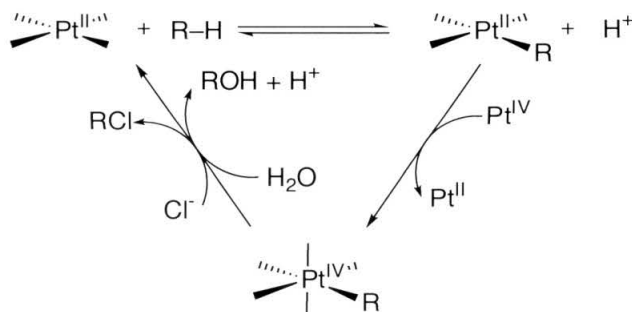


In contrast to most complexes that activate C–H bonds, the Shilov system is tolerant of water and dioxygen. Its selectivity pattern is opposite to that of radical reactions: C–H bonds follow the reactivity order, $1^\circ > 2^\circ \gg 3^\circ$, and $-\text{CH}_3 > -\text{CH}_2\text{OH}$.

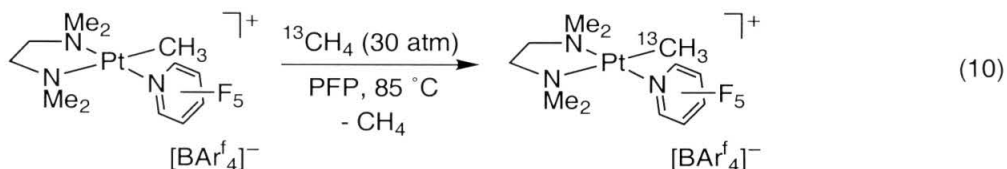
In the past decade, several groups have carried out mechanistic studies of the Shilov system.²⁸ A three-step catalytic cycle has been proposed in Scheme 1. In the first step, the alkane is activated by a platinum(II) complex, tentatively formulated as $(\text{H}_2\text{O})_2\text{PtCl}_2$, to afford a platinum(II) alkyl. Although the Shilov system was initially described as an example of “electrophilic” alkane activation, recent mechanistic studies suggested that the C–H bond-breaking step occurs through oxidative addition. The mechanism of this step was examined through the study of its microscopic reverse, the protonation of platinum(II) alkyls $(\text{tmeda})\text{Pt}(\text{CH}_3)\text{Cl}$ and $(\text{tmeda})\text{Pt}(\text{CH}_3)_2$.²⁹ These studies implied that the forward reaction starts with coordination of an alkane to platinum(II) to form a σ -complex, followed by an oxidative addition step to yield a platinum(IV)

(alkyl)hydride. The latter is then deprotonated by an external base to afford a platinum(II) alkyl species.

Scheme 1.



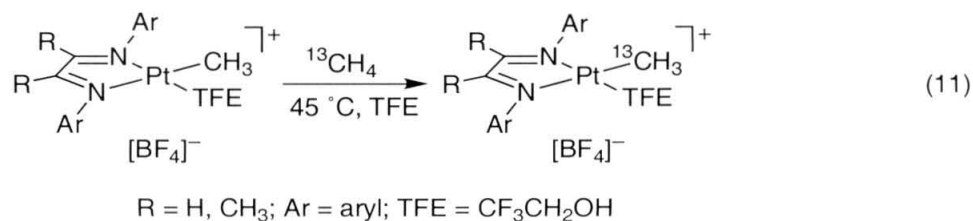
Using the clues provided by the mechanistic studies, several model platinum(II)-based systems were prepared for stoichiometric C–H bond activation. The first was reported by Labinger, Bercaw and co-workers in 1996 (eq. 10).³⁰



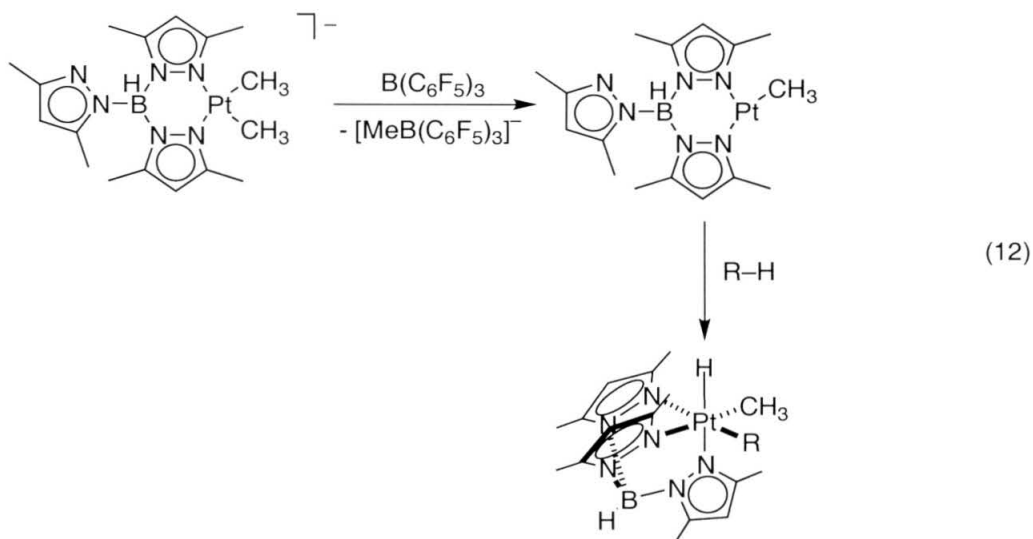
An electrophilic $[(\text{tmeda})\text{Pt}(\text{CH}_3)(\text{NC}_5\text{F}_5)][\text{BAr}^f_4]$ was prepared by treating $(\text{tmeda})\text{Pt}(\text{CH}_3)_2$ with HBar^f_4 in pentafluoropyridine. Reactions with hydrocarbons (methane, cyclohexane, benzene) were observed in pentafluoropyridine at 85°C . The mechanistic studies of C–H bond activation in this system are described in the second chapter of this thesis.

Low temperature alkane activation can be achieved with cationic α -diimine complexes of platinum(II) (eq. 11).³¹ The cationic species is generated by protonation of $(\alpha\text{-diimine})\text{Pt}(\text{CH}_3)_2$ with aqueous HBF_4 in trifluoroethanol. The

reaction with methane occurs at 45 °C, whereas benzene adds even at room temperature.



A highly electrophilic platinum(II) center can be generated by methide abstraction from $\text{K}[(\kappa^2\text{-Tp}^*)\text{Pt}(\text{CH}_3)_2]$, Tp^* = tris(3,5-dimethylpyrazolyl)borate, by BAr_3^f (eq. 12).³² The neutral intermediate adds to the C–H bonds of pentane, cyclohexane and benzene. The resulting platinum(IV) (alkyl)hydride is stabilized by coordination of the free arm of the tris(pyrazolyl)borate ligand.

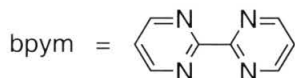
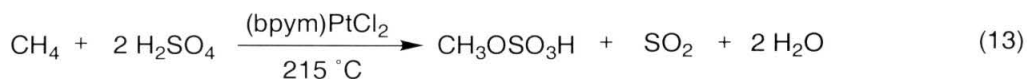


The second step of the Shilov cycle (Scheme 1) is oxidation of a platinum(II) alkyl to a platinum(IV) alkyl by PtCl_6^{2-} . Labeling studies have shown that oxidation occurs by electron transfer from Pt^{II} to Pt^{IV} .³³ Several oxidants (Cl_2 ,³⁴ $\text{K}_2\text{S}_2\text{O}_8$,³⁵ CuCl_2/O_2 and others) have been used in the Shilov oxidation instead of

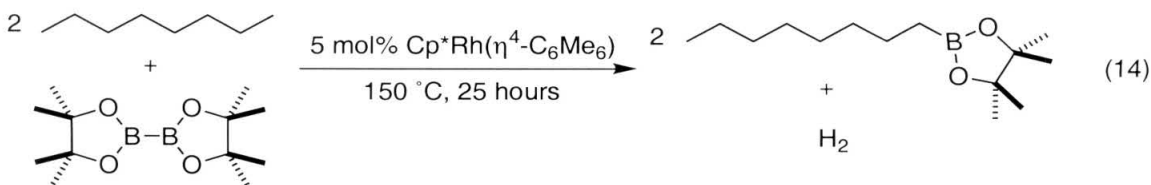
platinum(IV), but only with limited success. Of these, dioxygen is the most desirable oxidant for the Shilov system. Our studies of the reactions of dioxygen with platinum(II) complexes are described in the third chapter of this thesis.

The final step of the Shilov cycle is an S_N2-type displacement of platinum(IV) by water or chloride, which yields alcohol or alkyl chloride and regenerates the catalytically active platinum(II) species.³³

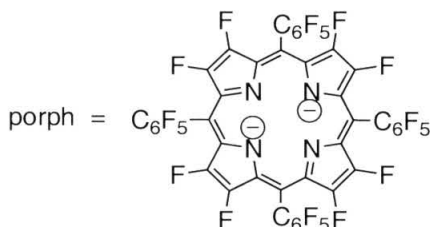
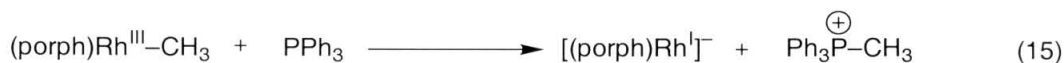
The main drawback is, of course, the stoichiometric use of platinum(IV). A practical platinum(II)-based system for alkane hydroxylation would have to use another, cheaper oxidant. A promising example was described by Periana and co-workers (eq. 13).³⁶ Using a remarkably robust platinum catalyst, methane can be converted to methyl bisulfate in 73% one-pass yield. Sulfuric acid or sulfur trioxide is the stoichiometric oxidant in this system.



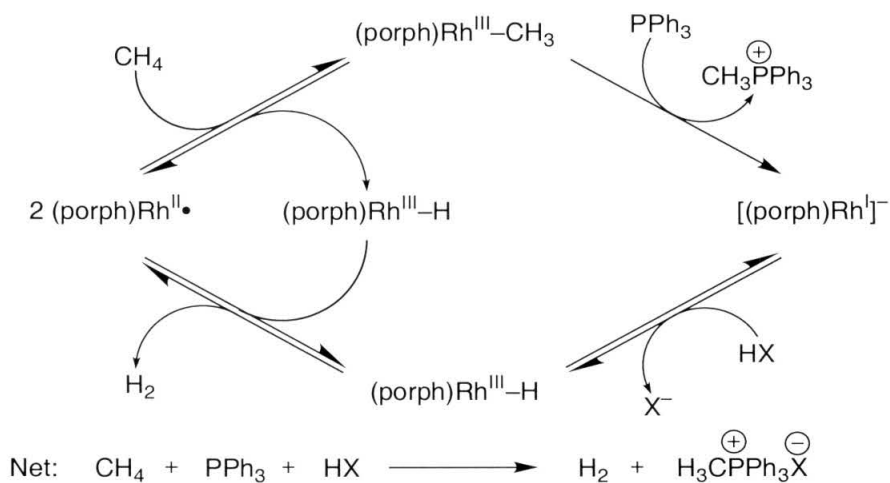
Some indirect approaches to alkane hydroxylation have been outlined. Hartwig and co-workers have recently described a rhodium(I)-catalyzed conversion of alkanes to alkylboranes (eq. 14).³⁷ Thus, *n*-octylborane is formed from *n*-octane with remarkable selectivity. Benzene, *n*-butylether and 2-methylpentane were also tested and straight chain alkyls were favored in all cases. The resulting boron-containing products can be further functionalized.³⁸



A recent work by DiMagno and co-workers suggests that metalloradical C–H bond activation might be made catalytic.¹⁰ Exhaustive fluorination of the porphyrin ligand leads to the reverse of Rh–C bond polarity making it susceptible to nucleophilic attack (eq. 15). Based on this result, the authors proposed a catalytic cycle for methane functionalization (Scheme 2). The resulting phosphonium cations can be used in a number of organic transformations.³⁹

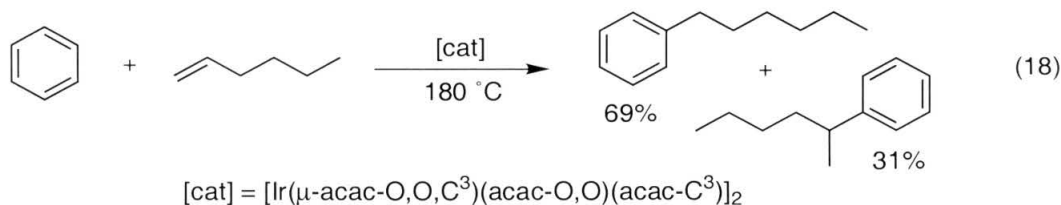
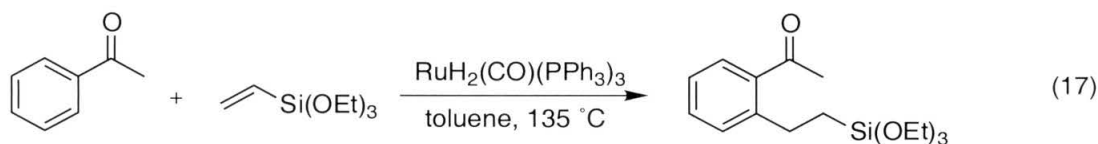
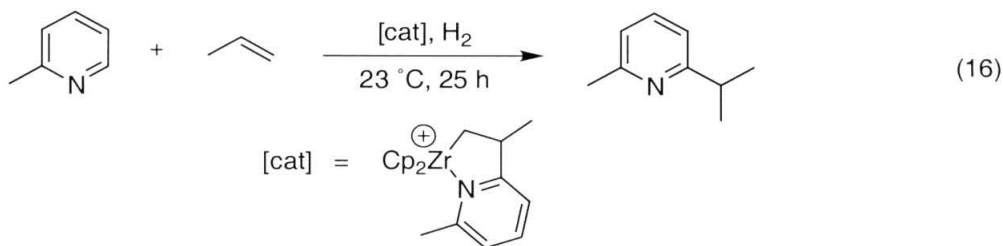


Scheme 2

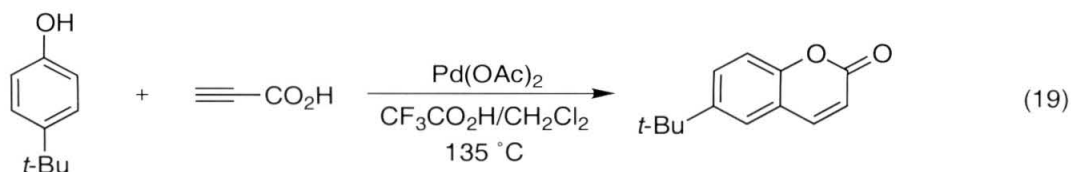


Insertion of Alkenes and Alkynes into C–H bonds. Insertion of alkenes or alkynes into C–H bonds constitutes another thermodynamically allowed approach to C–H activation. Insertion of olefins is of limited value since the reaction product is as inert as the starting material. Selective alkylation of arenes and insertion of acetylenes into C–H bonds are of greater utility.

In 1989, Jordan and co-workers reported a zirconium(IV)-catalyzed alkylation of α -picoline with propylene (eq. 16).⁴⁰ Ruthenium-catalyzed arene alkylation was developed by Murai and co-workers (eq. 17).⁴¹ The regioselectivity of this process is achieved through intramolecular chelation with the carbonyl group. Anti-Markovnikov iridium-catalyzed alkylation of benzene has been reported recently (eq. 18).⁴² In contrast to the Friedel-Crafts alkylation of benzene, the yield of the straight-chain alkane is remarkably high.



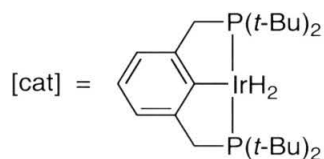
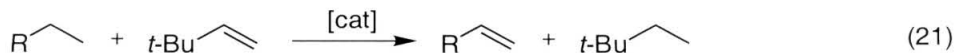
Palladium(II)-catalyzed insertion of alkynes into aromatic C–H bonds has been demonstrated recently (eq. 19).⁴³ Insertion of alkynes occurs both intra- and intermolecularly to give *cis*-alkenes. A number of oxygen- and nitrogen-containing functionalities are tolerated.



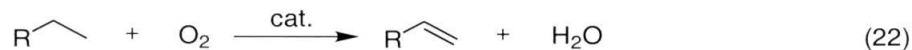
Alkane Dehydrogenation. Dehydrogenation of alkanes is another approach to alkane functionalization (eq. 20). Most of the chemical industry is geared towards the use of alkenes, the products of alkane dehydrogenation. Although the overall reaction is thermodynamically uphill if no dihydrogen scavenger is used, the highly positive entropy of the reaction allows the process to be driven to completion at high temperatures (typically $150\text{--}220\text{ }^\circ\text{C}$). For exploratory studies thermodynamic requirements can be eased by using dihydrogen acceptors such as norbornene or *tert*-butylethylene.



Alkane dehydrogenation with or without H_2 acceptors has been achieved with iridium(I) complexes of pincer-type ligands (eq. 21).⁴⁴ Due to the high thermal stability of these complexes, the catalytic reactions can be carried out at temperatures of $150\text{--}200\text{ }^\circ\text{C}$ with rates of up to 8 turnovers/min. However, in catalytic dehydrogenation without an H_2 acceptor, the final product distributions reflect relative thermodynamic stabilities of the olefins since dihydrogen elimination is slower than alkyl isomerization.



Oxidative alkane dehydrogenation uses dioxygen as H_2 scavenger (eq. 22). So far this reaction has only been demonstrated with heterogeneous systems.⁴⁵ Our attempts to develop a platinum(II)-catalyzed oxidative dehydrogenation of alkanes are described in Chapter 4 of this thesis.



Conclusions

The field of C–H bond activation has grown enormously in the last 20 years. A rarity not a long time ago, stoichiometric C–H activation reactions are becoming increasingly common. Except for “electrophilic” alkane activation, the mechanistic details of C–H bond breaking are well understood.

The progress in selective alkane functionalization has been much slower. Organometallic compounds are often incompatible with the conditions required for alkane functionalization. In that respect, the “electrophilic” systems, which can operate in strong acids, need to be studied in greater detail. A better understanding of the reaction mechanism, especially the C–H bond breaking step, will allow a greater control over the reactivity and selectivity of such systems. As described above, arene activation can be successfully coupled to

alkyne insertion. This chemistry can possibly be extended to other (cheaper) electrophilic metals such as cobalt(III).

The utility of alkane hydroxylation systems would be greatly increased if oxidation of alkanes could be coupled to dioxygen reduction. Despite its unique selectivity, the Shilov system is not practical since it uses stoichiometric amounts of platinum(IV). Dioxygen has been tested in this system: a few turnovers have been observed only in the presence of CuCl_2 or phosphomolybdates.⁴⁶ This problem can probably be solved by making the intermediate platinum(II) alkyl more electron-rich through ligand modification.

References

- (1) Parshall, G. W.; Ittel, S. D. *Homogeneous Catalysis*; 2nd ed.; John Wiley & Sons, Inc.: New York, 1992.
- (2) Mayer, J. M. *Acc. Chem. Res.* **1998**, *31*, 441-450.
- (3) Shilov, A. E.; Shul'pin, G. B. *Chem. Rev.* **1997**, *97*, 2879; Shilov, A. E.; Shul'pin, G. B. *Activation and Catalytic Reactions of Saturated Hydrocarbons in the Presence of Metal Complexes*; Kluwer Academic Publishers: Boston, 2000.
- (4) Arndtsen, B. A.; Bergman, R. G.; Mobley, T. A.; Peterson, T. H. *Acc. Chem. Res.* **1995**, *28*, 154-162.
- (5) Jones, W. D. In *Activation of Unreactive Bonds and Organic Synthesis*; Murai, S., Ed.; Springer-Verlag: Berlin, 1999; pp 9-46.
- (6) Geftakis, S.; Ball, G. E. *J. Am. Chem. Soc.* **1998**, *120*, 9933; Hall, C.; Perutz, R. N. *Chem. Rev.* **1996**, *96*, 3125.
- (7) Bennet, J. L.; Wolczanski, P. T. *J. Am. Chem. Soc.* **1997**, *119*, 10696; Slaughter, L. M.; Wolczanski, P. T.; Klinckman, T. R.; Cundari, T. R. *J. Am. Chem. Soc.* **2000**, *122*, 7953-7975.
- (8) Legzdins, P.; Tran, E. *J. Am. Chem. Soc.* **1997**, *119*, 5071.
- (9) Zhang, X. X.; Wayland, B. B. *J. Am. Chem. Soc.* **1994**, *116*, 7897-7898; Wayland, B. B.; Ba, S.; Sherry, A. E. *J. Am. Chem. Soc.* **1991**, *113*, 5305-5311; Sherry, A. E.; Wayland, B. B. *J. Am. Chem. Soc.* **1990**, *112*, 1259-1261.
- (10) Nelson, A. P.; DiMagno, S. G. *J. Am. Chem. Soc.* **2000**, *122*, 8569-8570.
- (11) Thompson, M. E.; Baxter, S. M.; Bulls, A. R.; Burger, B. J.; Nolan, M. C.; Santarsiero, B. D.; Schaefer, W. P.; Bercaw, J. E. *J. Am. Chem. Soc.* **1987**, *109*, 203-219.

- (12) Henry, P. M. *J. Org. Chem.* **1971**, 36, 1886-1890; Stock, L. M.; Tse, K.; Vorvick, L. J.; Walstrum, S. A. *J. Org. Chem.* **1981**, 46, 1757-1759.
- (13) Fujiwara, Y.; Takaki, K.; Taniguchi, Y. *Synlett* **1996**, 7, 591.
- (14) Larock, R. C. *Organomercury Compounds in Organic Synthesis*; Springer-Verlag: New York, 1985.
- (15) Usyatinskii, A. Y.; Bregadze, V. I. *Uspekhi Khimii* **1988**, 57, 1840-1866.
- (16) Lin, M.; Sen, A. *J. Am. Chem. Soc.* **1992**, 114, 7307-7308.
- (17) Periana, R. A. *Adv. Chem. Ser.* **1997**, 253, 61-78; Periana, R. A.; Taube, D. J.; Evitt, E. R.; Loffler, D. G.; Wentrcek, P. R.; Voss, G.; Masuda, T. *Science* **1993**, 259, 340.
- (18) Vargaftik, M. N.; Stolarov, I. P.; Moiseev, I. I. *J. Chem. Soc., Chem. Comm.* **1990**, 1049-1050.
- (19) Dihydrogen becomes more acidic when bound to transition metals. See Heinekey, D. M.; Oldham, W. J. *Chem. Rev.* **1993**, 93, 913-926; Jessop, P. G.; Morris, R. H. *Coord. Chem. Rev.* **1992**, 121, 155-284.
- (20) Jones, W. D. In *Selective Hydrocarbon Activation. Principles and Progress*; Davies, J. A., Watson, P. L., Greenberg, A., Liebman, J. F., Eds.; VCH Publishers, Inc.: New York, 1990.
- (21) Labinger, J. A. *Fuel Process. Technol.* **1995**, 42, 325-338.
- (22) Thomas, J. M. *Angew. Chem., Int. Ed.* **1999**, 38, 3589-3628; Thomas, J. M.; Raja, R.; Sankar, G.; Bell, R. G. *Nature* **1999**, 398, 227-230.
- (23) Valentine, J. S. In *Bioinorganic Chemistry*; Bertini, I., Gray, H. B., Lippard, S. J., Valentine, J. S., Eds.; University Science Books: Mill Valley, 1994.
- (24) Whittington, D. A.; Lippard, S. J. *J. Am. Chem. Soc.* **2001**, 123, 827-838.

- (25) Newcomb, M.; Shen, R.; Choi, S. Y.; Toy, P. H.; Hollenberg, P. F.; Vaz, A. D. N.; Coon, M. J. *J. Am. Chem. Soc.* **2000**, *122*, 2677-2686; Choi, S. Y.; Eaton, P. E.; Kopp, D. A.; Lippard, S. J.; Newcomb, M.; Shen, R. *J. Am. Chem. Soc.* **1999**, *121*, 12198-12199.
- (26) Gol'dshleger, N. F.; Tyabin, M. B.; Shilov, A. E.; Shteinman, A. A. *Zh. Fiz. Khim. (Engl. trans.)* **1969**, *43*, 1222.
- (27) Gol'dshleger, N. F.; Es'kova, V. V.; Shilov, A. E.; Shteinman, A. A. *Zh. Fiz. Khim. (Engl. trans.)* **1972**, *46*, 785.
- (28) For a review see: Stahl, S. S.; Labinger, J. A.; Bercaw, J. E. *Angew. Chem., Int. Ed.* **1998**, *37*, 2180.
- (29) Stahl, S. S.; Labinger, J. A.; Bercaw, J. E. *J. Am. Chem. Soc.* **1996**, *118*, 5961-5976.
- (30) Holtcamp, M. W.; Labinger, J. A.; Bercaw, J. E.; Henling, L. M.; Day, M. W. *Inorg. Chim. Acta* **1998**, *270*, 467-478; Holtcamp, M. W.; Labinger, J. A.; Bercaw, J. E. *J. Am. Chem. Soc.* **1997**, *119*, 848.
- (31) Johansson, L.; Tilset, M. *J. Am. Chem. Soc.* **2001**, *123*, 739-740; Johansson, L.; Tilset, M.; Labinger, J. A.; Bercaw, J. E. *J. Am. Chem. Soc.* **2000**, *122*, 10846-10855; Johansson, L.; Ryan, O. B.; Tilset, M. *J. Am. Chem. Soc.* **1999**, *121*, 1974-1975; Zhong, A. Z.; Labinger, J. A.; Bercaw, J. E. *J. Am. Chem. Soc.*,, to be submitted.
- (32) Wick, D. D.; Goldberg, K. I. *J. Am. Chem. Soc.* **1997**, *119*, 10235.
- (33) Luinstra, G. A.; Wang, L.; Stahl, S. S.; Labinger, J. A.; Bercaw, J. E. *J. Organomet. Chem.* **1995**, *504*, 75-91.
- (34) Horvath, I. T.; Cook, R. A.; Millar, J. M.; Kiss, G. *Organometallics* **1993**, *12*, 8.
- (35) Basickes, N.; Hogan, T. E.; Sen, A. *J. Am. Chem. Soc.* **1996**, *118*, 13111-13112.

- (36) Periana, R. A.; Taube, D. J.; Gamble, S.; Taube, H.; Satoh, T.; Fujii, H. *Science* **1998**, *280*, 560-564.
- (37) Chen, H.; Schlecht, S.; Semple, T. C.; Hartwig, J. F. *Science* **2000**, *287*, 1995-1997.
- (38) Brown, H. C. *Organic Syntheses via Boranes*; Wiley: New York, 1975.
- (39) Kolodiazhnyi, O. I. *Phosphorus Ylides*; Wiley-VCH: Weinheim, 1999.
- (40) Jordan, R. F.; Taylor, D. F. *J. Am. Chem. Soc.* **1989**, *111*, 778-779.
- (41) Sonoda, M.; Kakiuchi, F.; Chatani, N.; Murai, S. *Bull. Chem. Soc. Jpn.* **1997**, *70*, 3117-3128; Murai, S.; Chatani, N.; Kakiuchi, F. *Pure and Applied Chemistry* **1997**, *69*, 589-594; Murai, S.; Kakiuchi, F.; Sekine, S.; Tanaka, Y.; Kamatani, A.; Sonoda, M.; Chatani, N. *Nature* **1993**, *366*, 529-531.
- (42) Matsumoto, T.; Taube, D. J.; Periana, R. A.; Taube, H.; Yoshida, H. *J. Am. Chem. Soc.* **2000**, *122*, 7414-7415.
- (43) Jia, C. G.; Piao, D. G.; Oyamada, J. Z.; Lu, W. J.; Kitamura, T.; Fujiwara, Y. *Science* **2000**, *287*, 1992-1995.
- (44) Jensen, C. M. *Chem. Commun.* **1999**, 2443-2449.
- (45) Khodakov, A.; Olthof, B.; Bell, A. T.; Iglesia, E. *J. Catal.* **1999**, *181*, 205-216.
- (46) See Chapter 2.

Chapter II

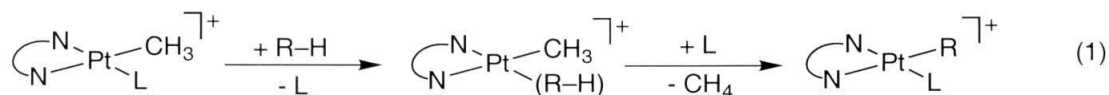
LIGAND SUBSTITUTION IN CATIONIC PLATINUM(II) COMPLEXES. IMPLICATIONS FOR THE MECHANISM OF C–H ACTIVATION WITH ELECTROPHILIC COMPLEXES OF PLATINUM(II).

Abstract

The displacement of pentafluoropyridine in $[(\text{tmeda})\text{Pt}(\text{CH}_3)(\text{NC}_5\text{F}_5)][\text{Bar}^{\text{f}}_4]$ (**1**) with γ -tetrafluoropicoline, a very poor nucleophile, was studied. The ligand substitution occurs by a dissociative interchange mechanism. This result implies that dissociative loss of pentafluoropyridine is the rate-limiting step in the C–H activation reactions of **1**. The proposed mechanism agrees with the results of the study of the reaction of **1** with $\text{C}_6\text{F}_5\text{CH}_3$ and C_6H_6 . The rate of the C–H activation reaction is independent of benzene concentration and no kinetic isotope effect was observed. Activation parameters for the reaction of **1** with pentafluorotoluene were determined ($\Delta H^\ddagger = 26 \pm 3 \text{ kcal mol}^{-1}$, $\Delta S^\ddagger = -5 \pm 7 \text{ kcal (K mol)}^{-1}$).

Introduction

Carbon-hydrogen bond activation by electrophilic platinum(II) complexes has been extensively studied (eq. 1).¹⁻⁵ The individual steps are hard to examine experimentally since a well-defined alkane σ -complex of platinum(II) has eluded isolation. Most of the information about the C–H bond breaking step has been obtained through isotope labeling, ligand modification studies²⁻⁵ or from studies of the microscopic reverse of C–H activation, protonolysis of platinum(II) alkyls.^{1,6}

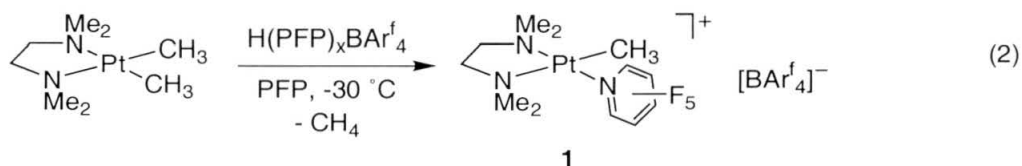


On the other hand, ligand substitution in platinum(II) complexes is one of the most exhaustively studied processes in inorganic chemistry.^{7,8} Associative or associative interchange mechanisms have been identified in an overwhelming number of cases.⁹ However, relatively little is known about substitution reactions with such weak nucleophiles as alkanes. Due to the low nucleophilicity of C–H bonds, a change from the ubiquitous associative mechanism to a dissociative one might be possible here.

An electrophilic platinum(II) complex, [(tmeda)Pt(CH₃)(NC₅F₅)] [BAr₄^f] (**1**, BAr₄^f = tetra-3,5-bistrifluoromethylphenyl borate), has been synthesized in our group and its reactions with alkanes have been examined.⁴ The studies of ligand substitution in **1** and their relevance to the C–H activation reactions are described here.

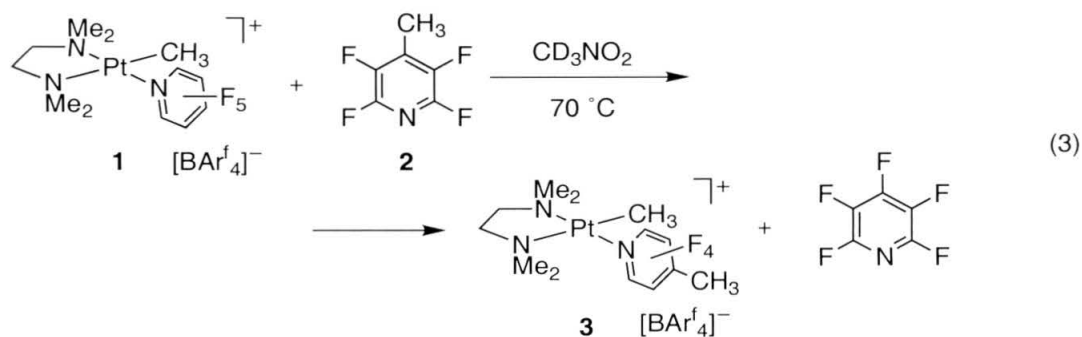
Results

Complex **1** was prepared by treating (tmeda)PtMe₂ with [H(NC₅F₅)_x][BAr^f₄] at -30 °C (eq. 2, PFP = pentafluoropyridine). The resulting compound is stable in pentafluoropyridine solution as well as in the solid state under inert atmosphere. It is also soluble in nitromethane and pentafluorotoluene (C₆F₅CH₃, PFT). Although not observed at room temperature, reaction with solvent becomes noticeable at higher temperatures. The product of the reaction with C₆F₅CH₃, [(tmeda)Pt(CH₂C₆F₅)(NC₅F₅)][BAr^f₄], can be isolated and characterized.



We first looked at the displacement of pentafluoropyridine from **1** with trimethylphosphine and pyridine. Unfortunately, only nucleophilic aromatic substitution of one of the fluorines on the perfluorinated aromatic ring occurred. With a weaker nucleophile, diethyl ether, no reaction was observed at 25 °C; higher temperatures resulted in C–H activation.

The substitution kinetics were then studied using γ -tetrafluoropicoline **2** (γ -TFP), a weak nucleophile with deactivated C–H bonds (eq. 3). The product of the reaction, [(tmeda)Pt(CH₃)(NC₅F₄CH₃)][BAr^f₄] (**3**), was isolated and characterized. Reactions were carried out in CD₃NO₂ at 70 °C (activation of the solvent C–D bonds was not observed under these conditions) and monitored by ¹⁹F NMR spectroscopy. The chemical shifts of the *ortho*-fluorines on the coordinated fluoroheterocycle are sensitive to the nature of the ligands on platinum (Table 1).



The reaction in eq. 3 is irreversible, $K_{eq} \geq 5.5$ at 70 °C. No intermediates were detected in the reaction mixture, except in the case with $[2]/[1]$ ratio of 2.6, when an extra peak with platinum satellites was found in the ^{19}F NMR spectrum at the late stages of the reaction. This peak was tentatively attributed to $[(\text{tmeda})\text{Pt}(\text{CD}_2\text{NO}_2)(\text{NC}_5\text{F}_5)][\text{BAr}_4^-]$.

Table 1. Selected ^{19}F NMR Data for Compounds **1**, **3-5**.

Compound	δ , ppm	$^3J_{\text{PtF}}$, Hz
$[(\text{tmeda})\text{Pt}(\text{CH}_3)(\text{PFP})][\text{BAr}_4^-]$ (1)	-78.0	352
$[(\text{tmeda})\text{Pt}(\text{CH}_3)(\gamma\text{-TFP})][\text{BAr}_4^-]$ (3)	-87.5	343
$[(\text{tmeda})\text{Pt}(\text{CH}_2\text{C}_6\text{F}_5)(\text{PFP})][\text{BAr}_4^-]$ (4)	-78.9	352
$[(\text{tmeda})\text{Pt}(\text{C}_6\text{H}_5)(\text{PFP})][\text{BAr}_4^-]$ (5)	-79.9	329

The initial rates of substitution were calculated by fitting the concentration–time data for the first 15% of the reaction to a 3rd order polynomial (eq. 4).¹⁰ The observed rate constants were obtained from eq. 6 (c_0 is the starting concentration of **1**) and are given in Table 2 (entries 1-4). Even though the concentration of incoming nucleophile increased by two orders of magnitude, the observed rate constants remained essentially the same. In addition, the rate

of substitution did not change when the reaction was carried out in 1:1 CD₃NO₂/C₆F₆ solvent mixture (entries 5 and 6, Table 2).

$$c(t) = a_0 + a_1 t + a_2 t^2 \quad (4)$$

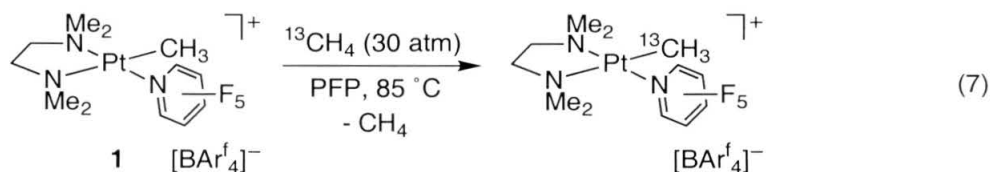
$$\text{initial rate} = \left[\frac{dc(t)}{dt} \right]_{t=0} = a_1 + 2a_2 t = a_1 = kc_0 \quad (5)$$

$$k = \frac{\text{initial rate}}{c_0} \quad (6)$$

Table 2. Kinetic data for the reaction of **1** with **2** in CD₃NO₂ at 70 °C. Entries 5 and 6: added [PFP] = 0.15 M. Entries 1-5: solvent = CD₃NO₂. Entry 6: solvent = 1:1 C₆F₆/CD₃NO₂. *k*_{obs} was obtained from the exponential fitting of the *c*(*t*)–time data.

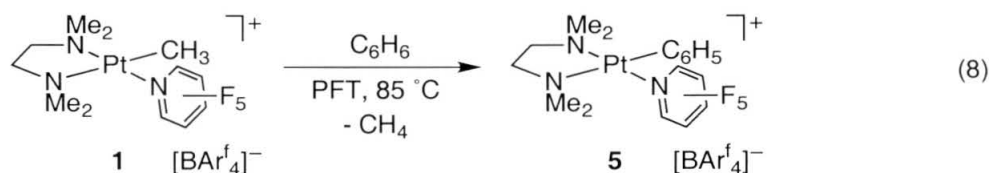
Entry	[1], mM	[2], M	[2]/[1]	<i>k</i> _{obs} ·10 ⁴ , s ⁻¹	Init.rate·10 ⁴ , M s ⁻¹	(Init.rate/[1])·10 ³ , s ⁻¹
1	19	0.05	2.6	1.8±0.4	1.0	5.2
2	19	0.34	18	2.7±0.2	1.8	9.5
3	34	1.67	49	2.5±0.3	2.5	7.3
4	34	3.03	89	2.4±0.5	2.1	6.2
5	28	0.55	20	1.5±0.1	–	–
6	28	0.55	20	1.5±0.1	–	–

Initially, the C–H activation reactions were carried out in pentafluoropyridine since it has no C–H bonds and is polar enough to dissolve cationic complex **1**.⁴ Thus, reaction of **1** with benzene afforded [(tmeda)Pt(C₆H₅)(NC₅F₅)]⁺[BAR^f₄][–] (**6**) in pentafluoropyridine at 85 °C. Remarkably, **1** was also shown to react with ¹³CH₄ under similar condition (eq. 7). The rates of C–H activation reactions were typically slow (several days).

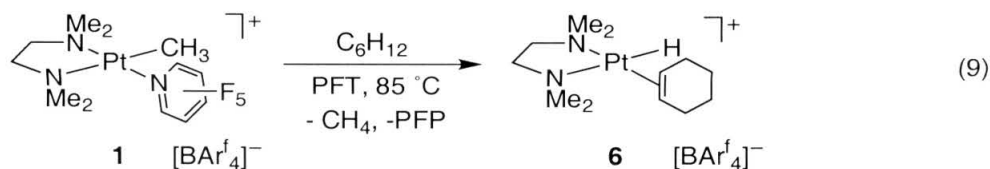


Whereas nitromethane proved to be too reactive to be used as a reaction medium, pentafluorotoluene turned out to be a suitable solvent for the observation of C–H activation reactions. Just as in γ -tetrafluoropicoline, the strong electron-withdrawing nature of the fluorinated substituent (pentafluorophenyl or tetrafluoropyridyl group) considerably decreases the reactivity of the benzylic C–H bonds. C–H activation reactions are typically faster in pentafluorotoluene than they are in pentafluoropyridine.

Reaction of **1** with benzene in PFP to give [(tmeda)Pt(C₆H₅)(PFP)][BAr^f₄] (**5**) takes several days at 85 °C while in C₆F₅CH₃ the reaction is complete in several hours (eq. 8). The rate of the C–H activation reaction in pentafluorotoluene does not depend on the concentration of benzene ($k_{\text{obs}}(93\text{ °C}) = 1.2 \cdot 10^{-4}\text{ s}^{-1}$ at [C₆H₆] = 0.2 M and $k_{\text{obs}}(99\text{ °C}) = 1.3 \cdot 10^{-4}\text{ s}^{-1}$ at [C₆H₆] = 1.2 M). No kinetic isotope effect was observed in reactions with C₆H₆ and C₆D₆. Deuterium incorporation into the Pt-CH₃ moiety along with the formation of the methane isotopomers (CH₃D, CH₂D₂) when the reaction is carried in C₆D₆/C₆F₅CH₃ mixture indicate that H/D exchange occurs prior to methane loss. Besides, protio benzene is generated in the reaction mixture even when all **1** is consumed. NMR integrations confirmed that both **1** and pentafluorotoluene are sources of protium. Only the starting material, **1**, and the product, **5**, were detected in the reaction mixtures by ¹⁹F NMR.



The olefin hydride complex **6** was formed in the reaction of cyclohexane with **1** in both pentafluoropyridine and pentafluorotoluene solvents, along with some platinum(0) (eq. 9). Isotopomers of methane (CH_3D and CH_2D_2) were observed in the reaction of **1** with cyclohexane- d_{12} .



The reaction of **1** with pentafluorotoluene was monitored by ^1H NMR at 84–120 °C (eq. 10). The disappearance of **1** is first order in the platinum complex (Figure 1). The rate of the reaction decreases with added pentafluoropyridine. The activation parameters, $\Delta H^\ddagger = 26 \pm 3 \text{ kcal mol}^{-1}$, $\Delta S^\ddagger = -5 \pm 7 \text{ kcal (K mol)}^{-1}$, were calculated from the Eyring plot (Figure 2).

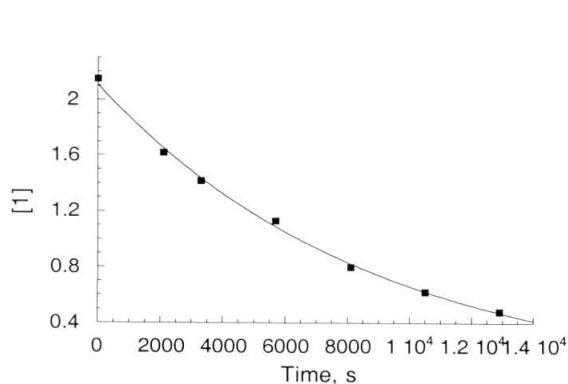
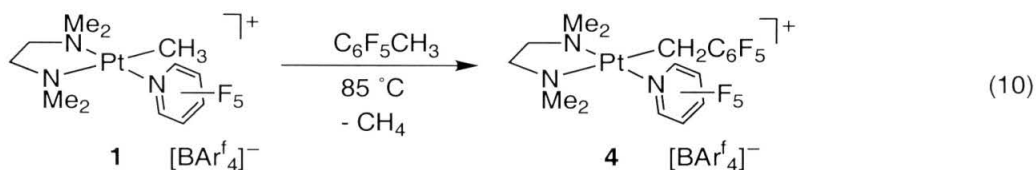


Figure 1. Disappearance of **1** in the reaction with pentafluorotoluene. $k_{\text{obs}} = (1.2 \pm 0.1) \cdot 10^{-4} \text{ s}^{-1}$. $T = 93^\circ\text{C}$.

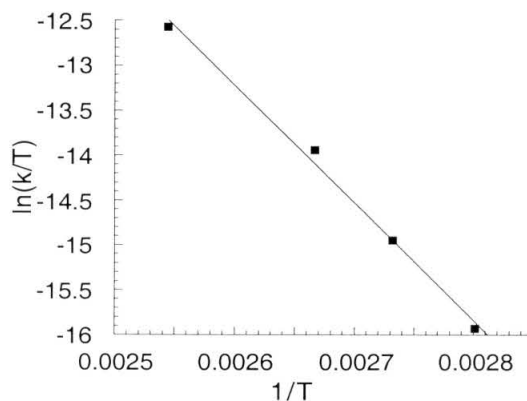
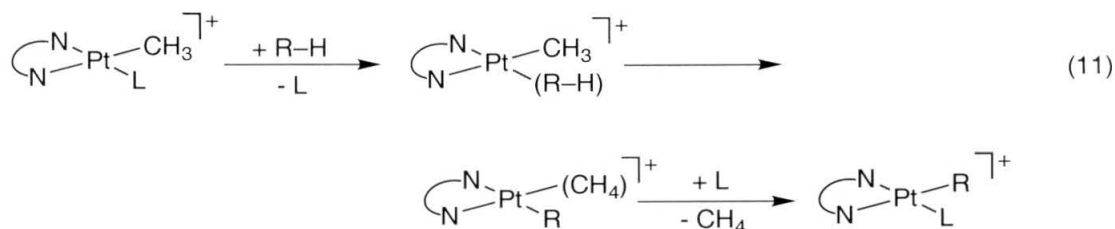


Figure 2. Eyring plot for the reaction of **1** with pentafluorotoluene. Calculated activation parameters: $\Delta H^\ddagger = 26 \pm 3 \text{ kcal mol}^{-1}$, $\Delta S^\ddagger = -5 \pm 7 \text{ kcal (K mol)}^{-1}$. Temperature range: 84–120 °C.

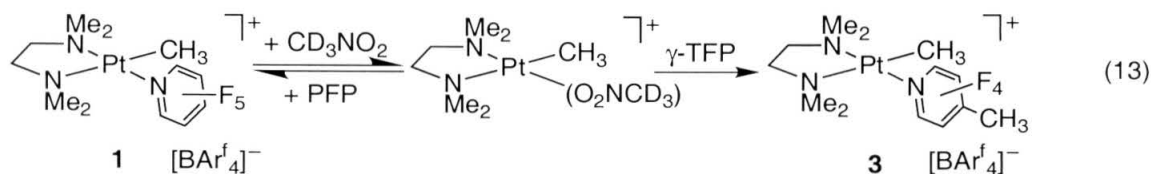
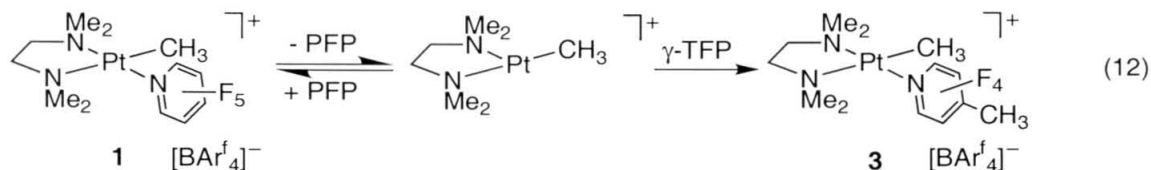
Discussion

Earlier studies of C–H activation by $[(\text{tmeda})\text{Pt}(\text{CH}_3)(\text{NC}_5\text{F}_5)][\text{BAr}_4^f]$ have established the presence of alkane σ -complexes on the reaction pathway.^{4,11} Therefore, the overall process can be divided into three parts: i) displacement of pentafluoropyridine in **1** by alkane to form a σ -complex, ii) C–H activation and iii) displacement of methane with pentafluoropyridine (eq. 11).



Direct study of ligand substitution in **1** using alkanes has not been possible, since alkane σ -complexes have not been detected in reaction mixtures and their independent synthesis has not been achieved yet. The susceptibility of pentafluoropyridine to nucleophilic attack prevents the use of common nucleophiles to study the substitution step. In any case, such reagents are not very good models of alkane C–H bonds, which have very low nucleophilicity. We were not able to observe exchange of the coordinated PFP ligand with free ligand by ^{19}F NMR even at elevated temperatures. We reasoned that if alkanes can successfully compete with pentafluoropyridine in the case of **1**, then perhaps γ -tetrafluoropicoline, which acts almost as a “labeled” pentafluoropyridine, can be used to study the substitution step. γ -Tetrafluoropicoline is more electron rich than pentafluoropyridine and, therefore, is a better nucleophile. We found that reaction of **1** with γ -TFP is irreversible under the reaction conditions that we used in this study.

As can be seen in Table 2, the rate of substitution did not change with increasing concentration of γ -TFP (entries 1-4). Addition of extra pentafluoropyridine slows down the substitution (entries 2 and 5, Table 2). Two possible substitution mechanisms can explain this behavior: a dissociative mechanism through the coordinatively unsaturated 14 electron platinum(II) intermediate (eq. 12) or a solvent-assisted associative pathway (eq. 13). The non-innocent nature of nitromethane in ligand substitution reactions of platinum(II) complexes was established as early as 1960.¹² To distinguish between the two mechanisms we carried out substitution reactions in diluted CD_3NO_2 (1:1 $\text{CD}_3\text{NO}_2/\text{C}_6\text{F}_6$). The observed rate constants remained unchanged (entries 5 and 6, Table 2). The experimental results indicate that displacement of pentafluoropyridine by **3** in **1** occurs by a dissociative interchange mechanism.



The mechanism of ligand substitution in square-planar platinum(II) complexes has been extensively studied.^{7,9} In the majority of cases, associative or associative interchange mechanisms have been identified. For example, a recent study by Romeo *et al.* showed that DMSO exchange in $[(\text{tmeda})\text{Pt}(\text{CH}_3)(\text{DMSO})][\text{BF}_4]$ occurs by an associative interchange mechanism.¹³

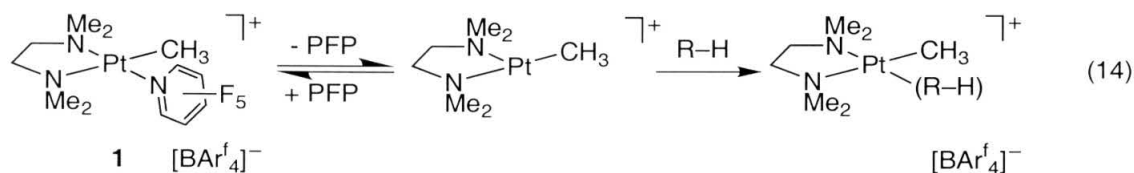
On the other hand, the coordinated diethyl ether in [(tmeda)Pt(CH₃)(OEt₂)] [BF₄] does not exchange with Et₂O-*d*₁₀ even at elevated temperatures. Instead, intramolecular C–H bond activation takes place.⁴

In several cases, ligand substitution in platinum(II) complexes has been shown to proceed by a dissociative interchange mechanism.¹⁴ Displacement of the coordinated dimethylsulfide or dimethylsulfoxide in *cis*-PtPh₂(L)₂ (L = Me₂S or Me₂SO) by a number of bidentate ligands as well as by pyridine occurs by a dissociative mechanism.¹⁵ Phosphine exchange in *cis*-(Ph₂MeSi)₂Pt(PMe₂Ph)₂ also occurs via a dissociative pathway.¹⁶

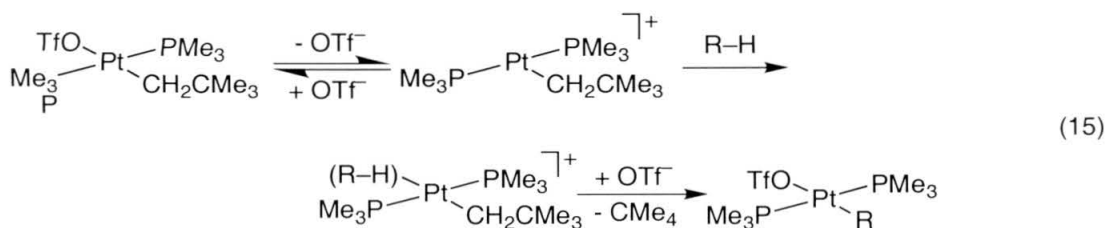
Several factors are responsible for the switch from an associative mechanism to a dissociative one, as exemplified by the substitution in PtPh₂(L)₂ and (Ph₂MeSi)₂Pt(PMe₂Ph)₂. Both ground state destabilization, through *trans*-influence and steric congestion, and the stabilization of the three-coordinate intermediate with strong σ-donors favor the dissociative mechanism. On the other hand, the presence of π-acceptors should stabilize the transition state for associative displacement (see below). The nature of the incoming nucleophile and the leaving group should also be taken into account. Whereas ligand exchange in [(tmeda)Pt(CH₃)(L)] [BF₄], when L is dimethylsulfoxide, occurs by an associative mechanism, exchange of a weaker nucleophile γ-TFP for a good leaving group (L = PFP) occurs through a dissociative pathway.

Since alkanes are even poorer nucleophiles than γ-tetrafluoropicoline we propose that the two substitution steps in the C–H activation reactions of **1** (eq. 11) also occur by a dissociative interchange mechanism (eq. 14). The C–H activation reactions are proposed to start by a rate-limiting loss of PFP followed

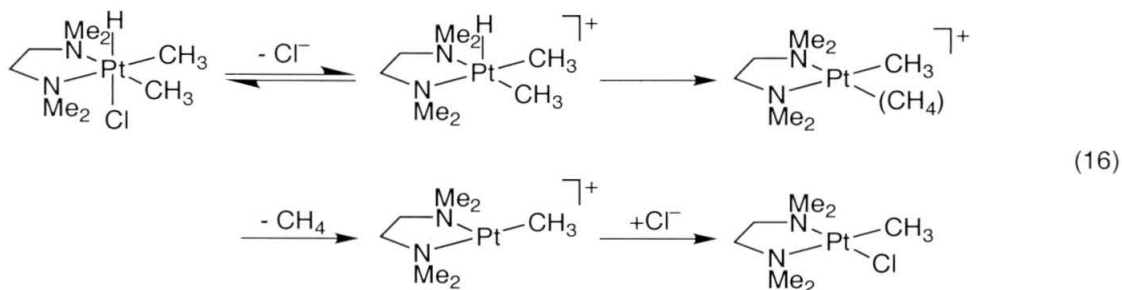
by coordination of alkane. In agreement with this proposal, the rate of the reaction between **1** and benzene (eq. 8) is independent of benzene concentration and there is no KIE in reactions with C₆H₆ and C₆D₆. The discriminating ability of the three-coordinate intermediate toward hydrocarbons is low: C₆F₅CH₃ and C₆H₆ react at approximately the same rate. As mentioned above, C–H activation reactions of **1** are faster in pentafluorotoluene compared to the reactions carried out in pentafluoropyridine. The entropy of activation for the reaction of **1** with C₆F₅CH₃ ($\Delta S^\ddagger = -5 \pm 7$ kcal (K mol)⁻¹), although smaller than typical values for a dissociative mechanism, does not contradict the proposed mechanism and, instead, might be largely defined by the changes in solvation.



The mechanism of C–H activation by electrophilic platinum(II) complexes has been studied in several systems. Whitesides and co-workers examined the C–H bond activation by *trans*-(PMe₃)₂Pt(CH₂C(CH₃)₃)(OTf) in neat benzene (eq. 15).³ Addition of [Bu₄N][BF₄] increases the rate of the reaction whereas addition of [Bu₄N][OTf] decreases it. The authors proposed that the loss of triflate to form the three-coordinate [(PMe₃)₂PtCH₂C(CH₃)₃]⁺ is the rate-determining step in this reaction.

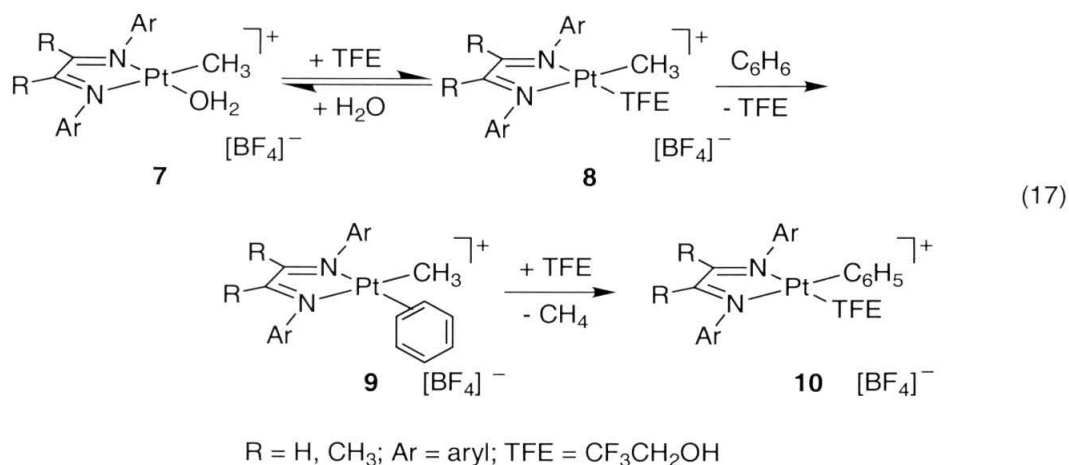


Indirect evidence for dissociative displacement of alkanes from the σ -complex comes from the protonolysis studies of dialkylplatinum(II) complexes (eq. 16).^{1,17} Reductive elimination from (tmeda)Pt(H)(CH₃)₂Cl in methanol or (tmeda)Pt(CH₂Ph)(H)Cl₂ in dichloromethane affords (tmeda)Pt(CH₃)Cl or (tmeda)PtCl₂, respectively. The rates of these reactions exhibit an inverse dependence on the concentration of chloride. In addition, H/D exchange shows an inverse dependence on [Cl⁻]. Assuming a fast pre-equilibrium chloride dissociation step precedes the rate-limiting alkane loss, these data point to dissociative mechanism of alkane displacement from the σ -complex (eq. 16). By microscopic reverse, chloride displacement by an alkane should also occur by a dissociative mechanism. On the other hand, an associative displacement of the coordinated methane was inferred from the studies of protonolysis of dimethylplatinum(II) complexes of α -diimines.⁶



The mechanism of C–H activation by cationic platinum(II) complexes of α -diimines was examined in several recent studies.^{5,18} A mechanism which

accounts for all experimental data is shown in eq. 17. Only the trifluoroethanol complex **8** reacts with benzene to give a π -bound intermediate **9** by an associative mechanism. The overall reaction is slowed down by the addition of water as the equilibrium concentration of **8** decreases in favor of the aquo complex **7**. The nature of the α -diimine ligand dictates the rate-determining step of the overall reaction. Either the ligand substitution or the C–H activation step can be rate-limiting.



It should be noted that the majority of, if not all, direct mechanistic studies of C–H activation with platinum(II) compounds have used benzene or its derivatives. Initial coordination of the aromatic π -system helps to bring the weakly nucleophilic C–H bonds close to an electrophilic platinum(II) center. It will be interesting to see whether less nucleophilic alkanes would react through similar pathways.

Both protonolysis studies and studies of ligand substitution and C–H activation reactions indicate that tmeda-chelated platinum(II) prefers dissociative substitution pathways while platinum(II) complexes of α -diimines favor associative mechanisms. This observation can be rationalized if we consider the

transition state for an associative ligand exchange. The five-coordinate transition structure is stabilized by π -acceptors in the equatorial plane. Therefore, α -diimines, which are better π -acceptors than diamines, are expected to stabilize the transition state for associative substitution. The same trend is also expected from the steric point of view.

Conclusions

The mechanism of C–H activation reactions by $[(\text{tmeda})\text{Pt}(\text{CH}_3)(\text{PFP})][\text{BAr}^{\text{f}}_4]$ was studied. Through model substitution studies and isotope labeling experiments it was established that displacement of pentafluoropyridine by a hydrocarbon is the rate-limiting step. The substitution step was studied using γ -tetrafluoropicoline as a nucleophile and found to occur by a dissociative interchange mechanism.

Experimental

All air and/or moisture sensitive compounds were manipulated using standard high-vacuum line, Schlenk or cannula techniques, or in a dry box under a nitrogen atmosphere.¹⁹ Glassware was flame-dried prior to use. Pentafluoropyridine (PFP), 1,2,3,4,5-pentafluorotoluene (PFT), 4-methyl-2,3,5,6-tetrafluoropyridine (γ -TFP), and N,N,N',N'-tetramethylethylenediamine (tmeda) were purchased from Aldrich. (COD)Pt(CH₃)₂ was purchased from Strem Chemicals. Solvents were dried over sodium/benzophenone (Et₂O, THF, petroleum ether), 4Å molecular sieves (CH₃OH, CH₃NO₂), or CaH₂ (CH₂Cl₂, pentafluoropyridine, 1,2,3,4,5-pentafluorotoluene, α,α,α -trifluorotoluene, 4-methyl-2,3,5,6-tetrafluoropyridine). The following compounds were prepared according to literature procedures: (tmeda)Pt(CH₃)₂,²⁰ [(tmeda)Pt(CH₃)(PFP)][BAR^f₄],⁴ and [H(OEt₂)₂][BAR^f₄].²¹

NMR spectra were recorded on General Electric QE300 (300 MHz for ¹H), Bruker AM 500 (500.13 MHz for ¹H, 125.03 MHz for ¹³C, 476.56 MHz for ¹⁹F) and Varian UNITY INOVA 500 (499.853 MHz for ¹H, 476.30 MHz for ¹⁹F) spectrometers. Multiplicities cited for NMR peaks do not include ¹⁹⁵Pt satellites; if the latter are present, a coupling constant is given. Elemental analyses were carried out at the Caltech Elemental Analysis Facility by Fenton Harvey.

[(tmeda)Pt(CH₃)(PFP)][BAR^f₄] (1). ¹⁹F NMR (PFT): δ -65.0 (s, 24F, -CF₃ in BAR^f₄), -78.0 (m, 2F, ³J_{PtF} = 352 Hz, *o*-F in Pt-NC₅F₅), -125.47 (m, 2F, *m*-F in Pt-NC₅F₅), -159.75 (m, 2F, *p*-F in Pt-NC₅F₅).

Reactions of 1 with deuterated alkanes and arenes in PFT. In an inert atmosphere drybox, [(tmeda)Pt(CH₃)(PFP)][BAR^f₄] (30 mg, 0.022 mmol) was

placed into a NMR tube. Pentafluorotoluene (~0.5 mL) and deuterated substrate (0.05 - 0.1 mL) were added by vacuum transfer and the tube was flame-sealed. The NMR tube was placed into an oil bath at 85 °C. Reactions were monitored by ^1H and ^{19}F NMR spectroscopy.

[(tmeda)Pt(CH₂C₆F₅)(PFP)][BAr^f₄] (5). In an inert atmosphere drybox, **1** (60 mg, 0.044 mmol) was placed into a 25 mL thick-walled glass bomb. Pentafluorotoluene (~2 mL) was added by vacuum transfer. The flask was placed into 85 °C oil bath for 15 hours. The product was precipitated with petroleum ether and purified by dissolving in pentafluorotoluene and precipitating with petroleum ether. The product was dried *in vacuo* to give dark-tan powder (35 mg, 0.023 mmol, 52%). Anal. Calcd. for C₅₀H₃₀F₃₄N₃BPt: C, 39.39%, H, 1.98%, N, 2.76%. Found: C, 38.93%, H, 2.64%, N, 2.87%. ^1H NMR (PFP): δ 7.72 (s, 8H, *o*-H in BAr^f₄), 7.32 (s, 4H, *p*-H in BAr^f₄), 3.30, 2.55 (m, 12H, -CH₂N(CH₃)₂), 3.11, 2.69 (s, 4H, -CH₂N(CH₃)₂), 2.87 (s, 3H, ^{195}Pt satellites are obscured by the tmeda resonances, Pt-CH₂C₆F₅). ^{19}F NMR (CD₃NO₂): δ -65.0 (s, 24F, -CF₃ in BAr^f₄), -78.9 (m, 2F, $^3J_{\text{PtF}}$ = 352 Hz, *o*-F in Pt-NC₅F₅), -122.9 (m, 1F, *p*-F in Pt-NC₅F₅), -158.3 (m, 2F, *m*-F in Pt-NC₅F₅). ^{13}C NMR (CD₃NO₂): δ 163.6 (q, $^1J_{\text{BC}}$ = 50 Hz, *i*-C in B(C₆H₂(CF₃)₂)₄), 136.4 (s, *o*-C in B(C₆H₂(CF₃)₂)₄), 130.5 (q, $^2J_{\text{CF}}$ = 31 Hz, *m*-C in B(C₆H₂(CF₃)₂)₄), 126.1 (q, $^1J_{\text{CF}}$ = 270 Hz, -CF₃ in B(C₆H₂(CF₃)₂)₄), 118.4 (s, *p*-C in B(C₆H₃(CF₃)₂)₄), 68.4, 61.1 (s, -CH₂N(CH₃)₂), 53.2, 50.4 (s, -CH₂N(CH₃)₂), -10.1 (s, $^1J_{\text{PtC}}$ = 716 Hz, Pt-CH₂C₆F₅).

[(tmeda)Pt(CH₃)(TFP)][BAr^f₄] (7). In an inert atmosphere drybox, **1** (0.1 g, 0.074 mmol) was placed into a 25 mL thick-walled glass bomb. γ -Tetrafluoropicoline (~2 mL) was added by vacuum transfer. The flask was

placed in an 85 °C oil bath for 15 hours. Volatiles were removed *in vacuo* to give dark-brown oil which was dissolved in nitromethane- d_3 to obtain NMR spectra. ^1H NMR (CD_3NO_2): δ 7.86 (s, 8H, *o*-H in BAr_4^f), 7.67 (s, 4H, *p*-H in BAr_4^f), 2.81, 3.08 (m, 6H, $-\text{CH}_2\text{N}(\text{CH}_3)_2$), 2.68, 3.0 (s, 4H, $-\text{CH}_2\text{N}(\text{CH}_3)_2$), 2.47 (s, 3H, $\text{Pt-NC}_5\text{F}_4\text{-CH}_3$), 0.28 (s, 3H, $^3J_{\text{PtH}} = 74\text{ Hz}$, Pt-CH_3). ^{19}F NMR: d -65.0 (s, 24F, $-\text{CF}_3$ in BAr_4^f), -87.5 (m, 2F, $^3J_{\text{PtF}} = 343\text{ Hz}$, *o*-F in $\text{Pt-NC}_5\text{F}_4\text{CH}_3$), -144.88 (m, 2F, *p*-F in $\text{Pt-NC}_5\text{F}_4\text{CH}_3$).

Data Analysis. Due to the fact that some reactions were run in neat pentafluorotoluene, the question of error analysis becomes very important. Data analysis, which mainly consisted of curve fitting, was carried out with the KaleidaGraphTM software package. Unfortunately, this particular program does not take into account uncertainty in measurements in calculation of slopes. A modified linear least-squares algorithm for analysis of data with uncertainties in both variables has been applied to our data.²² In analysis of the ^1H NMR-based kinetic experiments relative error of integration was set to 10%, and standard deviation, σ , was assigned the same value (the measured σ was equal to 5% of the intensity; for ^{19}F NMR spectra it was 2.5%). The algorithm was repeated until satisfactory convergence of the values of slope and intercept was achieved (usually 2-3 iterations). In all cases, the relative uncertainty in the observed rate constant was close to 15%. The same algorithm was applied to the Eyring plot data. The uncertainties were not substantially different from the ones calculated by KaleidaGraphTM: ΔH^\ddagger , ± 3 vs. $\pm 2\text{ kcal mol}^{-1}$; ΔS^\ddagger , ± 7 vs $\pm 5\text{ kcal (K mol)}^{-1}$

Ligand substitution in 1. In an inert atmosphere drybox, **1** was placed into a NMR tube. Pentafluoropyridine, γ -tetrafluoropicoline and nitromethane- d_3 were

added by syringe. The tube was sealed off under vacuum and placed into the NMR probe preheated to 343 K. Reactions were monitored by ^{19}F NMR.

Determination of the activation parameters for reaction of 1 with PFT. In an inert atmosphere drybox, **1** was placed into a NMR tube. Pentafluorotoluene was added by syringe. The tube was sealed off and placed into oil bath. Reactions were monitored by ^{19}F NMR.

References

- (1) Stahl, S. S.; Labinger, J. A.; Bercaw, J. E. *J. Am. Chem. Soc.* **1996**, *118*, 5961-5976.
- (2) Wick, D. D.; Goldberg, K. I. *J. Am. Chem. Soc.* **1997**, *119*, 10235.
- (3) Brainard, R. L.; Nutt, W. R.; Lee, T. R.; Whitesides, G. M. *Organometallics* **1988**, *7*, 2379-2386.
- (4) Holtcamp, M. W.; Labinger, J. A.; Bercaw, J. E.; Henling, L. M.; Day, M. W. *Inorg. Chim. Acta* **1998**, *270*, 467-478.
- (5) Johansson, L.; Tilset, M.; Labinger, J. A.; Bercaw, J. E. *J. Am. Chem. Soc.* **2000**, *122*, 10846-10855; Zhong, A. Z.; Labinger, J. A.; Bercaw, J. E. *J. Am. Chem. Soc.*, to be submitted.
- (6) Johansson, L.; Tilset, M. *J. Am. Chem. Soc.* **2001**, *123*, 739-740.
- (7) Wilkins, R. G. *Kinetics and Mechanism of Reactions of Transition Metal Complexes*; 2nd Edition ed.; VCH: Weinheim, New York, 1991.
- (8) Langford, C. H.; Gray, H. B. *Ligand Substitution Processes*; W. A. Benjamin, Inc.: New York, 1966.
- (9) Cross, R. J. *Adv. Inorg. Chem.* **1989**, *34*, 219-292.
- (10) Hall, K. J.; Quickenden, T. I.; Watts, D. W. *J. Chem. Educ.* **1976**, *53*, 493-494.

- (11) Holtcamp, M. W.; Labinger, J. A.; Bercaw, J. E. *J. Am. Chem. Soc.* **1997**, *119*, 848.
- (12) Pearson, R. G.; Gray, H. B.; Basolo, F. *J. Am. Chem. Soc.* **1960**, *82*.
- (13) Romeo, R.; Sclaro, L. M.; Nastasi, N.; Arena, G. *Inorg. Chem.* **1996**, *35*, 5087.
- (14) Romeo, R. *Comments Inorg. Chem.* **1990**, *11*, 21-57.
- (15) Alibrandi, G.; Bruno, G.; Lanza, S.; Minniti, D.; Romeo, R.; Tobe, M. L. *Inorg. Chem.* **1987**, *26*, 185-190; Lanza, S.; Minniti, D.; Moore, P.; Sachinidis, J.; Romeo, R.; Tobe, M. L. *Inorg. Chem.* **1984**, *23*, 4428-4433.
- (16) Wendt, O. F.; Deeth, R. J.; Elding, L. I. *Inorg. Chem.* **2000**, *39*, 5271-5276.
- (17) Stahl, S. S. *Ph.D. Thesis*; California Institute of Technology: Pasadena, California, 1997.
- (18) Johansson, L.; Ryan, O. B.; Tilset, M. *J. Am. Chem. Soc.* **1999**, *121*, 1974-1975.
- (19) Shriver, D. F.; Drezdson, M. A. *The Manipulation of Air-Sensitive Compounds*; 2nd ed.; John Wiley & Sons: New York, 1986.
- (20) Clark, H. C.; Manzer, L. E. *J. Organomet. Chem.* **1973**, *59*, 411-428.
- (21) Brookhart, M.; Grant, B.; Volpe, A. F. *Organometallics* **1992**, *11*, 3920-3922.
- (22) Ogren, P. J.; Norton, J. R. *J. Chem. Educ.* **1992**, *69*, A130.

Chapter III

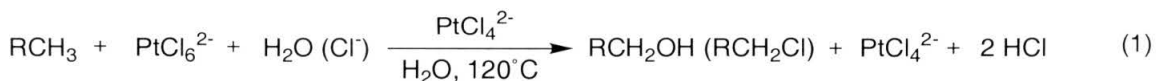
OXIDATION OF DIMETHYLPLATINUM(II) COMPLEXES WITH DIOXYGEN

Abstract

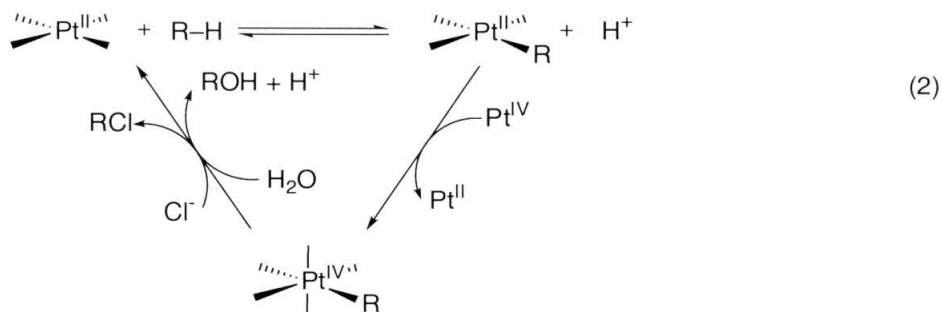
Dimethylplatinum(II) complexes $(\text{N-N})\text{Pt}(\text{CH}_3)_2$ ($\text{N-N} = \text{tmeda}(\mathbf{1})$, α -diimines) are oxidized by dioxygen in methanol to the corresponding hydroxoplatinum(IV) complexes $(\text{N-N})\text{Pt}(\text{OH})(\text{OCH}_3)(\text{CH}_3)_2$. Mechanistic studies suggest a two-step mechanism. First, a hydroperoxoplatinum(IV) complex is formed in a reaction between $(\text{N-N})\text{Pt}(\text{CH}_3)_2$ and dioxygen. Next, the hydroperoxy complex reacts with a second equivalent of $(\text{N-N})\text{Pt}(\text{CH}_3)_2$ to afford the final product, $(\text{N-N})\text{Pt}(\text{OH})(\text{OCH}_3)(\text{CH}_3)_2$. The hydroperoxy intermediate, $(\text{tmeda})\text{Pt}(\text{OOH})(\text{OCH}_3)(\text{CH}_3)_2$ ($\mathbf{2}$), was isolated and characterized. The reactivity of $\mathbf{2}$ with several dimethylplatinum(II) complexes is reported.

Introduction

The selective catalytic oxidation of alkanes by aqueous platinum salts was originally reported by Shilov in 1972 (eq. 1).¹ The mechanism of this unique catalytic cycle, a topic of extensive mechanistic studies in a number of research

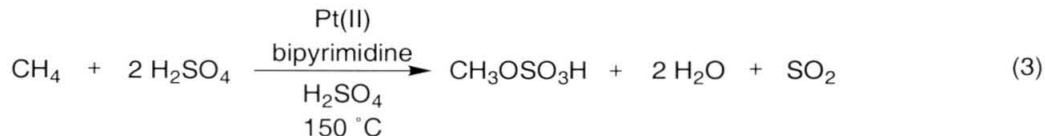


groups, consists of three steps and is shown in eq. 2.² Alkane activation results in the formation of a platinum(II) alkyl complex, which is then oxidized by $[\text{PtCl}_6]^{2-}$. The resulting platinum(IV) alkyl then undergoes an $\text{S}_{\text{N}}2$ -type displacement to afford the alcohol (or alkyl chloride) and regenerate the active platinum(II) species. The oxidation is typically carried out in water or aqueous acetic acid at 100-120 °C. A wide range of hydrocarbons can be converted to the corresponding alcohols or alkyl chlorides. Remarkably, oxidation is most selective towards the strongest and most electron rich C–H bonds. One of the main drawbacks of the Shilov system is the use of stoichiometric platinum(IV). Fortunately, the oxidation step was shown to proceed by an electron transfer mechanism, thus potentially allowing the use of common, inexpensive oxidants instead of hexachloroplatinate.³



Several oxidants have been examined in place of platinum(IV). Chlorine gas,⁴ peroxydisulfate,⁵ hydrogen peroxide,⁶ and an electrochemical cell⁷ were tested with limited success (low turnovers and low turnover rates). Most of the strong oxidants used in the systems above are not selective with respect to alkylplatinum(II) intermediates and, instead, all platinum(II) is converted to platinum(IV). A successful oxidant should have a redox potential in a window between alkylplatinum(II) intermediates and the rest of platinum(II) salts present in the reaction solution. Unfortunately, due to the poor reversibility of Pt^{II}/Pt^{IV} potentials in most complexes of platinum, it is hard to estimate the gap in oxidation potentials.⁸

Periana and co-workers have recently reported a platinum(II)-catalyzed oxidation of alkanes with oleum (eq. 3).⁹



Dioxygen is undoubtedly the most attractive reagent for catalytic alkane oxidation. Shilov and co-workers reported that combinations of cupric or cuprous chloride, quinones or polyoxometallates with air can be used instead of platinum(IV) salts.¹⁰ In a recent publication, Sen and co-workers applied the Na₂PtCl₄/CuCl₂/O₂ system to the oxidation of a number of alkylsulfonic acids. However, these oxidations were carried out under harsh reaction conditions (160-200 °C). Mild, facile air-oxidations may point the way toward more efficient catalytic systems.

Here we report our studies of the oxidation of dimethylplatinum(II) complexes with dioxygen.¹¹ We have synthesized the proposed intermediate of

this reaction, a hydroperoxoplatinum(IV) complex, (tmeda)Pt(OOH)(OCH₃)(CH₃)₂ (**2**, tmeda = N,N,N',N'-tetramethylethylenediamine) and explored its reactivity.

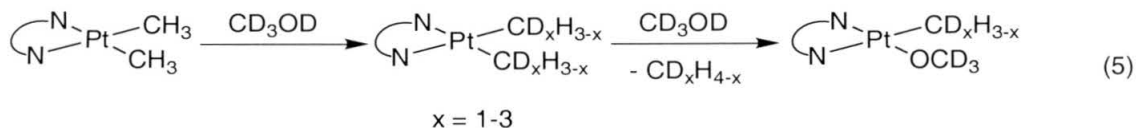
Results

In 1984, Puddephatt and Monaghan reported that several dimethylplatinum(II) complexes can be oxidized to dimethylplatinum(IV) compounds by alcohols (eq. 4).¹² The authors proposed an electron-transfer mechanism for this oxidation, not unlike that of the reaction between alkali metals and water. Based on our interest in the oxidation of platinum alkyls as well as the apparent contradiction with the proposed last step in the Shilov cycle—in which water reduces platinum(IV) to platinum(II)—we decided to reinvestigate the reported results.

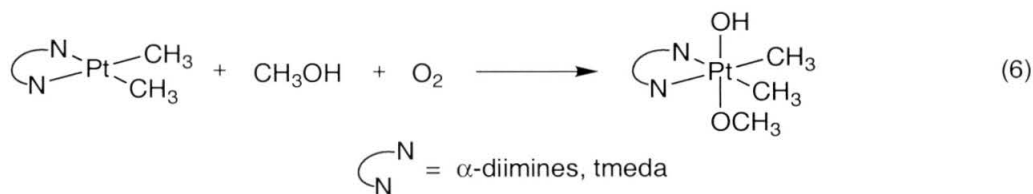


Under an argon atmosphere, oxidation of dimethylplatinum(II) complexes was not observed. Analysis of the solutions of (phen)Pt(CH₃)₂ (**3**, phen = 1,10-phenanthroline) and (tmeda)Pt(CH₃)₂ (**1**) in methanol-*d*₄ by ¹H NMR spectroscopy revealed that slow deuterium incorporation into Pt-CH₃ groups, followed by the formation of methane isotopomers (CH₃D, CH₂D₂, and CHD₃) and (N-N)Pt(OCH₃)(CH₃) were the major processes occurring in the solution (eq. 5). This reactivity is most likely due to the formation of dimethylhydridoplatinum(IV) intermediates formed by protonation of dimethylplatinum(II) complexes with methanol. It has been previously shown

that reductive elimination of methane from dimethylhydridoplatinum(IV) complexes competes with H/D exchange (see eq. 16 in Chapter 2).¹³



The formation of dimethylplatinum(IV) complexes occurs only in the presence of dioxygen. Oxidation of (tmeda)Pt(CH₃)₂, (phen)Pt(CH₃)₂ and (bipy)Pt(CH₃)₂ (bipy = 2,2'-bipyridine) results in the formation of hydroxo(methoxo)platinum(IV) complexes as evidenced by ¹H NMR spectroscopy (eq. 6). The spectra of platinum(IV) complexes are identical to those reported by Puddephatt and Monaghan for (N–N)Pt(OH)(OCH₃)(CH₃)₂ (N–N = phen, bipy).¹²



Oxidation of (tmeda)Pt(CH₃)₂. Exposure of the solution of (tmeda)Pt(CH₃)₂ in methanol to air led to the formation of several intermediates, observed by ¹H NMR and UV-Vis spectroscopies, which ultimately gave rise to a single product, (tmeda)Pt(OH)(OCH₃)(CH₃)₂ (**4**, eq. 6). The hydroxoplatinum(IV) complex was isolated and characterized by ¹H NMR spectroscopy, elemental analysis and X-ray crystallography (see below).

Two colored intermediates were observed during the course of oxidation. When exposed to air, the solution of (tmeda)Pt(CH₃)₂ in methanol turns pale

yellow ($\lambda_{\text{max}} = 480 \text{ nm}$). The yellow intermediate fades away as the solution develops a blue color ($\lambda_{\text{max}} = 640 \text{ nm}$). The blue color was most intense at low dioxygen pressures and high concentrations of $(\text{tmeda})\text{Pt}(\text{CH}_3)_2$. Addition of radical scavengers (2,6-di-*tert*-butyl-4-methylphenol or BHT, *p*-methoxyphenol) quenches the blue intermediate(s). If the radical scavenger was present in the reaction mixture before addition of dioxygen, the colored intermediates did not form at all. In both cases, the presence of radical scavengers did not influence the rate or the outcome of the oxidation.

The reaction of dioxygen with $(\text{tmeda})\text{PtMe}_2$ dissolved in aprotic solvents (THF, CH_2Cl_2 , toluene) also led to the formation of blue-colored solutions. Only a small fraction of $(\text{tmeda})\text{PtMe}_2$ (<10%) was converted to the colored intermediates, as observed by ^1H NMR spectroscopy. These solutions were EPR active (Figure 1) and displayed broad peaks in the ^1H NMR spectra.

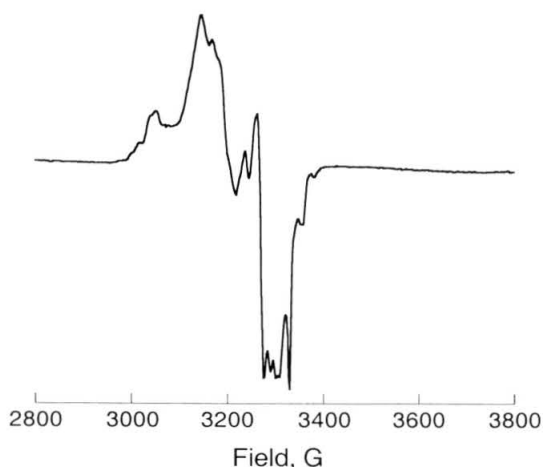


Figure 1. EPR spectrum of the frozen blue-colored benzene solution formed after $(\text{tmeda})\text{Pt}(\text{CH}_3)_2$ was exposed to 1 atm of O_2 .

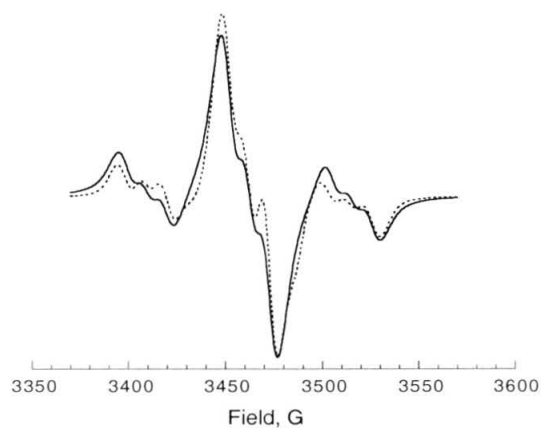
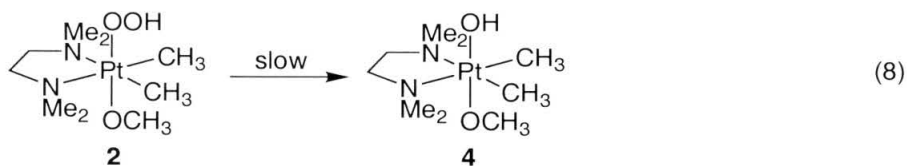
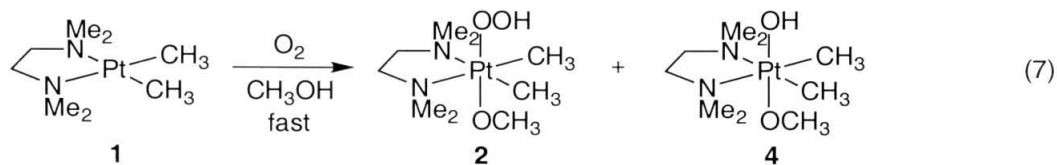


Figure 2. Room temperature EPR spectra of $[(\text{tmeda})\text{Pt}^{\text{III}}(\text{'N})(\text{CH}_3)_2]^+$ in CH_2Cl_2 . Solid line – acquired spectrum, dotted line – simulated spectrum ($A = 106 \text{ G}$ and 10 G).

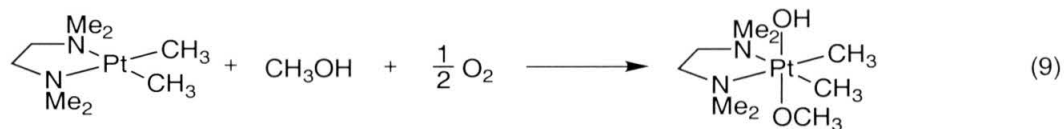
Although too complicated to analyze without any structural information, the EPR data tentatively suggest that the paramagnetic species most likely consists of several platinum atoms linked together to form a “stacked” mixed-valent oligomer. The formation of colored intermediates can be prevented by addition of radical scavengers (BHT, *p*-methoxyphenol). Quenching of blue solutions with methanol gives an intractable mixture of platinum(IV)-containing products.

Reaction of nitrosobenzene with (tmeda)Pt(CH₃)₂ resulted in the formation of a red paramagnetic solution. EPR spectra were acquired in CH₂Cl₂, benzene or THF. A representative room temperature spectrum is shown in Figure 2. It displays a typical 1:4:1 pattern ($A = 106$ G)¹⁴ of a mononuclear platinum-based radical with $g_e = 2.014700$. The electron is also coupled to one nitrogen nucleus ($S=1$) with $A = 10$ G.



At high dioxygen pressures (0.6-1 atm) in methanol, (tmeda)Pt(CH₃)₂ cleanly reacts to form a mixture of (tmeda)Pt(OH)(OCH₃)(CH₃)₂ (4) and (tmeda)Pt(OOH)(OCH₃)(CH₃)₂ (2, eq. 7). The oxidation is complete within minutes at room temperature. Conversion of (tmeda)Pt(OOH)(OCH₃)(CH₃)₂ to (tmeda)Pt(OH)(OCH₃)(CH₃)₂ occurs more slowly, over hours or days (eq. 8). Eventually, all (tmeda)Pt(CH₃)₂ is converted to (tmeda)Pt(OH)(OCH₃)(CH₃)₂.

The dioxygen uptake under conditions of high (tmeda)Pt(CH₃)₂ and low O₂ concentrations was measured using a Toepler pump. One equivalent of dioxygen is consumed per two equivalents of (tmeda)Pt(CH₃)₂ (eq. 9).



The relative ratios of **2** to **4** (measured by ¹H NMR spectroscopy shortly after all (tmeda)Pt(CH₃)₂ is consumed) are strongly dependent on the concentration of both (tmeda)Pt(CH₃)₂ and O₂. A high concentration of O₂ (4-8.1 mM) and a low concentration of (tmeda)Pt(CH₃)₂ (0.05 mM) favor the formation of **2**, while more **4** is formed at low O₂ concentration (0.7-4 mM) and high concentrations of (tmeda)Pt(CH₃)₂ (50-190 mM) as shown in Figure 3.

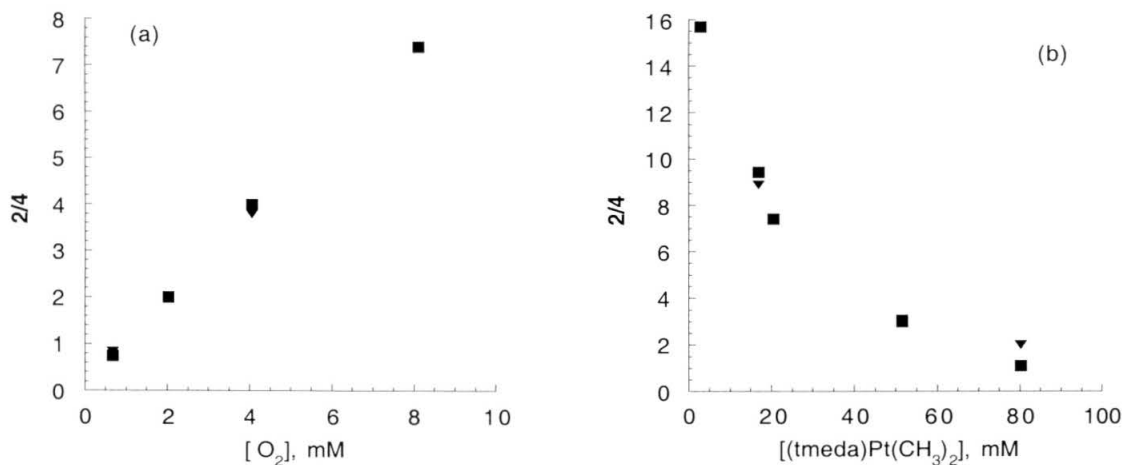
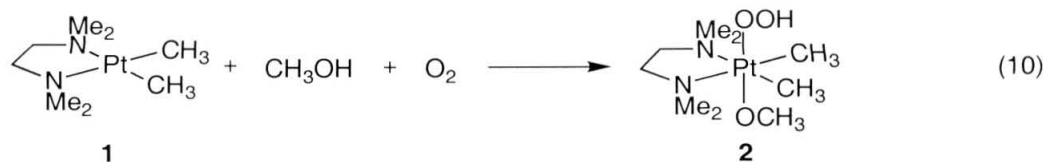


Figure 3. Ratios of **2** to **4** (■) at various concentrations of (tmeda)Pt(CH₃)₂ and O₂. (a) [(tmeda)Pt(CH₃)₂] = 21 mM, rt. (b) [O₂] = 8.1 mM, rt. Theoretical values (▼) were calculated for a consecutive mechanism with $k_1/k_2 = 18$ using the point from plot (a) with highest [O₂] as a reference (see Discussion).

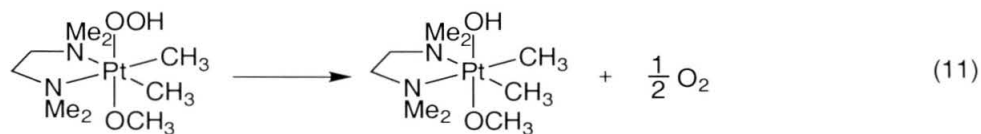
Even at higher pressures of dioxygen, the outcome of the reaction between (tmeda)Pt(CH₃)₂ and dioxygen depends on the concentration of the protic solvents. At low methanol concentration, the blue color of the reaction solution is more pronounced. In acetonitrile/methanol solvent mixture (1:1), both methoxy complex **4** and cationic [(tmeda)Pt(OH)(NCCH₃)(CH₃)₂]⁺ are formed.

Isolation and Reactivity of (tmeda)Pt(OOH)(OCH₃)(CH₃)₂. The observed dependence of the hydroperoxy/hydroxy ratio (**2/4**) on O₂ and (tmeda)Pt(CH₃)₂ concentrations can be used to prepare pure samples of (tmeda)Pt(OOH)(OCH₃)(CH₃)₂. Stirring a dilute solution of (tmeda)Pt(CH₃)₂ in methanol (*ca.* 5 mM) under 1 atm of dioxygen resulted in clean formation of (tmeda)Pt(OOH)(OCH₃)(CH₃)₂ (**2**, eq. 10). The hydroperoxy complex was isolated and characterized by elemental analysis, ¹H and ¹⁹⁵Pt NMR spectroscopy, and X-ray crystallography (see below). The ¹H and ¹⁹⁵Pt NMR data for **2** and **4** are very similar, except for the hydroxperoxy and hydroxy protons. The latter resonates at δ 6.48 ppm while the former shifts to δ -2.5 ppm. This upfield shift probably occurs because the hydroxy proton is closer to the metal than the hydroxperoxy proton and its chemical shift is thus more influenced by the temperature-independent paramagnetism of the transition metal center. The hydroperoxy complex **2** is not stable in the solid state for long periods of time and decomposes to an unidentified mixture of platinum(IV)-containing compounds.



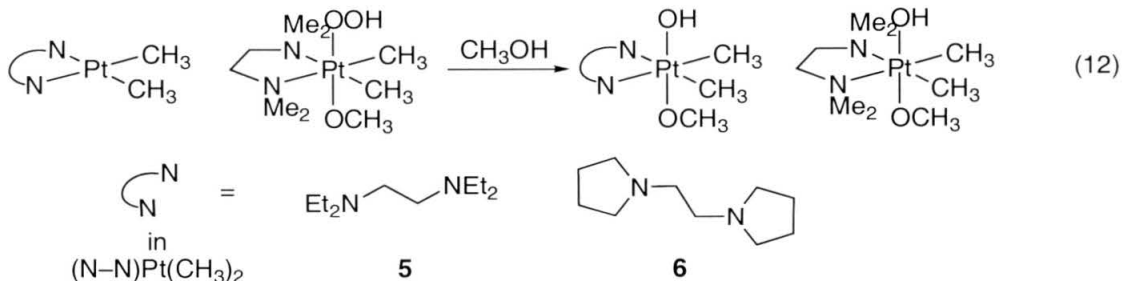
Formation of (tmeda)Pt(OOH)(OCH₃)(CH₃)₂ is irreversible. We prepared ¹⁸O-containing **2** by treating (tmeda)Pt(CH₃)₂ with isotopically enriched dioxygen. A degassed solution of ¹⁸O-enriched **2** in methanol was stirred under air for 30 min at room temperature. Mass-spectroscopic analysis of a sample of gas from the reaction headspace revealed that ¹⁸O was present only at the natural abundance level.

A solution of (tmeda)Pt(OOH)(OCH₃)(CH₃)₂ in methanol slowly disproportionates to (tmeda)Pt(OH)(OCH₃)(CH₃)₂ and O₂ over several days at room temperature (eq. 11). One-half equivalent of dioxygen is formed in this reaction as measured by Toepler pump; the identity of the gas was confirmed by mass spectroscopy. Irreproducible rates and fluctuations in the reaction order were found when the disproportionation reaction was monitored by ¹H NMR spectroscopy at 50–60 °C.



Several dimethylplatinum(II) complexes can be oxidized by the hydroperoxy complex **2**. The reaction between (tmeda)Pt(CH₃)₂ and **2** in methanol cleanly affords two equivalents of (tmeda)Pt(OH)(OCH₃)(CH₃)₂ (eq. 12). The rate of oxidation is too fast to measure by ¹H NMR spectroscopy even at –80 °C (*t*_{1/2} is

about 300 s). Increased steric bulk around platinum(II) slows this reaction, so that the oxidation of (teeda)Pt(CH₃)₂ (**5**) with (tmeda)Pt(OOH)(OCH₃)(CH₃)₂ can



be monitored by ¹H NMR spectroscopy around 0 °C (eq. **12**, N-N = teeda). The reaction is first order in both platinum reagents with $k_2(-9\text{ °C}) = 7.6 \cdot 10^{-3} \text{ (M s)}^{-1}$ (Figure 4a). The temperature dependence of the rate constant was also studied and the activation parameters were calculated from the Eyring plot, $\Delta H^\ddagger = 13.6 \text{ kcal mol}^{-1}$, $\Delta S^\ddagger = -16.5 \text{ kcal mol}^{-1} \text{ K}^{-1}$ (Figure 4b). 1,2-Dipyrrolidinoethane (dpe) is not as bulky as *N,N,N',N'*-tetraethylethylenediamine and, as expected, oxidation of (dpe)Pt(CH₃)₂ (**6**) by (tmeda)Pt(OOH)(OCH₃)(CH₃)₂ occurs at a faster rate compared to (teeda)Pt(CH₃)₂: $k_{\text{obs}}(\times 10^{-4} \text{ s}^{-1}, 0\text{ °C}) = 16.7 \pm 0.3$ vs. 9.3 ± 0.3 at **[2]** = 41mM, respectively.

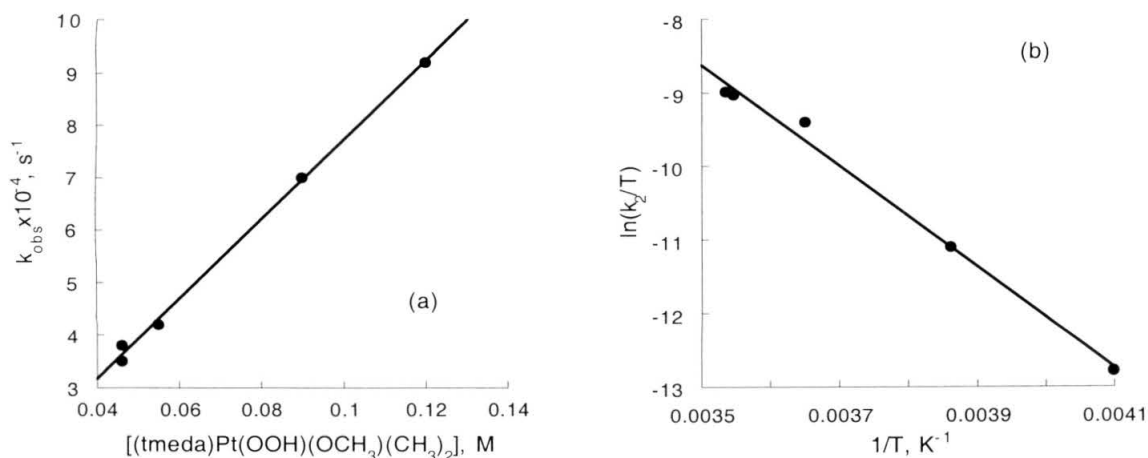
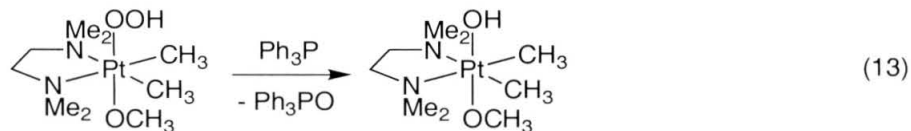


Figure 4. Oxidation of $(\text{tmeda})\text{Pt}(\text{CH}_3)_2$ with $(\text{tmeda})\text{Pt}(\text{OOH})(\text{OCH}_3)(\text{CH}_3)_2$. (a) Rate of oxidation vs. concentration of $(\text{tmeda})\text{Pt}(\text{OOH})(\text{OCH}_3)(\text{CH}_3)_2$, in CD_3OD , $T = -9^\circ\text{C}$. (b) Eyring plot, $\Delta T = -30$ to $+10^\circ\text{C}$, $[(\text{tmeda})\text{Pt}(\text{OOH})(\text{OCH}_3)(\text{CH}_3)_2] = 41 \text{ mM}$.

Dimethylplatinum(II) complexes of α -diimines are also oxidized by **2**, but these oxidations are not as straightforward as the ones described above. With one equivalent each of $(\text{N-N})\text{Pt}(\text{CH}_3)_2$ and $(\text{tmeda})\text{Pt}(\text{OOH})(\text{OCH}_3)(\text{CH}_3)_2$, $\text{N-N} = \text{phen}$ (**3**) or CyDA B^{H} (**7**, eq. 14), equimolar amounts of $(\text{N-N})\text{Pt}(\text{OH})(\text{OCH}_3)(\text{CH}_3)_2$ and **4** are formed. However, if more than one equivalent of $(\text{tmeda})\text{Pt}(\text{OOH})(\text{OCH}_3)(\text{CH}_3)_2$ is used in the oxidation, all of **2** is converted to $(\text{tmeda})\text{Pt}(\text{OH})(\text{OCH}_3)(\text{CH}_3)_2$ (**4**) even though only a stoichiometric amount of $(\text{N-N})\text{Pt}(\text{OH})(\text{OCH}_3)(\text{CH}_3)_2$ is formed.



The reactivity of $(\text{tmeda})\text{Pt}(\text{OOH})(\text{OCH}_3)(\text{CH}_3)_2$ is of limited scope. Besides the oxidation of dimethylplatinum(II) complexes mentioned above, it is capable of converting triphenylphosphine to triphenylphosphine oxide (eq. 13). It does

not react with Me_2S , Me_2SO , cyclohexene or styrene. Addition of strong acids does not enhance the oxidizing ability of the hydroperoxy complex.

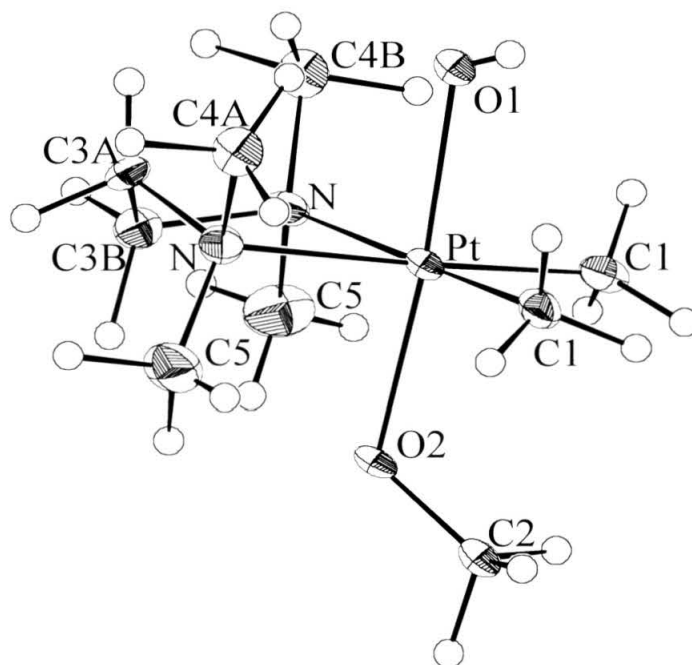


Figure 5. Labeled Diamond view of **4**, with 50% ellipsoids. Hydrogen atoms other than the hydroxy proton are omitted for clarity.

X-ray Structure Determination of $(\text{tmeda})\text{Pt}(\text{OH})(\text{OCH}_3)(\text{CH}_3)_2$. The molecule lies on a mirror plane, which contains the heavy atoms Pt, O1, O2, C2 and bisects the tmeda ligand (Figure 5). The tmeda backbone carbon C3 and one of the methyl groups, C4, are disordered over two sites with occupancies 1/2, since C3A is bonded to the mirror image of C3B. Bond lengths and angles around platinum are within the limits expected for Pt–O, Pt–N and Pt–C bonds. Selected bond lengths and angles are shown in Table 1. There is an intermolecular

hydrogen bond between O1 and O2 (at $x, y, z-1$) of 2.946(9)Å (the O1-H1A-O2 angle is 172(18)°), which forms a linear chain along the O2–Pt–O1 axis (c axis).

Table 1. Selected bond lengths (in Å) and angles (in °) for **4**.

Pt-O1	1.995(7)	O1-Pt-C1	90.8(3)
Pt-C1	2.007(8)	C1 ⁱ -Pt-C1	89.6(5)
Pt-O2	2.028(6)	O1-Pt-O2	174.9(3)
Pt-N	2.229(6)	C1-Pt-O2	92.8(3)
O1-H0A	0.55(12)	O1-Pt-N	87.6(2)
O2-C2	1.362(13)	C1 ⁱ -Pt-N	176.1(3)
C4A-C4B	0.60(3)	C1-Pt-N	93.9(3)
C3A-C3B	0.74(2)	O2-Pt-N	88.6(2)
		N-Pt-N ⁱ	82.5(3)
		Pt-O1-H0A	113(10)
		C2-O2-Pt	119.5(6)

Symmetry transformations used to generate equivalent atoms: (i) $x, -y + 3/2, z$

X-ray Structure Determination of (tmeda)Pt(OOH)(OCH₃)(CH₃)₂ (Figure 6). This structure is both twinned and disordered. The asymmetric unit consists of one molecule of (tmeda)Pt(CH₃)₂(OOH)(OCH₃), which is disordered ~1:1 over two orientations. All atoms except the platinum were split and modeled with two sites. The major difference between the two orientations is the position of the terminal hydroperoxy oxygen atom; it can lie under either of the two methyl groups. The rest of the molecule tilts to accommodate these two positions (see Appendix B). Orientation A has a slightly more reasonable structure than orientation B, which has a carbon atom (C1B of the tmeda backbone) with distorted geometry. This distortion is most likely due to additional disorder of the tmeda ligand, a failing to which this ligand is all too prone: see, for example, the structure of (tmeda)Pt(CH₃)₂(OH)(OCH₃) above.

The selected bond lengths and angles for both orientations are shown in Table 2. All dimensions around the central platinum atom are within the limits

expected for Pt^{IV}-O, Pt^{IV}-N and Pt^{IV}-C bonds. The O-O bond lengths (1.44(2) and 1.48(2) Å) are very close to the ones reported in the literature (1.481(5) Å in Tp*Pt(OOH)(CH₃)₂, 1.465(3) Å in **12** and 1.394(6) Å in (phen)Pt(OOi-Pr)(CH₃)₂Cl).

An analysis of intermolecular contacts suggests two potential hydrogen bonds, each between a donor hydroperoxy group and an acceptor methoxy group. One bond is between two molecules of orientation A translated one unit along the *a*-axis; the other between two molecules of orientation B similarly related. However, the intermolecular distances also reveal some impossibly short contacts, such as 2.08 Å between O2A (*x,y,z*) and C5A (*x*+1,*y,z*). Therefore, two molecules of orientation A cannot be adjacent along the *a*-axis and thus molecules of orientation A must comprise no more than 50% of the total molecules in the crystal. The population parameter for orientation A refined to 0.508(9), or essentially 1:1. Thus, orientations A and B must alternate along the *a*-axis. This alternation must be occasionally broken since no evidence of a larger cell is seen. There are no appreciable intermolecular platinum – hydroperoxy or hydroperoxy – hydroperoxy interactions. As shown in the hydrogen bond table (Appendix B), there is a good hydrogen bond between the hydroperoxy group of one orientation and the methoxy oxygen of the other orientation. These close intermolecular contacts that would explain the low stability of **2** in the solid.

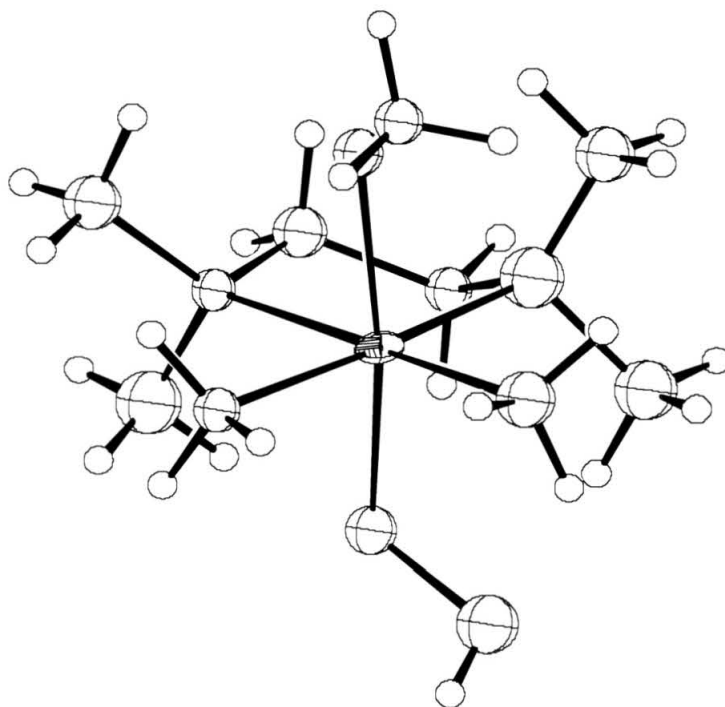


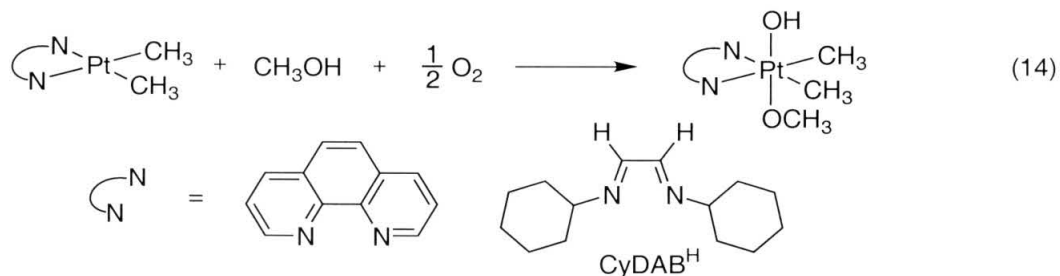
Figure 6. Labeled Diamond view of **2**, with 50% ellipsoids.

Table 2. Selected bond lengths (in Å) and angles (in °) for **2**.

Pt-O1A	2.006(16)	Pt-O1B	2.015(16)
Pt-O3A	2.051(13)	Pt-O3B	2.033(13)
Pt-C8A	2.069(18)	Pt-C8B	2.04(2)
Pt-C9A	2.01(2)	Pt-C9B	2.05(2)
Pt-N1A	2.276(16)	Pt-N1B	2.200(16)
Pt-N2A	2.17(2)	Pt-N2B	2.281(16)
O1A-O2A	1.48(2)	O1B-O2B	1.44(2)
O3A-C7A	1.40(2)	O3B-C7B	1.39(3)
O1A-Pt-O3A	170.5(6)	O1B-Pt-O3B	170.8(5)
C8A-Pt-N2A	174.1(7)	C9B-Pt-N1B	173.9(7)
C9A-Pt-N1A	179.2(8)	C8B-Pt-N2B	177.0(8)
O2A-O1A-Pt	112.7(10)	O2B-O1B-Pt	116.0(11)
C7A-O3A-Pt	120.0(12)	C7B-O3B-Pt	121.9(15)

Oxidation of (α -diimine)Pt(CH₃)₂. Several (α -diimines)platinum(II) dimethyl complexes were prepared, and their reactions with dioxygen were studied by ¹H NMR and UV-Vis spectroscopies (eq. 14). The red-orange solution of

(phen)Pt(CH₃)₂ in methanol-*d*₄ slowly fades to pale yellow under dioxygen to form (phen)Pt(OH)(OCH₃)(CH₃)₂ (**8**). At least one dimethylplatinum(IV) intermediate was observed in the reaction mixture. Unlike (tmeda)Pt(CH₃)₂, (phen)Pt(CH₃)₂ is stable in inert solvents (THF, C₆H₆, toluene) under a dioxygen atmosphere. Dioxygen also reacts with (CyDAB^H)Pt(CH₃)₂ in methanol to give (CyDAB^H)Pt(OH)(OCH₃)(CH₃)₂ (**9**). Although several intermediates were observed during the course of the oxidation by ¹H NMR spectroscopy, all of them eventually converted to the final product. It should be noted that oxidation of (phen)Pt(CH₃)₂ or (CyDAB^H)Pt(CH₃)₂ with (tmeda)Pt(OOH)(OCH₃)(CH₃)₂ is faster than their reaction with dioxygen to give the hydroxomethoxoplatinum(IV) products.



Oxidation of both (phen)Pt(CH₃)₂ and (CyDAB^H)Pt(CH₃)₂ was monitored by UV-Vis spectroscopy (at 412 and 364 nm, respectively). The reaction was first-order in both platinum(II) and dioxygen [Figure 7, the non-zero intercept of the (phen)Pt(CH₃)₂ line is due to the parallel conversion to (phen)Pt(CH₃)(OCH₃)]. The second-order rate constants are 0.11 and 0.08 (M s)⁻¹ for (phen)Pt(CH₃)₂ and (CyDAB^H)Pt(CH₃)₂, respectively. Addition of radical scavengers (BHT) or exclusion of light did not change the observed rate of oxidation. The rate of oxidation did not change in 1.0 M LiClO₄ solution in methanol. Deviations from

the first-order behavior were detected at low dioxygen pressures: the absorbance-time graphs had a distinct S-shape (Figure 8). This behavior may result from any of the following causes: autocatalysis, slow approach to the equilibrium distribution of dioxygen between gas and liquid phases, or a complicated reaction mechanism. Additional experiments, including the addition of an aliquot of the starting material to the reaction mixture after the first half-life and the use of solvents presaturated with dioxygen, ruled out autocatalysis and gas solubility problems, respectively. Based on the results of ^1H NMR studies, it seems likely that non-first-order behavior at low O_2 pressure is due to a complicated reaction mechanism (see Discussion).

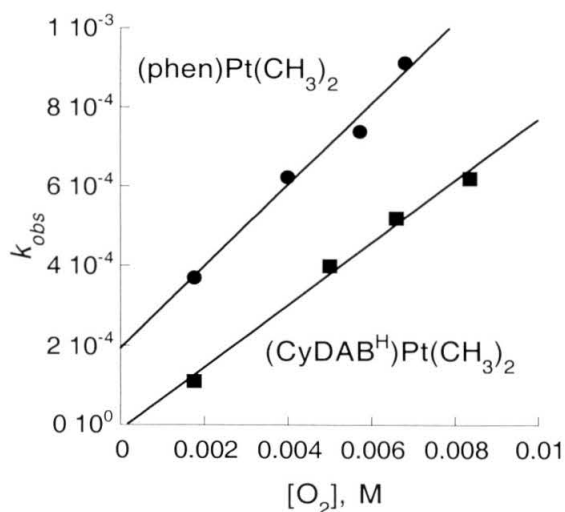


Figure 7. First-order dependence of the observed rate of oxidation of (phen)Pt(CH₃)₂ (●) and (CyDAB^H)Pt(CH₃)₂ (■) on [O₂]. T = 23 °C.

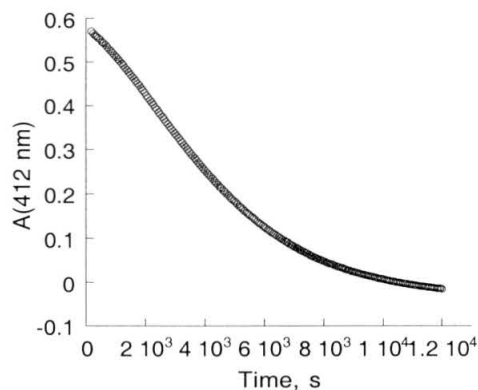
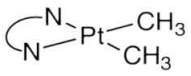
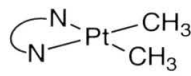
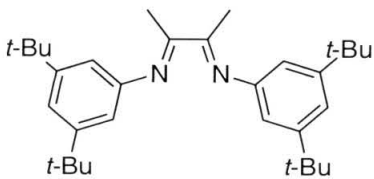
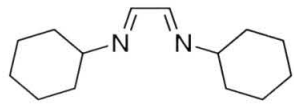
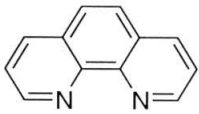
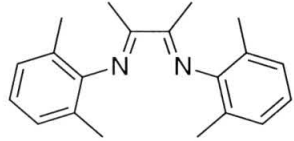
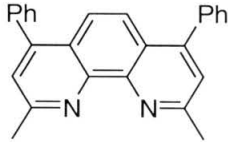
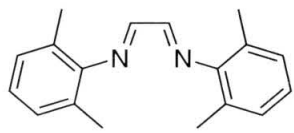
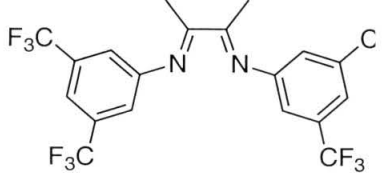
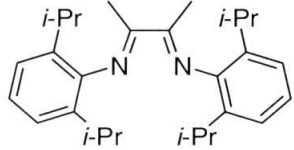


Figure 8. Kinetic trace of the oxidation of (phen)Pt(CH₃)₂ with O₂. [O₂] = 1.6 mM, λ = 412 nm, T = 23 °C.

Oxidation of a number of (α-diimine)Pt(CH₃)₂ complexes was monitored by UV-Vis spectroscopy to assess the influence of steric and electronic factors on the

observed rate of oxidation (Table 3). The electronic character of the ligands is reflected by the stretching frequency of the corresponding carbonyl cation, where a lower frequency indicates stronger Lewis basicity. The observed rate constants span only a small range of values from $2.7 \cdot 10^{-4}$ to $14.5 \cdot 10^{-4} \text{ s}^{-1}$. It is evident that the oxidation reaction may be slowed greatly or suppressed by bulky ligands.

Table 3. Relative rates of oxidation for $(\alpha\text{-diimine})\text{Pt}(\text{CH}_3)_2$. $k_{\text{obs}}((\text{CyDAB}^{\text{H}})\text{Pt}(\text{CH}_3)_2) = 2.7 \cdot 10^{-4} \text{ s}^{-1}$ at $[\text{O}_2] = 7 \text{ mM}$, 1:25 $\text{CH}_3\text{CN}/\text{CH}_3\text{OH}$, $T = 23^\circ \text{C}$. Carbonyl stretching frequencies ν_{CO} are for $[(\alpha\text{-diimine})\text{Pt}(\text{CH}_3)(\text{CO})]\text{BF}_4$ complexes, cm^{-1} .

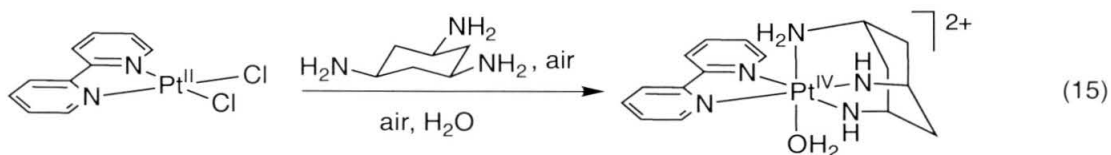
	Relative rates (ν_{CO})		Relative rates (ν_{CO})
	6 (2104.6)		1 (2104.7)
	4 (2108.4)		v. slow (2109.6)
	2		NR (2114.9)
	1.4 (2113.5)		NR (2108.7)

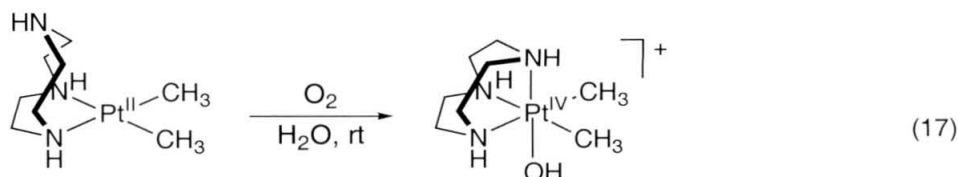
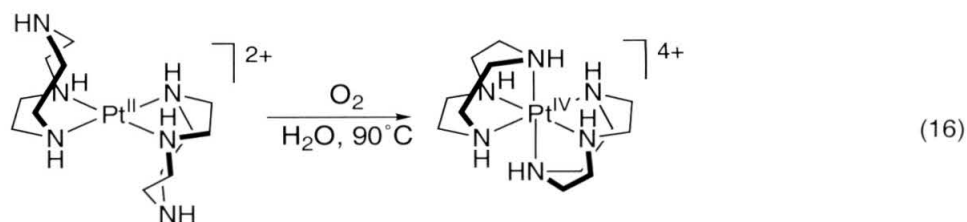
Oxidation of Various Platinum(II) Complexes. The ability of a platinum(II) complex $(\text{N-N})\text{PtX}_2$ to react with dioxygen depends not only on the nature of the

chelating ligand but also on the character of the X-type substituent. Whereas both (tmeda)Pt(CH₃)₂ and (CyDAB^H)Pt(CH₃)₂ are oxidized by dioxygen, their diphenyl analogs, (tmeda)PtPh₂ and (CyDAB^H)PtPh₂, are stable under the analogous reaction conditions. No oxidation occurs with (tmeda)Pt(CH₃)Cl and (tmeda)PtCl₂. On the other hand, (tmeda)Pt(CH₃)Ph is converted to (tmeda)Pt(OH)(OCH₃)(CH₃)Ph in methanol under dioxygen. Similarly, only (CyDAB^H)Pt(CH₃)Ph was consumed when a mixture of (CyDAB^H)Pt(CH₃)Ph and (CyDAB^H)PtPh₂ was exposed to dioxygen.

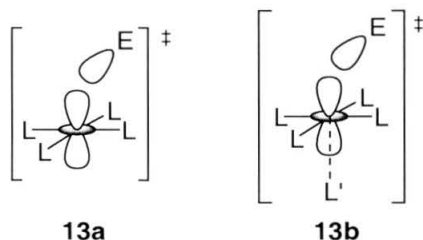
Discussion

Oxidation of Platinum(II) Complexes with Dioxygen. There are only a few examples of the oxidation of platinum(II) complexes with dioxygen. In 1977, Sarneski and co-workers reported that [(bipy)Pt(κ²-tach)]²⁺, generated *in situ*, was converted to [(bipy)Pt(κ³-tach)(OH₂)]²⁺ in water under air (eq. 15).¹⁵ Six years later, Wieghardt and co-workers described the aerobic oxidation of [(κ²-tacn)₂Pt]²⁺ to [(κ³-tacn)₂Pt]⁴⁺ in water at 90 °C (eq. 16).¹⁶ Most recently, Puddephatt and co-workers found that (κ²-tacn)Pt(CH₃)₂ is oxidized to [(κ³-tacn)Pt(CH₃)₂(OH)]⁺ with dioxygen (eq. 17).¹⁷ It is noteworthy that in all cases a κ²-bound tridentate ligand is coordinated to platinum(II).





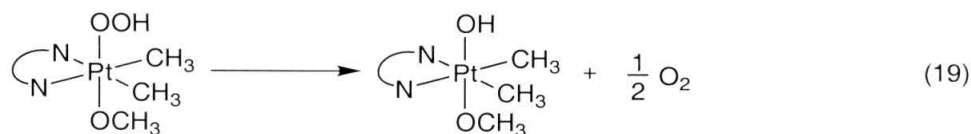
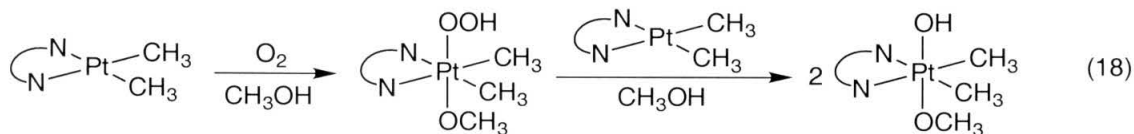
Proposed mechanism. The oxidation of platinum(II) complexes has been extensively studied.^{18,19} Halogens,^{20,21} peroxides,^{22,23} platinum(IV) complexes^{24,25} and a number of other oxidizing agents²⁶ can be used in this reaction. The generally accepted mechanism involves an axial electrophilic attack of the oxidizing agent on the square-planar platinum(II) complex (see **13a**). In some cases, ligand pre-coordination prior to the oxidation step was found (**13b**).¹⁹ The majority of such reactions can formally be viewed as a two-electron redox processes. However, dioxygen is reduced by four electrons in the reaction with (tmeda)Pt(CH₃)₂. How does this happen?



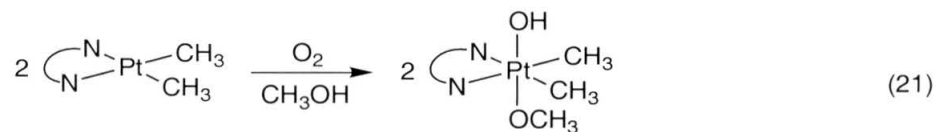
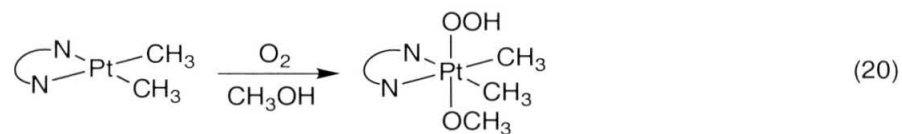
Formation of paramagnetic blue-colored intermediates²⁷ during the course of the reaction, which initially led us to propose a radical-based mechanism for the

oxidation, can be inhibited by addition of radical scavengers. Since the outcome of the oxidation—i.e., formation of a mixture of (tmeda)Pt(OOH)(OCH₃)(CH₃)₂ and (tmeda)Pt(OH)(OCH₃)(CH₃)₂—is not influenced by the presence of radical scavengers, we believe that single-electron transfer pathways are minor side reactions.

We propose that the reduction of dioxygen occurs in two consecutive steps (eqs. 18 and 19). In the first step, (N–N)Pt(CH₃)₂ reacts with dioxygen to give (N–N)Pt(OOH)(OCH₃)(CH₃)₂, which was isolated from reaction mixtures and characterized (eq. 18). In the second step, the hydroperoxo complex oxidizes the second equivalent of (N–N)PtMe₂ to form two equivalents of (N–N)Pt(OH)(OCH₃)(CH₃)₂ (eq. 18). Disproportionation of (N–N)Pt(OOH)(OCH₃)(CH₃)₂ to (N–N)Pt(OH)(OCH₃)(CH₃)₂ and O₂ occurs at a slower rate (eq. 19). Therefore, the overall stoichiometry of the reaction for the formation of the hydroxy complex is two equivalents of platinum(II) per one equivalent of dioxygen. The predicted stoichiometry was confirmed experimentally. An analogous mechanism was proposed by Davies and Hambley²² as well as by Puddephatt and co-workers.¹⁷



According to the proposed mechanism, the ratio of the platinum(IV) products (hydroperoxy/hydroxy) should depend on the concentrations of (tmeda)Pt(CH₃)₂ and dioxygen. At high concentrations of O₂, all (tmeda)Pt(CH₃)₂ is converted to (tmeda)Pt(OOH)(OCH₃)(CH₃)₂, whereas at higher concentrations of platinum or lower concentrations of O₂, a higher proportion of (tmeda)Pt(OOH)(OCH₃)(CH₃)₂ is converted to (tmeda)Pt(OH)(OCH₃)(CH₃)₂ by reaction with (tmeda)Pt(CH₃)₂. Therefore, the **2/4** ratio should decrease as the concentration of O₂ is decreased or the concentration of (tmeda)Pt(CH₃)₂ is increased. As can be seen from Figure 3, these trends are observed experimentally. The product ratios can also be predicted by kinetic simulation using one of the data points as a reference. The calculated values are in good agreement with the experimental values as shown on Figure 3. The dependence of the **2/4** ratio on [O₂] also rules out an alternative mechanism in which (tmeda)Pt(OOH)(OCH₃)(CH₃)₂ and (tmeda)Pt(OH)(OCH₃)(CH₃)₂ are formed in parallel reactions (eqs. 20 and 21). According to such a kinetic scheme, the ratio of platinum(IV) products should be independent of dioxygen concentration.



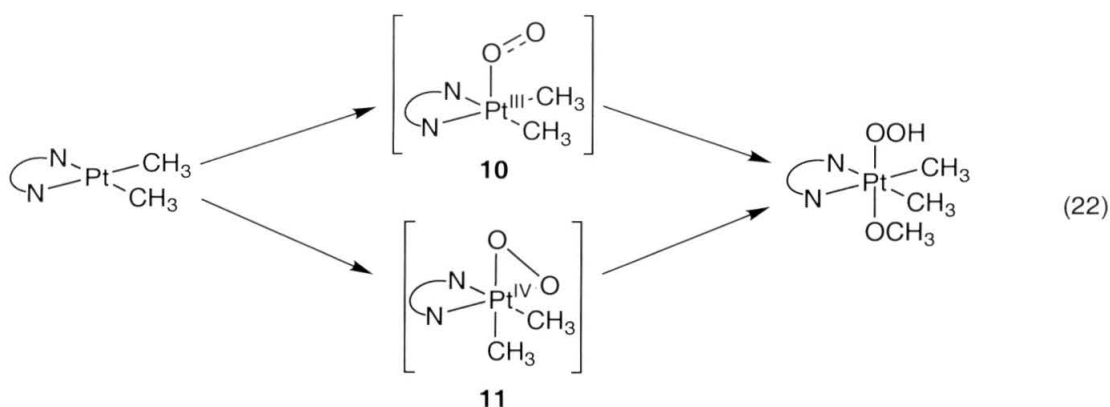
Oxidation of α -diimine complexes of platinum(II) is slower than that of diamine complexes. This difference in rates can be correlated with the expected electron-density at the metal center. α -Diimines, weaker σ -donors and better π -

acceptors than diamines, should give less electron-rich platinum complexes (in $[(N-N)Pt(CH_3)(CO)]BF_4$, $\nu_{CO} = 2102.0\text{ cm}^{-1}$ for $N-N = tmeda$ and 2108.4 cm^{-1} for $N-N = phen$; see also Table 3).

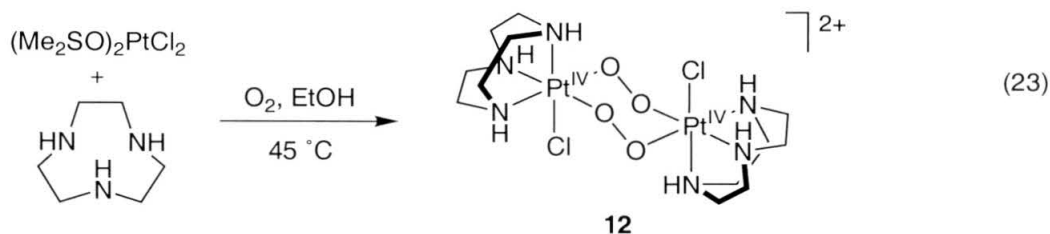
A more pronounced difference in reactivity occurs between dimethylplatinum(II) and methylchloroplatinum(II) complexes. Whereas $(tmeda)Pt(CH_3)_2$ or $(phen)Pt(CH_3)_2$ are oxidized by dioxygen in methanol at room temperature, $(tmeda)Pt(CH_3)Cl$ and $(phen)Pt(CH_3)Cl$ do not react with dioxygen under analogous reaction conditions. It is also evident from Table 3 that steric bulk along the axial approaches to the metal center greatly influences the rate of oxidation and, in some cases, overrides the electronic effects. Thus, bulky α -diimines with substituents in the ortho positions of the aryl ring do not react with dioxygen. Increased steric bulk around the platinum center in diphenyl complexes $(CyDAB^H)PtPh_2$ and $(tmeda)PtPh_2$ might also be responsible for their stability toward dioxygen.

Formation of the Hydroperoxy Intermediate. At least two reaction pathways were identified in the reaction of dimethylplatinum(II) complexes with dioxygen. The radical pathway discussed above is a minor side-reaction. We believe that the majority of platinum(II) in solution reacts with dioxygen and forms the hydroperoxy complex. Dioxygen can approach platinum(II) either end-on, to form η^1 -complex **10**, or side-on, to form η^2 -complex **11** (eq. 22). Platinum(0) reacts with dioxygen to form η^2 -complexes.²⁸ Reaction of O_2 with Vaska's complex, which is isoelectronic with $(N-N)Pt(CH_3)_2$, results in the formation of an η^2 -adduct.²⁹ On the other hand, there are no examples of η^1 -dioxygen coordination to platinum(II). It should be noted that end-on coordination of

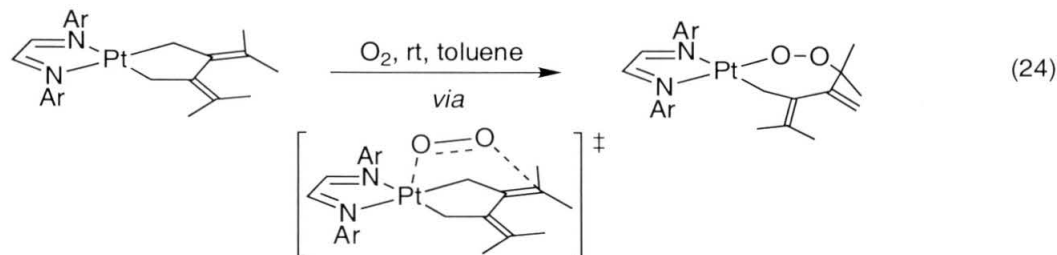
dioxygen to dimethylplatinum(II) complex might result in the formation of a platinum(III) superoxide complex. Unfortunately, the scarcity of experimental data does not allow us to distinguish between the two alternatives. In either case, protonation of the dioxygen intermediate is the step that affords the hydroperoxy complex (eq. 22). The protonation of η^2 -peroxo complexes of iridium(III) and platinum(II) to give binuclear μ_2, η^1 -peroxo complexes or hydrogen peroxide³⁰ has precedent in the literature.³¹ Additional studies will be needed to determine the mode of dioxygen activation.



Interestingly, Davies and Hambley have recently isolated the bis(μ^2 -peroxo) platinum(IV) dimer **12**, which is thought to form by dimerization of a platinum(IV) peroxo intermediate in aerobic oxidation of a κ^2 -tacn-containing platinum(II) complex (eq. 23).²²

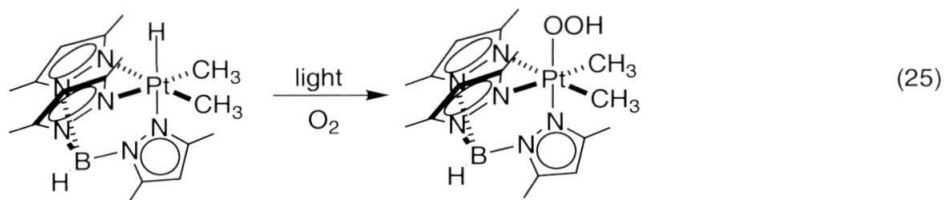


An interesting reaction of a platinum(II) complex with dioxygen was reported by tom Dieck and co-workers (eq. 24, Ar is 2,6-di-isopropylphenyl, 2,6-dimethylphenyl).³² 1,4-Addition of dioxygen to platinum allyl moiety resulted in the formation of an alkylperoxoplatinum(II) complex. The authors proposed that reaction occurs in a concerted manner through a 6-membered transition state. Note that this reaction was reported for α -diimines with bulky aryl groups. The analogous dimethyl complexes do not react with dioxygen (see Table 3). This apparent discrepancy can be reconciled. Equilibrium ligand pre-coordination prior to the oxidation step was found in a number of platinum(II) oxidation reactions.^{20,25,33} Thus, oxidation of the dimethylplatinum(II) complexes might require the presence of both dioxygen and methanol in the coordination sphere, thereby amplifying the steric influence of the ligand.



A recent result by Wick and Goldberg brings up another possible mechanism for the formation of (tmeda)Pt(OOH)(OCH₃)(CH₃)₂. The authors reported that Tp*Pt(CH₃)₂H reacts with dioxygen in benzene to afford Tp*Pt(CH₃)₂(OOH) by a radical mechanism (eq. 25).³⁴ It is well-established that, in protic solvents, dimethylplatinum(II) complexes are in equilibrium with alkylhydridoplatinum(IV) species.¹³ The insertion of O₂ into Pt^{IV}-H bond would afford the hydroperoxy complex. Although, in contrast to the Tp*Pt(CH₃)₂(OOH) case, formation of (tmeda)Pt(OOH)(OCH₃)(CH₃)₂ occurs by a non-radical

pathway, a change in mechanism due to differences in the nature of the complexes cannot be ruled out.



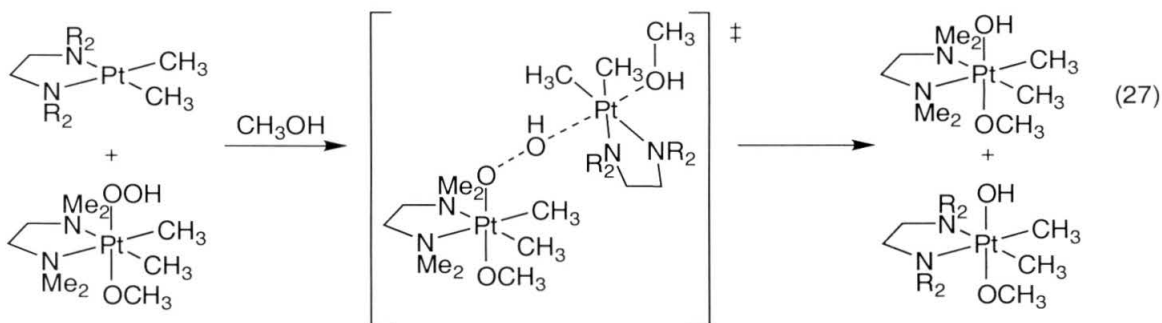
Reaction of (tmeda)Pt(CH₃)₂ with PhNO. The use of nitrosobenzene as a dioxygen model has allowed isolation and characterization of important reaction intermediates and provided valuable structural and mechanistic information about the reactions of transition metal complexes with dioxygen.³⁵ Despite the different electronic states of PhNO and O₂, the coordination preferences of nitrosobenzene in platinum complexes closely resemble those of dioxygen. In complexes with platinum(0), nitrosobenzene binds through the π -bond of the N=O moiety.³⁶ On the other hand, both the lone pair on the nitrogen atom and the N=O π -bond can be used in complexes of PhNO with platinum(II).³⁷

Reaction of (tmeda)Pt(CH₃)₂ with PhNO affords a red paramagnetic solution. The EPR spectrum is best interpreted as that of a mononuclear platinum(III) compound with one strongly bound nitrogen-based ligand.¹⁴ It is most likely that this ligand is either nitrosobenzene or its reduced derivative. This result implies that formation of blue-colored intermediates starts by one-electron oxidation of (tmeda)Pt(CH₃)₂. The resulting platinum(III) species then forms mixed-valent oligomers by associating with the remaining (tmeda)Pt(CH₃)₂.

Reactivity of $(tmeda)Pt(OOH)(OCH_3)(CH_3)_2$. The mechanism of oxidation of dimethylplatinum(II) complexes with $(tmeda)Pt(OOH)(OCH_3)(CH_3)_2$ resembles that of the reaction between alkyl- or hydrogen peroxides and triphenylphosphine, dimethylsulfide or other oxidizable nucleophiles.³⁸ The lone



pair of the nucleophile—in this case, a pair of electrons in the d_{z^2} orbital of platinum(II) complex—attacks the antibonding molecular orbital of the O-O bond (eq. 26). In the case of $(tmeda)Pt(OOH)(OCH_3)(CH_3)_2$, the attack most likely occurs at the β -oxygen of the hydroperoxy ligand (eq. 27). The increased steric bulk of $(teeda)Pt(CH_3)_2$ *vs.* $(tmeda)Pt(CH_3)_2$ destabilizes the transition state and slows down the rate of the reaction. Oxidation of triphenylphosphines probably occurs through an analogous transition state. The reaction of $(tmeda)Pt(OOH)(OCH_3)(CH_3)_2$ with $(N-N)Pt(CH_3)_2$ ($N-N$ = phen, CyDAB^H) is slower than with $(tmeda)Pt(CH_3)_2$, mainly because the platinum center is less electron-rich in complexes with α -diimines.



Disproportionation of $(tmeda)Pt(OOH)(OCH_3)(CH_3)_2$ to dioxygen and $(tmeda)Pt(OH)(OCH_3)(CH_3)_2$ is not unique – analogous chemistry was reported

for hydroperoxy complexes of platinum(IV), $\text{Tp}^*\text{Pt}(\text{CH}_3)_2(\text{OOH})$,³⁴ and cobalt(III), $[(\text{CN})_5\text{CoOOH}]^{3-}$.³⁹ Unlike the hydroperoxy complex studied here, disproportionation of the cobalt hydroperoxy complex is first order in $[(\text{CN})_5\text{CoOOH}]^{3-}$ at 35–50 °C with an activation barrier of 24 kcal mol⁻¹. Irregular kinetics was observed at higher temperatures. Taking into account the substitutional inertness of octahedral platinum(IV) complexes,⁴⁰ it seems likely that formation of O₂ is initiated by a homolytic cleavage of the O–O bond. A similar mode of activation has been proposed for the disproportionation of *t*-BuOOH to *t*-BuOH and O₂.⁴¹

It is noteworthy that if bidentate ligands are bound to platinum(II), only neutral platinum(II) complexes with such good σ -donors as methyl groups react with dioxygen, whereas with κ^2 -bound tridentate ligands even cationic platinum(II) complexes with weaker nitrogen-based σ -donors (amines, imines) are converted to platinum(IV) products with air (eqs. 15-17). This difference in reactivity is best understood in light of the proposal put forth by Wieghardt and co-workers.¹⁶ The authors invoked electron-electron repulsion between the lone pair on the free arm of the κ^2 -bound ligand and the d_{z^2} orbital of the square-planar platinum(II) complex (Figure 9, left side). This interaction raises the energy of HOMO of the platinum complex (σ -antibonding d_{z^2} -based orbital) and facilitates oxidation. This interaction is absent in platinum(II) complexes with bidentate ligands, so the HOMO is relatively low in energy and, therefore, the metal complex is resistant to oxidation. In dimethylplatinum(II) complexes, strong σ -bonds raise the energy of the HOMO, making it more susceptible to oxidation (Figure 9, right side).

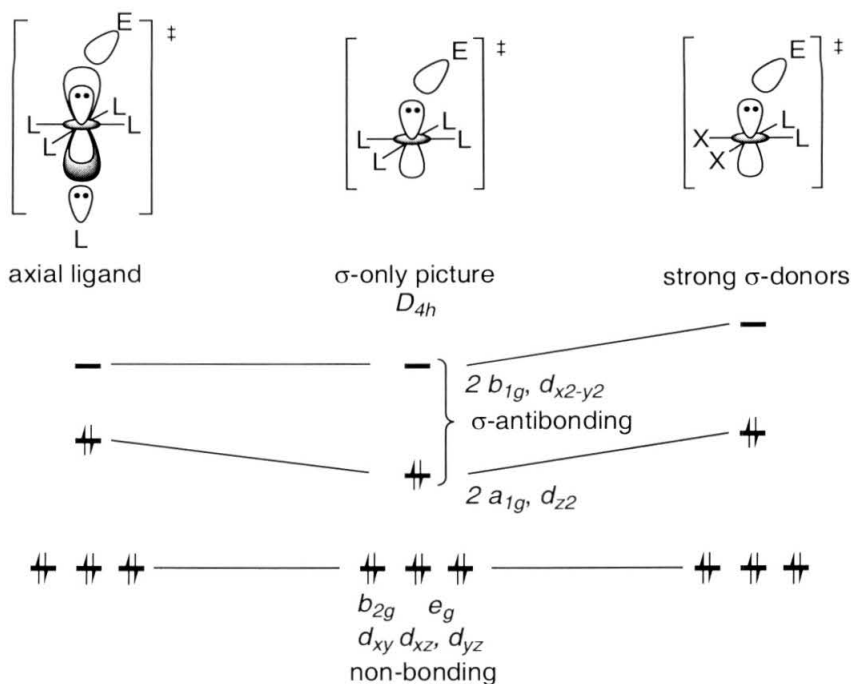


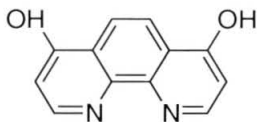
Figure 9. MO diagram of a square-planar platinum(II) complex. Effects of axial ligands and strong σ -donors on HOMO energy.

Conclusions

Of the three steps of the Shilov system, the oxidation step is solely responsible for the limitations of this catalytic reaction. Replacement of PtCl_6^{2-} by another oxidant would greatly increase the utility of the Shilov oxidation. Fortunately, the mechanism of the oxidation step allows the use of other oxidizing reagents. Dioxygen, perhaps the most desired oxidant, does react with platinum(II) complexes. The reaction works with sterically unencumbered and electron-rich dimethylplatinum(II) compounds. However, most complexes capable of C–H activation are cationic and not as electron rich as the dimethylplatinum(II) systems used here.

Several approaches can be used to enhance the reactivity of platinum(II) complexes toward dioxygen. From an MO theory point of view, the ability of a platinum complexes to react with O₂ is largely determined by the energy of the d_{z^2} -based HOMO: the higher it is, the easier it is to oxidize the platinum(II). Ligands with a “free” arm situated in the axial position of the platinum complex should raise the energy of HOMO. Alternatively, oxidation can be carried out in strong donor solvents or with excess of chloride or similar anions.

Another approach is based on the observation that neutral platinum(II) complexes are easier to oxidize than cationic ones. With ligands containing acidic functionalities positioned on the periphery (**13**), the overall cationic charge may be offset by deprotonation of these functionalities.



13

Experimental

General Considerations. All air and moisture sensitive compounds were manipulated using standard high-vacuum line, Schlenk or cannula techniques, or in a dry box under a nitrogen atmosphere, as described previously.⁴² *N,N,N',N'*-Tetramethylethylenediamine (tmeda) and 1,10-phenanthroline (phen) was purchased from Aldrich. (COD)Pt(CH₃)₂ was purchased from Strem Chemicals. Ultra-high purity oxygen was purchased from Liquid Air Products and used without further purification. Solvents were dried over sodium/benzophenone ketyl (Et₂O, THF, petroleum ether), 4Å molecular sieves (CH₃OH, CH₃NO₂), or CaH₂ (CH₂Cl₂). The following compounds were prepared according to literature procedures: (CH₃)₂Pt(μ₂-(CH₃)₂S)₂Pt(CH₃)₂,⁴³ ((CH₃)₂S)₂PtPh₂,⁴⁴ ((CH₃)₂S)₂Pt(CH₃)Cl,⁴³ (tmeda)Pt(CH₃)₂,⁴⁵ (phen)Pt(CH₃)₂,⁴⁵ 1,2-dipyrrolidinoethane (dpe),^{4 6} and *trans*-*N,N,N',N'*-tetramethyl-1,2-cyclohexanediamine (tmcdca).⁴⁶ Dimethylplatinum(II) complexes of α-diimines were prepared from (CH₃)₂Pt(μ₂-(CH₃)₂S)₂Pt(CH₃)₂ by the method published by Bercaw and co-workers.⁴⁷ α-Diimines were prepared as described earlier.⁴⁸ Abbreviations: teeda - *N,N,N',N'*-tetraethylethylenediamine; dptmeda – (1*S*, 2*S*)-1,2-diphenyl-*N,N,N',N'*-tetramethylethylenediamine. NMR spectra were acquired on Varian ^{UNITY}INOVA 500 (499.853 MHz for ¹H), Varian *MERCURY-VX* 300 (300.08 MHz for ¹H), General Electric QE300 (300 MHz for ¹H) and Bruker AM500 (500.13 MHz for ¹H) spectrometers. All ¹H NMR shifts are relative to the residual NMR solvent. ¹⁹⁵Pt NMR shifts were referenced with respect to a saturated aqueous solution of K₂PtCl₄. UV-vis Spectra were recorded on a HP8452A diode array spectrophotometer. EPR spectra were acquired on a

Bruker X-band EPR spectrometer. Elemental analyses were carried out either at the Caltech Elemental Analysis Facility by Mr. Fenton Harvey or by Midwest Microlab, Indianapolis, IN. Kinetic data were processed and fitted using KaleidaGraphTM software package (version 3.08d, Synergy Software).

(tmeda)Pt(C₆H₅)₂. (Me₂S)₂PtPh₂ was prepared as described by Puddephatt and co-workers.⁴⁴ To a slurry of (Me₂S)₂PtCl₂ (0.3 g, 0.77 mmol) in Et₂O (15 mL) cooled to 0 °C, a toluene/Et₂O solution of PhLi (1.05 mL, 1.8 M) was slowly added by syringe. The reaction mixture, initially yellow, was stirred at 0 °C until a beige suspension was obtained. Excess tmeda (0.2 mL, 1.3 mmol) was added via syringe and the reaction mixture was stirred for an additional 30 minutes at room temperature. The reaction mixture was quenched with a cold saturated aqueous solution of NH₄Cl (10 mL). The organic layer was separated and the aqueous layer was washed with Et₂O (2×20 mL). The combined organic portions were dried over MgSO₄, treated with 0.1 g of charcoal and filtered. Evaporation of Et₂O gave a white powder. Yield: 30 mg (9%). ¹H NMR (CD₂Cl₂/CD₃OD, δ): 2.46 (s, 12H, ³J_{PHH} = 22.2 Hz, NCH₃), 2.69 (s, 4H, ³J_{PHH} = 11.1 Hz, NCH₂CH₂N), 6.61 (m, 2H, *p*-H in Pt-C₆H₅), 6.75 (m, 4H, *m*-H in Pt-C₆H₅), 7.38 (m, 4H, ³J_{PHH} = 75.0 Hz, *o*-H in Pt-C₆H₅).

(tmeda)Pt(C₆H₅)(CH₃). Phenyllithium (0.25 mL, 1.8 M ether solution, 0.45 mmol) was added by syringe to a slurry of (Me₂S)₂Pt(CH₃)Cl (150 mg, 0.41 mmol) in 20 mL of dry Et₂O at -78 °C. The reaction mixture was stirred for 15 minutes, then warmed to 0 °C and stirred for additional 25 minutes. Tmeda (0.5 mL) was added via syringe, and the resulting suspension was kept at room temperature for another 15 minutes, then quenched with a cold saturated aqueous solution of

NH₄Cl (10 mL). The organic layer was separated and the aqueous layer was washed with Et₂O (2×20 mL). The combined organic portions were dried over MgSO₄, treated with charcoal (0.1 g) and filtered. Evaporation of Et₂O gave a white powder. Yield: 30 mg (18%). ¹H NMR (CDCl₃, δ): 0.45 (s, 3H, ²J_{PtH} = 88.5 Hz, PtCH₃), 2.54 (s, 6H, NCH₃), 2.72 (s, 6H, NCH₃), 6.83 (pseudo d, 1H, *p*-H in PtC₆H₅), 6.93 (pseudo dd, 2H, *m*-H in PtC₆H₅), 7.38 (d, 2H, ³J_{PtH} = 73 Hz, *o*-H in PtC₆H₅).

General Procedure for the synthesis of (N–N)Pt(CH₃)₂ (X–X). In a 50 mL Schlenk flask, Me₂Pt(μ₂-Me₂S)₂PtMe₂ (0.5–0.8 mmol) was dissolved in 10 mL of dry THF. The desired diamine (2 equivalents, 1.0–1.6 mmol) was added to the solution. The resulting mixture was stirred for 8 hours at room temperature. The solution was occasionally purged with argon to remove the liberated dimethylsulfide. Removal of volatiles under vacuum provided the desired compound. If necessary, the resulting complex was purified by recrystallization from THF/pentane or toluene/pentane mixtures.

(teeda)PtMe₂ (5). The general procedure afforded the title compound as a white solid. Yield 0.22 mg (55%) after recrystallization from THF. ¹H NMR (C₆D₆, δ): 0.97 (s, 6H, ²J_{PtH} = 88.0 Hz, Pt–CH₃), 1.08 (t, 12H, ³J_{HH} = 7 Hz, NCH₂CH₃), 1.96 (s, 4H, NCH₂CH₂N), 2.44 (dq, 4H, ²J_{HH} = 13 Hz, ³J_{HH} = 7 Hz, NCH₂CH₃), 2.68 (dq, 4H, ²J_{HH} = 13.5 Hz, ³J_{HH} = 7 Hz, N–CH₂–CH₃). Anal. Calcd. for C₁₂H₃₀N₂Pt: C 36.26%; H 7.61%; N 7.05%. Found: C 36.03%; H 7.48%; N 6.78%.

(dpe)PtMe₂ (6). The general procedure afforded the title compound as a white solid. The product was recrystallized from toluene/PE. ¹H NMR (CD₃CN,

δ): 0.07 (s, 6H, $^2J_{\text{PtH}} = 86.0$ Hz, PtCH₃), 1.78 (m, 8H, N(*c*-C₄H₈)), 2.62 (s, 4H, $^3J_{\text{PtH}} = 12.4$ Hz, NCH₂CH₂N), 2.86 (m, 4H, N(*c*-C₄H₈)), 3.21 (m, 4H, N(*c*-C₄H₈)).

(tmeda)Pt(OH)(OCH₃)(CH₃)₂ (4). A solution of (tmeda)Pt(CH₃)₂ (341 mg, 1 mmol) in methanol (10 mL) was stirred under air for 20 h, then concentrated *in vacuo*. The residual solid was taken up in CH₂Cl₂ (5 mL), treated with charcoal and filtered. Addition of petroleum ether gave pale yellow (tmeda)Pt(OH)(OCH₃)(CH₃)₂ (370 mg, 95%). ¹H NMR (CD₂Cl₂, 200K, δ): -2.5 (s, 1H, Pt-OH), 0.99 (s, 6H, $^2J_{\text{PtH}} = 74$ Hz, PtCH₃), 2.39 (m, 4H, NCH₂CH₂N), 2.56 (overlapping s, 12H, NCH₃), 2.82 (s, 3H, $^3J_{\text{PtH}} = 42$ Hz, PtOCH₃). ¹⁹⁵Pt NMR (CD₃OD, δ): -727.76. This preparation of **4** did not give satisfactory elemental analyses, but an analytically pure sample was obtained by oxidizing (tmeda)Pt(CH₃)₂ with a slight excess of 30% aqueous H₂O₂ and following a similar workup; the NMR spectrum was identical. Anal. Calcd. for C₉H₂₈N₂O₃Pt ((tmeda)Pt(OH)(OCH₃)(CH₃)₂·H₂O): C 26.56%; H 6.93%; N 6.88%. Found: C 26.37%; H 6.55%; N 6.70%.

(tmeda)Pt(OOH)(OCH₃)(CH₃)₂. In a drybox, (tmeda)Pt(CH₃)₂ (19 mg, 0.056 mmol) was placed in a 100-mL round bottom flask, which was then fitted with 180° Kontes valve. The flask was removed from the box, and dry methanol (50 mL) was added by cannula. The resulting solution was degassed at -78 °C and the flask was filled with dioxygen (1 atm). The reaction mixture was stirred for 2 hours. Volatiles were removed *in vacuo* to give the title compound as a white solid. Yield: 21 mg (96%). ¹H NMR (toluene-*d*₈, δ): 1.64 (s, 6H, $^2J_{\text{PtH}} = 76$ Hz, PtCH₃), 1.95 (broad s, 4H, NCH₂CH₂N), 2.18 (s, 6H, NCH₃), 2.24 (s, 6H, NCH₃), 3.27 (s, 3H, $^3J_{\text{PtH}} = 41.5$ Hz, PtOCH₃), 6.48 (s, 1H, $^3J_{\text{PtH}} = 13$ Hz, PtOOH). ¹⁹⁵Pt NMR

(CD₃OD, δ): -716.89. Anal. Calcd. for C₉H₂₆N₂O₃Pt: C 26.66%; H 6.46%; N 6.91%. Found: C 26.67%; H 6.52%; N 6.90%.

Determination of O₂ Stoichiometry. A solution of (tmeda)Pt(CH₃)₂ (341 mg, 1 mmol) in methanol (20 mL) was stirred under 2 equiv. of dioxygen for 2.5 days. The leftover gas was quantified by a Toepler pump.

Conversion of 2 to 4. A freshly prepared solution of **2** in methanol was placed into a medium-walled glass bomb. The solution was degassed and placed into a 65 °C oil bath for 20 hours. The evolved gas was quantified by a Toepler pump.

General Procedure for the NMR Tube Reaction of (N-N)Pt(CH₃)₂ with Dioxygen. The appropriate platinum complex (~5 mg, 0.015 mmol) was placed into an NMR tube equipped with a J Young valve. Methanol-*d*₄ (0.6 mL) was added by vacuum transfer. The NMR tube was filled with dioxygen (1 atm) at -78 °C. The sample was vigorously shaken as it was warmed to room temperature. The reaction was usually complete within several minutes. In some cases (see main text), the solution turned pale pink or pale blue.

General Procedure for Monitoring the Oxidation of Dimethylplatinum(II) Complexes with Dioxygen by UV/Vis spectroscopy. In a drybox, a stock solution of a platinum complex in acetonitrile or toluene (50 μ L, 2-5 mM) was placed in a 1-cm UV cell equipped with a magnetic stirbar, a 14/20 ground glass adapter at 120° to the UV cell axis, and a side-arm with a magnetic stirbar (5-mL round bottom flask at 90° to the UV cell axis). The cell was capped, taken out the drybox and attached to a vacuum line through a 128.2 mL gas bulb. Dry methanol (2.5 mL) was added via syringe into the sidearm. The entire cell was

cooled to $-78\text{ }^{\circ}\text{C}$ and degassed. The gas bulb was filled with the appropriate amount of dioxygen (100-630 Torr). After dioxygen was admitted into the UV cell at $-78\text{ }^{\circ}\text{C}$, both the solution of platinum complex and the methanol were allowed to stir for 3 minutes as they warmed to room temperature, to ensure that a sufficient amount of dioxygen dissolved in the liquid phase. The methanol was then added to the UV cell by tipping the cell. The reaction mixture was vigorously stirred in the cell holder. Reactions were monitored for at least 3 half-lives.

General Procedure for Monitoring the Oxidation of (teeda)Pt(CH₃)₂ with (tmeda)Pt(OOH)(OCH₃)(CH₃)₂ by ¹H NMR spectroscopy. In a drybox, a stock solution of (tmeda)Pt(OOH)(OCH₃)(CH₃)₂ (0.6-0.7 mL, 40-120 mM) in CD₃OD was placed into a Wilmad NMR tube equipped with a screw cap with Teflon insert. An aliquot of (teeda)Pt(CH₃)₂ solution in methanol (50 mL) was added by syringe to the cold NMR tube ($-78\text{ }^{\circ}\text{C}$). The NMR tube was vigorously shaken, placed into the spectrometer and allowed to equilibrate to the probe temperature while the sample was shimmed. Arrayed spectra were scaled to the first spectrum in the series, and kinetic fits were done using *kini* and *kind* functions built into VNMR software (version 6.1B, Varian Associates, Inc.).

Structure Determination of (tmeda)Pt(OH)(OCH₃)(CH₃)₂. The title complex was crystallized from methanol at $-78\text{ }^{\circ}\text{C}$. Four crystals were examined on the diffractometer, but only one was eventually used. The first three crystals were discarded due to broad diffraction peaks and severe indexing problems. The crystals were mounted on a glass fiber with Paratone-N oil. Data were collected with 1.5° ω -scans because of the poor crystal quality. The individual backgrounds were replaced by a background function of 2θ derived from weak

reflections with $I < 3\sigma(I)$. The $\text{GOF}_{\text{merge}}$ was 1.08 (1203 multiples); R_{int} was 0.013 for 94 duplicates (there are a small number of duplicates since four equivalent sets of reflections were collected). Ψ -scan data were used for the absorption correction. There was no decay. No outlying reflections were omitted from the refinement. Weights were calculated as $1/s^2(F_o^2)$; variances ($s^2(F_o^2)$) were derived from counting statistics plus an additional term, $(0.014I)^2$; variances of the merged data were obtained by propagation of error plus another additional term, $(0.014\langle I \rangle)^2$. No reflections were specifically omitted from the final processed dataset; 2095 reflections were rejected, with 33 space group-absence violations and 32 inconsistent equivalents. Refinement of F^2 was against all reflections. The weighted R-factor (wR) and goodness of fit (S) are based on F^2 , conventional R-factors R are based on F , with F set to zero for negative F^2 . The threshold expression of $F^2 > 2\sigma(F^2)$ is used only for calculating R-factors(gt). *etc.*, and is not relevant to the choice of reflections for refinement. The coordinates of all hydrogen atoms including the half-populated sites were refined with U_{iso} 's fixed at 120% of the U_{eq} of the attached atom. There are 17 peaks in the final difference map with intensities $\geq |1| \text{ e}\cdot\text{\AA}^{-3}$; the two largest are $-2.31 \text{ e}\cdot\text{\AA}^{-3}$ (0.92\AA from Pt) and $1.62 \text{ e}\cdot\text{\AA}^{-3}$ (0.89\AA from Pt). Nine of these peaks, with intensities up to $1.45 \text{ e}\cdot\text{\AA}^{-3}$ and $-1.53 \text{ e}\cdot\text{\AA}^{-3}$, are in the vicinity of the disordered region. The largest shift/esd of 0.155 is for the x coordinate of the half-hydrogen H3AA which oscillates approximately 0.05 \AA . Crystallographic data have been deposited at the CCDC, 12 Union Road, Cambridge CB2 1EZ, UK, and copies can be obtained on request, free of charge, by quoting the publication citation and the deposition number 160706.

Structure Determinations for (tmeda)Pt(OOH)(OCH₃)(CH₃)₂. A semi-opaque, rounded thin wedge was selected from a batch of crystals, which were freshly grown from acetone at -35 °C, and mounted on a glass fiber with Paratone-N oil. This sample was the best of many chosen from a number of crystallizations; data collected at room temperature were no better than low-temperature data. Five runs of data were collected with 15 second long, -0.3° wide ω -scans at five values of φ (0, 120, 240, 180, and 300°) with the detector 5 cm (nominal) distant at a θ of -28°. The spots were broad and sometimes split. The initial cell for data reduction was calculated from 999 centered reflections chosen from throughout the data frames. A total of 41 reflections were discarded in the triclinic least-squares with a reciprocal lattice vector tolerance of 0.008 (0.005 is customary). Of the rejects, 20 had substantially non-integral indices and presumably are from a small fragment with a different orientation. There was no evidence of a larger cell. For data processing with SAINT v6.02, all defaults were used, except: a fixed box size of 2.0 x 2.0 x 1.2 was used, periodic orientation matrix updating was disabled, the instrument error was set to zero, no Laue class integration restraints were used, and for the post-integration global least squares refinement, no constraints were applied. The profiles exhibited an apparently considerable truncation of many reflections, especially in the z-direction. A number of both larger and smaller box sizes were tried but gave worse refinements of the structure. Both the initial cell refinement and the global cell refinement gave an ω zero \sim 0.4° too negative. No decay correction was needed. The crystal boundaries were rudely indexed as faces; these were not good enough for a face-indexed absorption correction. A SADABS v2.03 beta

correction was applied (relative correction factors: 1.000 to 0.471) with $g = 0.113$, 100 refinement cycles, and defaults for the remaining parameters. Again, a number of other options such as discarding portions of the data and using different orders of Bessel functions did not lead to a better model refinement.

No reflections were specifically omitted from the final processed dataset but the data were truncated at a 2θ of 50° as the high angle spots seemed fuzzier; 3469 reflections were rejected, with 20 space group-absence violations, 0 inconsistent equivalents, and no reflections suppressed. Refinement of F^2 was against all reflections. The weighted R-factor (wR) and goodness of fit (S) are based on F^2 , conventional R-factors R are based on F , with F set to zero for negative F^2 . The threshold expression of $F^2 > 2\sigma(F^2)$ is used only for calculating R-factors(gt), *etc.*, and is not relevant to the choice of reflections for refinement.

The platinum atom was refined anisotropically, all other non-hydrogen atoms isotropically. The solvents form layers perpendicular to the c -axis at $z \sim 0, \frac{1}{2}$, and 1, but do not appear to interact. All hydrogen atoms were placed at calculated positions with U_{iso} 's fixed at 120% of the U_{iso} 's of the attached atoms. No restraints or constraints were used. Of the 20 largest peaks in the final difference map, 6 are greater than $|2| \text{ e}\cdot\text{\AA}^{-3}$ and another 12 are greater than $|1| \text{ e}\cdot\text{\AA}^{-3}$. Seven of these 18 peaks are near the platinum atom, including the largest positive peak of $2.98 \text{ e}\cdot\text{\AA}^{-3}$ at a distance of 0.89 \AA . The largest negative peak of $-2.73 \text{ e}\cdot\text{\AA}^{-3}$ is 0.75 \AA from N2B (anomalously small U_{iso}); the other big excursions not near the platinum are $2.29 \text{ e}\cdot\text{\AA}^{-3}$ at 0.88 \AA from C8B, $1.79 \text{ e}\cdot\text{\AA}^{-3}$ at 0.67 \AA from C6B, $-1.66 \text{ e}\cdot\text{\AA}^{-3}$ at 1.45 \AA from O2B, $1.63 \text{ e}\cdot\text{\AA}^{-3}$ at 0.68 \AA from N2B, $-1.23 \text{ e}\cdot\text{\AA}^{-3}$ at

0.99 Å from H8BC, $-1.21 \text{ e} \cdot \text{Å}^{-3}$ at 1.07 Å from O2A, $1.13 \text{ e} \cdot \text{Å}^{-3}$ at 0.76 Å from C4B, and $1.06 \text{ e} \cdot \text{Å}^{-3}$ at 0.80 Å from O1B.

The 6 most disagreeable reflections all have $k = 5$ and F_{calc} weak and less than F_{obs} . This suggests twinning. The 20 reflections discarded in the initial unit cell determination could not be indexed by themselves. No other effort was made to investigate this fairly minor problem.

Crystallographic data have been deposited with the Cambridge Crystallographic Data Centre as supplementary publication no. CCDC 163314. Copies of the data can be obtained, free of charge, on application to CCDC, 12 Union Road, Cambridge CB2 1EZ, UK, (fax: +44 1223 336033 or e-mail:deposit@ccdc.cam.ac.uk). Structure factors are available from the authors via e-mail:xray@caltech.edu

References

- (1) Gol'dshleger, N. F.; Es'kova, V. V.; Shilov, A. E.; Shteinman, A. A. *Zh. Fiz. Khim. (Engl. trans.)* **1972**, 46, 785.
- (2) Stahl, S. S.; Labinger, J. A.; Bercaw, J. E. *Angew. Chem., Int. Ed.* **1998**, 37, 2180.
- (3) Luinstra, G. A.; Wang, L.; Stahl, S. S.; Labinger, J. A.; Bercaw, J. E. *J. Organomet. Chem.* **1995**, 504, 75-91.
- (4) Horvath, I. T.; Cook, R. A.; Millar, J. M.; Kiss, G. *Organometallics* **1993**, 12, 8.
- (5) Basickes, N.; Hogan, T. E.; Sen, A. *J. Am. Chem. Soc.* **1996**, 118, 13111-13112.
- (6) Thorn, D. L., Personal Communication.
- (7) Freund, M. S.; Labinger, J. A.; Lewis, N. S.; Bercaw, J. E. *J. Mol. Cat. A: Chem.* **1994**, 87, L11-L15.
- (8) Based on irreversible one electron oxidation potentials, dimethylplatinum(II) compounds are almost 0.5 V easier to oxidize than chloromethylplatinum(II) complexes, which in turn are about 0.5 V easier to oxidize than dichloroplatinum(II) complexes. J. D. Scollard, J. A. Labinger, J. E. Bercaw, unpublished results.
- (9) Periana, R. A.; Taube, D. J.; Gamble, S.; Taube, H.; Satoh, T.; Fujii, H. *Science* **1998**, 280, 560-564.
- (10) Geletii, Y. V.; Shilov, A. E. *Kinet. Katal.* **1983**, 24, 486-489; Shilov, A. E.; Shteinman, A. A. *Coord. Chem. Rev.* **1977**, 24, 97-143.

- (11) A preliminary account of this work has been published. See Rostovtsev, V. V.; Labinger, J. A.; Bercaw, J. E.; Lasseter, T. L.; Goldberg, K. I. *Organometallics* **1998**, *17*, 4530-4531.
- (12) Monaghan, P. K.; Puddephatt, R. J. *Organometallics* **1984**, *3*, 444.
- (13) Stahl, S. S.; Labinger, J. A.; Bercaw, J. E. *J. Am. Chem. Soc.* **1996**, *118*, 5961-5976.
- (14) Shagisultanova, G. A.; Karaban, A. A. *Zh. Fiz. Khim.* **1971**, *45*, 2918-2919; Boucher, H. A.; Lawrance, G. A.; Lay, P. A.; Sargeson, A. M.; Bond, A. M.; Sangster, D. F.; Sullivan, J. C. *J. Am. Chem. Soc.* **1983**, *105*, 4652-4661.
- (15) Sarneski, J. E.; McPhail, A. T.; Onan, K. D.; Erickson, L. E.; Reilley, C. N. *J. Am. Chem. Soc.* **1977**, *99*, 7376-7378.
- (16) Wieghardt, K.; Koeppen, M.; Swiridoff, W.; Weiss, J. *J. Chem. Soc., Dalton Trans.* **1983**, 1869-1872.
- (17) Prokopchuk, E. M.; Jenkins, H. A.; Puddephatt, R. J. *Organometallics* **1999**, *18*, 2861-2866.
- (18) Peloso, A. *Coord. Chem. Rev.* **1973**, *10*, 123-181.
- (19) Gossage, R. A.; Ryabov, A. D.; Spek, A. L.; Stufkens, D. J.; van Beek, J. A. M.; van Eldik, R.; van Koten, G. *J. Am. Chem. Soc.* **1999**, *121*, 2488-2497.
- (20) Drougge, L.; Elding, L. I. *Inorg. Chem.* **1985**, *24*, 2292-2297.
- (21) Drougge, L.; Elding, L. I. *Inorg. Chem.* **1988**, *27*, 795-798; Elding, L. I.; Gustafson, L. *Inorg. Chim. Acta* **1976**, *19*, 165-171.
- (22) Davies, M. S.; Hambley, T. W. *Inorg. Chem.* **1998**, *37*, 5408-5409.
- (23) Aye, K. T.; Vittal, J. J.; Puddephatt, R. J. *J. Chem. Soc., Dalton Trans.* **1993**, 1835-1839.
- (24) Rich, R. L.; Taube, H. *J. Am. Chem. Soc.* **1954**, *76*, 2608-2611.

- (25) Mason, W. R. *Coord. Chem. Rev.* **1972**, 7, 241-255.
- (26) Berglund, J.; Voigt, R.; Fronaeus, S.; Elding, L. I. *Inorg. Chem.* **1994**, 33, 3346-3353; Drougge, L.; Elding, L. I. *Inorg. Chem.* **1987**, 26, 1703-1707; Hindmarsh, K.; House, D. A.; van Eldik, R. *Inorg. Chim. Acta* **1998**, 278, 32-42.
- (27) Matsumoto, K.; Sakai, K. *Adv. Inorg. Chem.* **2000**, 49, 375-427.
- (28) Nyman, C. J.; Wymore, C. E.; Wilkinson, G. J. *Chem. Soc. A* **1968**, 561-563.
- (29) Lawson, H. J.; Atwood, J. D. *J. Am. Chem. Soc.* **1989**, 111, 6223-6227.
- (30) Our attempts to detect hydrogen peroxide in reaction mixtures by electrochemical methods were unsuccessful.
- (31) Bianchini, C.; Meli, A.; Peruzzini, M.; Vizza, F. *J. Am. Chem. Soc.* **1990**, 112, 6726-6728; Bhaduri, S.; Casella, L.; Ugo, R.; Raithby, P. R.; Zuccaro, C.; Hursthouse, M. B. *J. Chem. Soc., Dalton Trans.* **1979**, 1624-1629; Hughes, G. R.; Mingos, D. M. P. *Transition Met. Chem.* **1978**, 3, 381-382; Muto, S.; Kamiya, Y. *Bull. Chem. Soc. Jpn.* **1976**, 49, 2587-2589.
- (32) tom Dieck, H.; Fendesak, G.; Munz, C. *Polyhedron* **1991**, 10, 255-260.
- (33) Drougge, L.; Elding, L. I. *Inorg. Chim. Acta* **1986**, 121, 175-183.
- (34) Wick, D. D.; Goldberg, K. I. *J. Am. Chem. Soc.* **1999**, 121, 11900-11901.
- (35) Hoard, D. W.; Sharp, P. R. *Inorg. Chem.* **1993**, 32, 612-620; Thiyagarajan, B.; Kerr, M. E.; Bruno, J. W. *Inorg. Chem.* **1995**, 34, 3444-3452; Moeller, E. R.; Joergensen, K. A. *J. Am. Chem. Soc.* **1993**, 115, 11814-11822; Sharp, P. R.; Hoard, D. W.; Barnes, C. L. *J. Am. Chem. Soc.* **1990**, 112, 2024-2026.
- (36) Otsuka, S.; Aotani, Y.; Tatsuno, Y.; Yoshida, T. *Inorg. Chem.* **1976**, 15, 656-660.
- (37) Clark, R. J. H.; Fanizzi, F. P.; Natile, G.; Pacifico, C.; van Rooyen, C. G.; Tocher, D. A. *Inorg. Chim. Acta* **1995**, 235, 205-213; Fanizzi, F. P.; Maresca, L.;

- Natile, G.; Lanfranchi, M.; Tiripicchio, A.; Pacchioni, G. *J. Chem. Soc., Chem. Commun.* **1992**, 333-335; Gowenlock, B. G.; Orrell, K. G.; Sik, V.; Vasapollo, G. *Polyhedron* **1998**, 17, 3495-3500.
- (38) Conte, V.; Di Furia, F.; Modena, G. In *Organic Peroxides*; Ando, W., Ed.; John Wiley & Sons: Chichester, 1992; pp 559-598.
- (39) Pregaglia, G.; Morelli, D.; Conti, F.; Gregorio, G.; Ugo, R. *Faraday Discuss. Chem. Soc.* **1968**, 110-121.
- (40) No exchange was observed between (tmeda)Pt(OH)(OCH₃)(CH₃)₂ and H₂¹⁷O after several days at room temperature. (phen)Pt(OH)(OCH₃)(CH₃)₂ is stable in 1M HCl for days (see ref 12).
- (41) Hiatt, R.; Mill, T.; Mayo, F. R. *J. Org. Chem.* **1968**, 33, 1416-1420.
- (42) Shriver, D. F.; Drezdson, M. A. *The Manipulation of Air-Sensitive Compounds*; 2nd ed.; John Wiley & Sons: New York, 1986.
- (43) Hill, G. S.; Irwin, M. J.; Levy, C. J.; Rendina, L. M.; Puddephatt, R. J. *Inorg. Synth.* **1998**, 32, 149-153.
- (44) Rashidi, M.; Fakhroieian, Z.; Puddephatt, R. J. *J. Organomet. Chem.* **1991**, 406, 261-267.
- (45) Clark, H. C.; Manzer, L. E. *J. Organomet. Chem.* **1973**, 59, 411-428.
- (46) Remenar, J. F.; Lucht, B. L.; Collum, D. B. *J. Am. Chem. Soc.* **1997**, 119, 5567-5572.
- (47) Johansson, L.; Tilset, M.; Labinger, J. A.; Bercaw, J. E. *J. Am. Chem. Soc.* **2000**, 122, 10846-10855.
- (48) Tom Dieck, H.; Svoboda, M.; Greiser, T. Z. *Naturforsch., B: Anorg. Chem., Org. Chem.* **1981**, 36B, 823-832.

Chapter IV

APPROACHES TO CATALYTIC OXIDATIVE DEHYDROGENATION OF ALKANES. SYNTHESIS AND REACTIVITY OF OLEFIN COMPLEXES OF PLATINUM(II).

Abstract

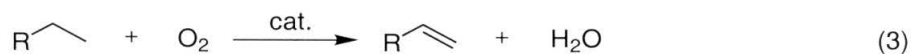
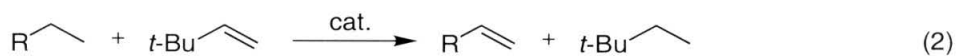
The studies described in this chapter are directed toward the development of a platinum(II)-catalyzed oxidative alkane dehydrogenation. Stoichiometric conversion of alkanes (cyclohexane, ethane) to olefins (cyclohexene, ethylene) is achieved by C–H activation with $[(N-N)Pt(CH_3)(CF_3CH_2OH)]BF_4$ (**1**, N–N is N,N'-bis(3,5-di-*t*-butylphenyl)-1,4-diazabutadiene) which results in the formation of olefin hydride complexes. The first step in the C–H activation reaction is formation of a platinum(II) alkyl which undergoes β -hydrogen elimination to afford the olefin hydride complex. The cationic ethylplatinum(II) intermediate can be generated *in situ* by treating diethylplatinum(II) compounds with acids. Treatment of (phen)PtEt₂ with $[H(OEt_2)_2]BAr^f_4$ at low temperatures resulted in the formation of a mixture of $[(phen)PtEt(OEt_2)]BAr^f_4$ (**8**) and $[(phen)Pt(C_2H_4)H] BAr^f_4$ (**7**). Excess diethyl ether converted olefin hydride **7** to the ethyl complex **8**. The cationic olefin complexes are unreactive toward dioxygen or hydrogen peroxide. Since the success of the overall catalytic cycle depends on our ability to oxidize the olefin hydride complexes, we have also prepared and characterized a series of neutral olefin complexes of platinum(II) with monoanionic ligands (derivatives of pyrrole-2-carboxyaldehyde N-aryl imines). Unfortunately, these are also stable to oxidation.

Introduction

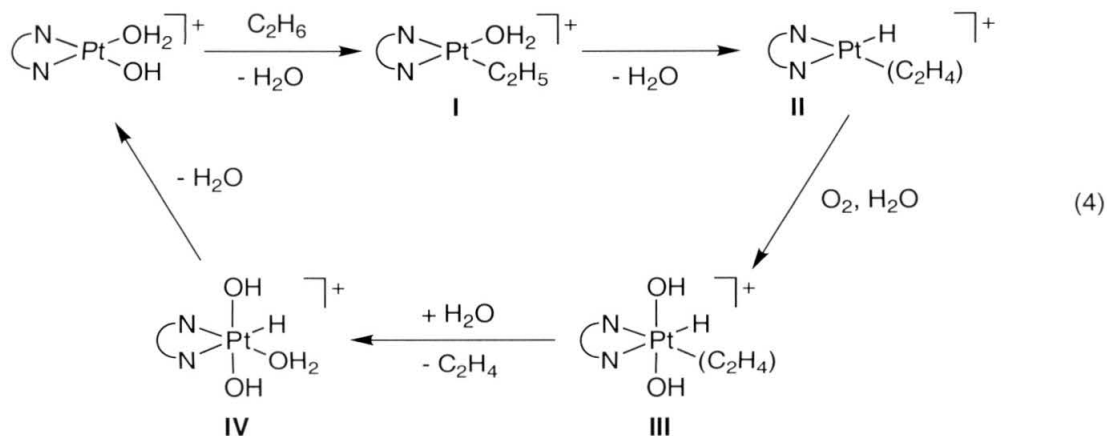
Alkane dehydrogenation is one of the approaches to catalytic functionalization of hydrocarbons.¹ Olefins, the products of alkane dehydrogenation, are widely used in chemical industry.^{2,3} The overall reaction as shown in eq. 1 is thermodynamically uphill. Taking advantage of highly positive standard entropy of the reaction, the process can be driven to completion by increased temperatures (150-200 °C).



Another approach is to capture dihydrogen with an acceptor molecule such as *t*-butylethylene thus relaxing thermodynamic requirements (eq. 2).⁴ Oxidative dehydrogenation uses dioxygen to capture H₂ (eq. 3).⁵ Reduction of dioxygen to water provides the driving force for the overall reaction.



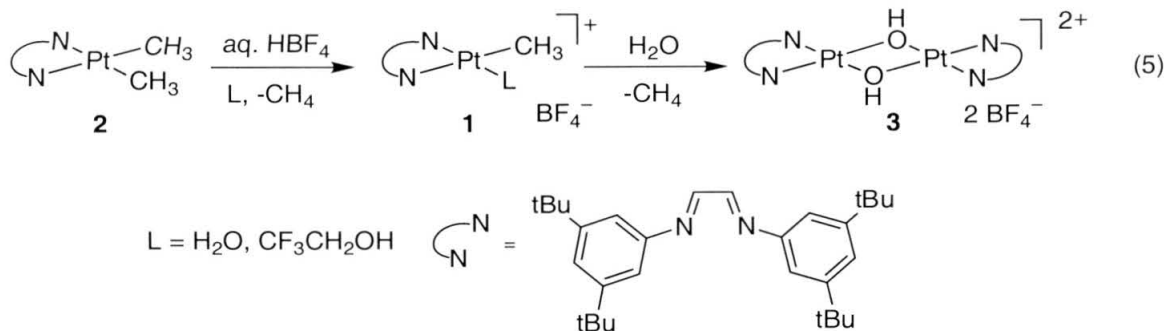
A possible catalytic cycle for oxidative alkane dehydrogenation with electrophilic platinum(II) complexes is shown below (eq. 4). Selective activation of terminal C–H bonds of an alkane would yield a platinum(II) alkyl **I**. β-Hydrogen elimination followed by oxidation of **II** with dioxygen should afford a platinum(IV) hydroxide **III** (assuming that reactions are carried out in water). Loss of ethylene and deprotonation of **IV** would regenerate the active catalyst.



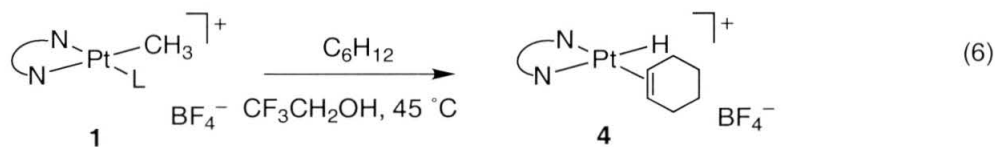
Studies of the individual steps of the proposed catalytic cycle are summarized in this chapter. First, we describe the reactivity of platinum(II) cations toward alkanes with β -hydrogens. Next, generation of a cationic olefin hydride complex of platinum(II) is reported, followed by the summary of the synthesis and reactivity of neutral chloro and methyl olefin complexes of platinum(II).

Results

C-H Activation of Ethane and Cyclohexane with a Cationic Platinum(II) Complex. Cation **1** was prepared *in situ* by treatment of the α -diimine complex **2** with aqueous HBF_4 in $\text{CF}_3\text{CD}_2\text{OD}$ ($\text{TFE-}d_3$).⁶ At room temperature, formation of the hydroxy dimer **3** was observed (eq. 5). Reactions with cyclohexane and ethane were carried out at 45 °C.

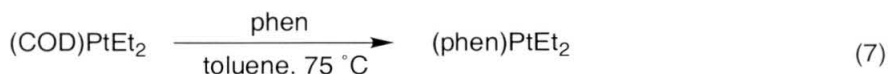


With cyclohexane, a mixture of the hydroxy dimer **3** and cyclohexene hydride **4** formed after several days at room temperature (eq. 6). Both hydride and olefin protons are coupled to platinum (Pt-H: δ -22.44 ppm, $^1J_{\text{PtH}} = 1332.3$ Hz; Pt-(C₆H₁₀): δ 4.85 ppm, $^1J_{\text{PtH}} = 58.8$ Hz).

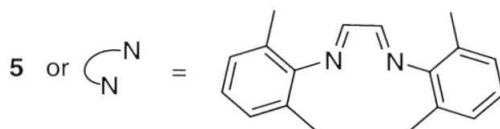
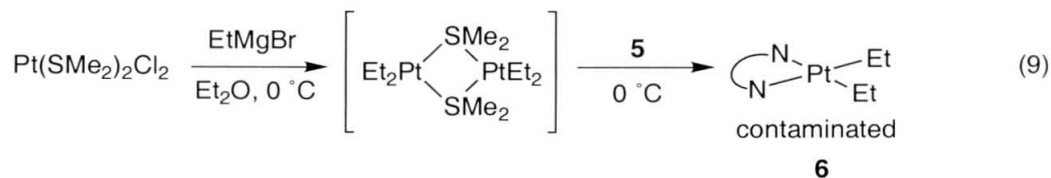
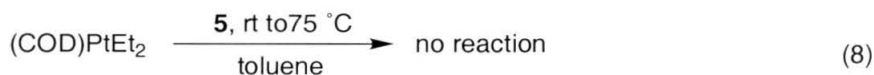


Reaction of **1** with ethane gave two products: the hydroxy dimer **3** and a platinum(II) hydride (δ -19.3 ppm). We were unable to detect either free or coordinated ethylene by ^1H NMR spectroscopy.

Preparation of Diethylplatinum(II) Complexes. Both (NBD)PtEt₂ and (COD)PtEt₂ can be used to prepare (phen)PtEt₂. Heating the solution of (COD)PtEt₂ and phenanthroline in toluene at 85 °C gave red-orange crystals of (phen)PtEt₂ in 79% yield (eq. 7). The product was characterized by ^1H and ^{13}C NMR spectroscopy and elemental analysis.

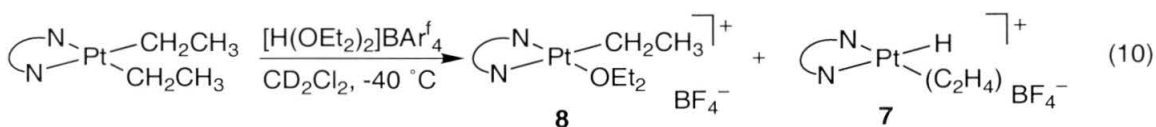


Our repeated attempts to prepare diethylplatinum(II) complexes of α -diimines using a number of platinum(II) starting materials were unsuccessful. No reaction was observed with (NBD)PtEt₂ or (COD)PtEt₂ at room temperature, whereas higher temperatures brought about decomposition of the starting material (eq. 8). Me₂Pt(μ_2 -SMe₂)₂PtMe₂ is a convenient starting material for the preparation of a number of dimethylplatinum(II) complexes. Unfortunately, its diethyl analog is not known. However, the reaction between α -diimine **5** and generated *in situ* Et₂Pt(μ_2 -SMe₂)₂PtEt₂ afforded contaminated samples of complex **6** (eq. 9).



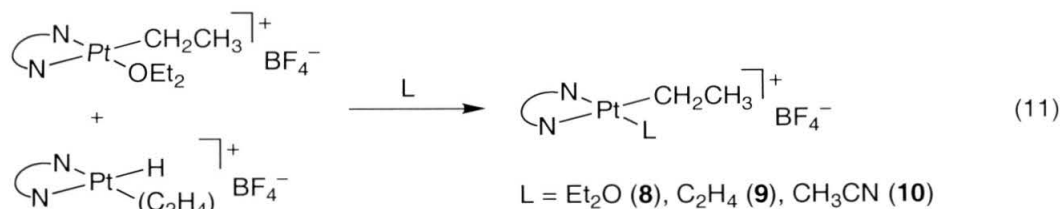
Protonation of Diethylplatinum(II) Complexes. Several acids (HBF₄, [H(OEt₂)₂]BAr^f₄ and CF₃CH₂OH) were used in protonation studies. Reaction between [H(OEt₂)₂]BAr^f₄ and (phen)PtEt₂ in CD₂Cl₂ at -40 °C gave two major products, the olefin hydride **7** and the solvento complex **8** in (eq. 10). The olefin hydride complex was identified by its characteristic olefin (δ 4.61 ppm, ²J_{PtH} = 65 Hz) and hydride peaks (δ -21.4 ppm, ¹J_{PtH} = 1227 Hz). NOE difference NMR

spectra confirmed that both moieties reside in the same molecule. Olefin rotation in **7** is fast at $-40\text{ }^{\circ}\text{C}$ and only starts to broaden at $-85\text{ }^{\circ}\text{C}$. Two sets of diastereotopic methylene protons of the coordinated diethyl ether were observed in ^1H NMR of **8** at δ 3.83 and 4.1 ppm ($-40\text{ }^{\circ}\text{C}$). The signals broaden at higher temperatures. The ratio of the two products (**7**/**8**) varied from 1.2 to 3. The ether complex was favored at higher temperatures.

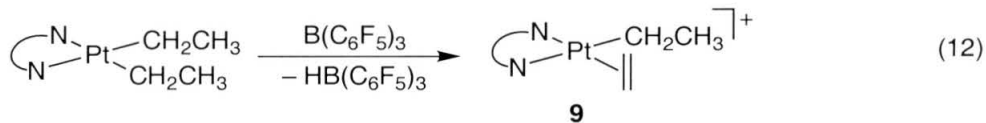


The olefin hydride **7** is stable for several hours at low temperatures (up to $-20\text{ }^{\circ}\text{C}$), but several new species were observed in ^1H NMR at higher temperatures. At least three more resonances with platinum satellites appeared in the olefinic region and several Pt-H peaks could be seen between δ -19 and -22 ppm. One of the olefin compounds was tentatively identified as the complex of platinum(II) with vinyl ether. After several days at room temperature, the amount of ethane in the NMR tube doubled and all intermediates converted to a single platinum hydride species (δ -22.3 ppm, $^1J_{\text{PtH}} = 540$ Hz), tentatively identified as a platinum(II) carbene hydride.

Addition of strong donors (C_2H_4 , CH_3CN) to the mixture of **7** and **8** at $-40\text{ }^{\circ}\text{C}$ resulted in the formation of cationic ethyl complexes $[(\text{phen})\text{Pt}(\text{CH}_2\text{CH}_3)\text{L}]\text{BAr}_4^f$, where L is C_2H_4 (**9**) or CH_3CN (**10**) (eq. 11). Excess diethyl ether converted olefin hydride **7** to **8**.



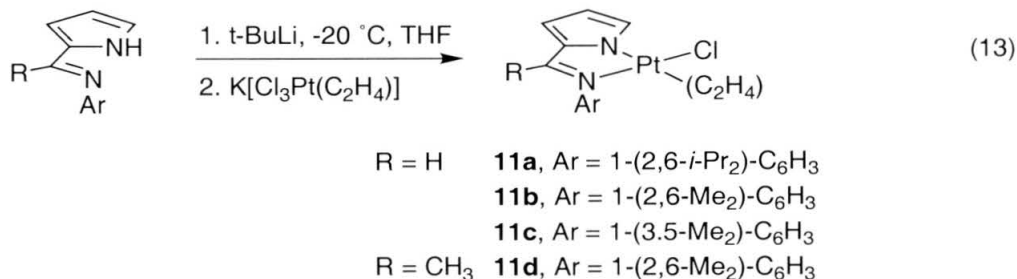
The ethylene complex **9** was also prepared by β -hydride abstraction from (phen)PtEt₂ (eq. 12). The barrier for olefin rotation in **9** was determined (ΔG^\ddagger (-50 °C) = 10.9 kcal mol⁻¹, ΔH^\ddagger = 11.5 kcal mol⁻¹, ΔS^\ddagger = 2.8 cal mol⁻¹ K⁻¹). Generation of olefin complexes by β -hydride abstraction from transition metal alkyl complexes has precedent.⁷



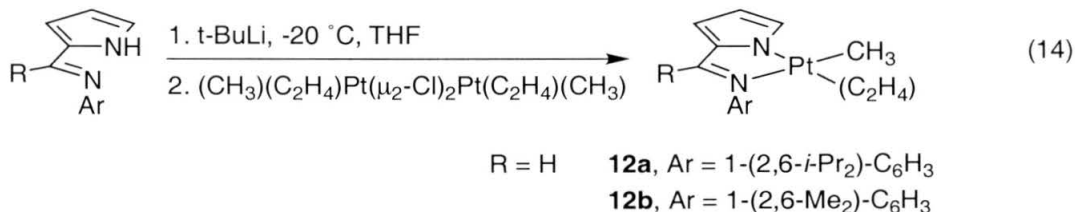
Addition of a diethyl ether solution of HBF₄ to (phen)PtEt₂ in CD₂Cl₂ resulted in sample decomposition even at low temperatures. In THF-*d*₈, the treatment of (phen)PtEt₂ with HBF₄/Et₂O followed by the addition of CD₃CN gave the ethylation **10**. Formation of ethane was observed when (phen)PtEt₂ was dissolved in CF₃CD₂OD. Unfortunately, we could not identify the platinum-containing products of the reaction.

Synthesis of Neutral Complexes of Platinum(II) with Ethylene. The ethylene chloride complexes **11a-d** were prepared using Zeise's salt, K[PtCl₃(C₂H₄)] as the starting material. Treatment of K[PtCl₃(C₂H₄)] with the deprotonated pyrrole ligand (*t*-BuLi, -20 °C) in THF at -20 °C gave the olefin chloride complexes **11a-d** in 75-90% yields (eq. 13). The crystal structure analysis by X-ray diffractometry established that ethylene is positioned trans to the pyrrole ligand in **11a** (Figure

1). The NOE difference NMR spectroscopy confirmed that **11a** retains its geometry in solution.



The methyl ethylene complexes **12a-b** were prepared by the procedure described above for the preparation of **11a-d** and using (C₂H₄)(CH₃)Pt(μ₂-Cl)₂Pt(CH₃)(C₂H₄) instead of the Zeise's salt (eq. 14). The geometry of **12a** in solution (CD₂Cl₂) was determined by NOE difference NMR spectroscopy: ethylene resides trans to the pyrrole ligand.



The ethylene complexes **11** and **12** are air- and moisture-stable solids. Compounds **11a** and **12b** do not react with dioxygen or hydrogen peroxide (in CH₃OH, at 25-60 °C). Coordinated ethylene is also unreactive towards Et₂NH (**11a**) and NH₄OH (**12b**).

We have also measured the barriers of olefin rotation in **11a** and **12a**. Contrary to our expectations, the barrier of olefin rotation in **12a** (ΔG[‡](-50 °C) = 7.2 kcal mol⁻¹, ΔH[‡] = 8.0 kcal mol⁻¹, ΔS[‡] = -3.8 cal mol⁻¹ K⁻¹) is lower than the one in **11a** (ΔG[‡](-50 °C) = 10.8 kcal mol⁻¹, ΔH[‡] = 11.1 kcal mol⁻¹, ΔS[‡] = -1.2 cal mol⁻¹ K⁻¹).

We carried out DFT calculations on the 2,6-dimethylphenyl derivatives **11b** and **12b** to determine the geometry and relative energy of the transition states for olefin rotation. For both complexes, the in-plane orientation of ethylene molecule was the highest energy point on the rotation profile. The calculated relative energies are listed in Table 1.

Table 1. Selected Data from DFT Calculations. Dihedral angle is the angle between the Pt-N(imine) bond and C=C bond of the coordinated ethylene.

Compound	Ground State		Transition State	
	Relative Enthalpy, in kcal mol ⁻¹	Dihedral Angle	Relative Enthalpy, in kcal mol ⁻¹	Dihedral Angle
12b	0	90°	9.2	0°
11b	0	90°	11.4	0°

Table 2. Selected Calculated Bond Lengths and Angles for **11b** and **12b** as well as for the Transition States for Ethylene Rotation.

Parameter X = Cl or CH ₃	11b , ground state	11b , transition state	12b , ground state	12b , transition state
Pt-X	2.365 Å	2.40 Å	2.064 Å	2.10 Å
Pt-N(imine)	2.092 Å	2.126 Å	2.240 Å	2.247 Å
Pt-N(pyr)	2.027 Å	2.031 Å	2.044 Å	2.060 Å
Pt-olefin centroid	2.097 Å	2.193 Å	2.061 Å	2.114 Å
C=C	1.390 Å	1.371 Å	1.398 Å	1.382 Å
N(im)-Pt-X	173.0°	166.3°	171.3°	162.9°

X-ray Structure of 11a. The structure of the olefin chloride complex **11a** was established by X-ray crystallography (Figure 1). Selected bond lengths and distances are shown in Table 4. As mentioned above, ethylene is positioned trans to the pyrrolide moiety perpendicular to the plane of the platinum

complex. The 2,6-di-*iso*-propylphenyl group is parallel to the ethylene molecule, blocking the axial approaches to platinum.

Table 3. Selected bond lengths (in Å) and angles (in °) for **11a**.

Pt-N(2)	1.988(4)	N(2)-Pt-N(1)	79.3(2)
Pt-N(1)	2.034(4)	N(2)-Pt-C(1)	159.0(2)
Pt-C(1)	2.129(5)	N(1)-Pt-C(1)	97.1(2)
Pt-C(2)	2.154(5)	N(2)-Pt-C(2)	163.1(2)
Pt-Cl	2.295(1)	N(1)-Pt-C(2)	96.9(2)
C(1)-C(2)	1.373(7)	C(1)-Pt-C(2)	37.4(2)
		N(2)-Pt-Cl	94.1(1)
		N(1)-Pt-Cl	173.3(1)
		C(1)-Pt-Cl	89.5(2)
		C(2)-Pt-Cl	89.2(2)

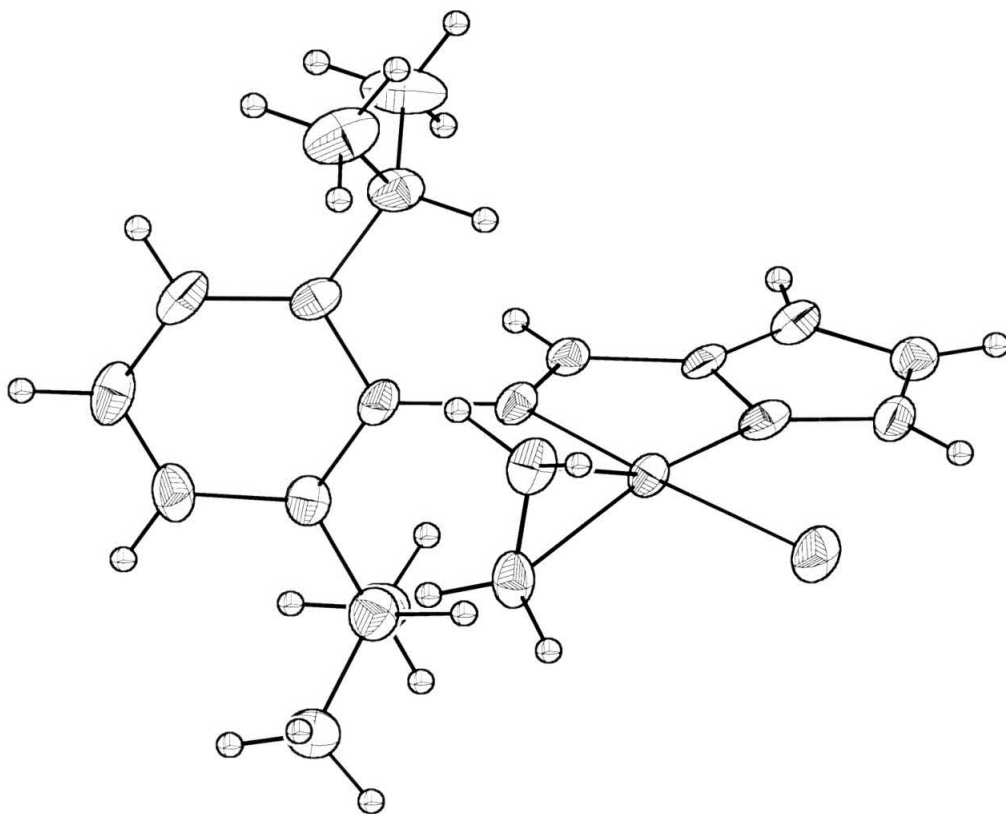
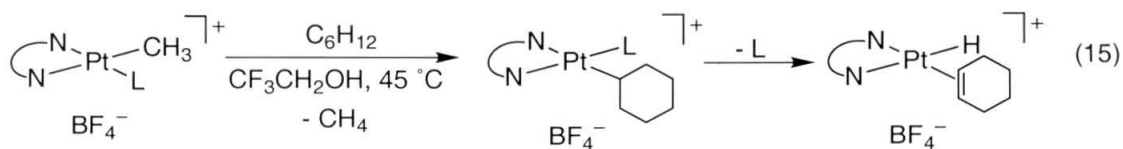


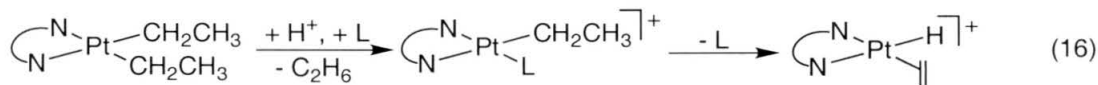
Figure 1. Structure of **11a**.

Discussion

Chemistry of Cationic Complexes. C–H activation of alkanes with β -hydrogens by cationic **1** results in the formation of olefin hydride complexes of platinum(II) (eq. 6). It was proposed that the initially formed platinum(II) alkyl undergoes β -hydrogen elimination to give the final product (eq. 15).^{6,8} In case of ethane, the coordinated ethylene is then displaced by solvent.

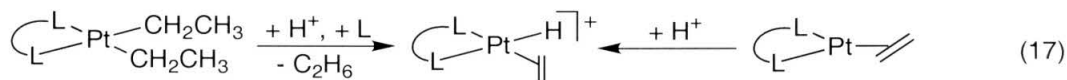


β -Hydrogen elimination in cationic alkylplatinum(II) complexes can be studied directly through generation of ethylplatinum(II) cations by protonation of the corresponding diethyl compounds (eq. 16). With this goal in mind we have prepared (phen)PtEt₂ and examined its reactions with acids. Puddephatt and Chaudhury reported the synthesis of (bipy)PtEt₂ from (COD)PtEt₂ and bipy in 40% yield.⁹ Although (phen)PtEt₂ is quite stable in solid state, it slowly reacts with methylene chloride under inert atmosphere at room temperature.

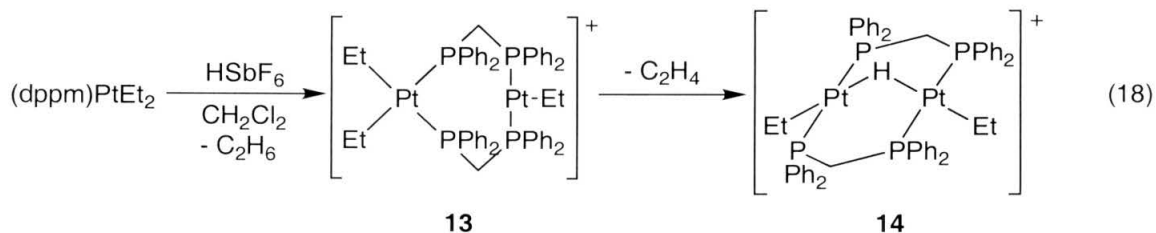


Olefin hydride complexes of platinum(II) were proposed as intermediates in such catalytic processes as alkene hydrogenation,¹⁰ hydroformylation¹¹ and hydrosilation.¹² These complexes are also thought to form during the thermal decomposition of platinum dialkyls.¹³⁻¹⁶ Several groups have studied the

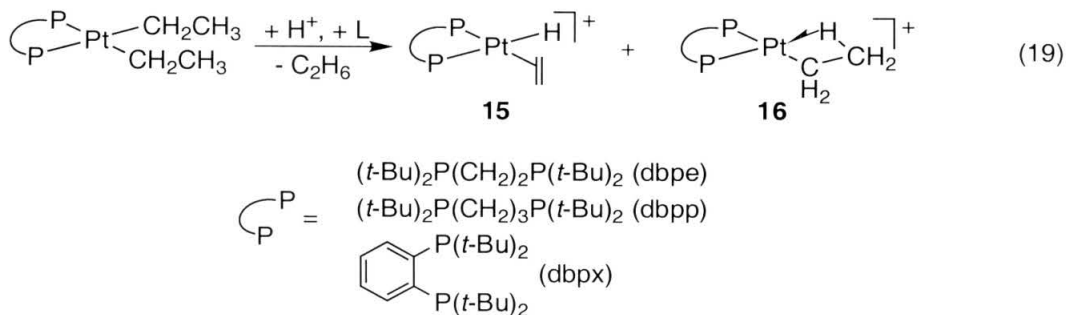
chemistry of cationic olefin hydrides.¹⁷⁻²⁰ The complexes can be prepared by protonation of either platinum(0) olefin or diethyl platinum(II) complexes



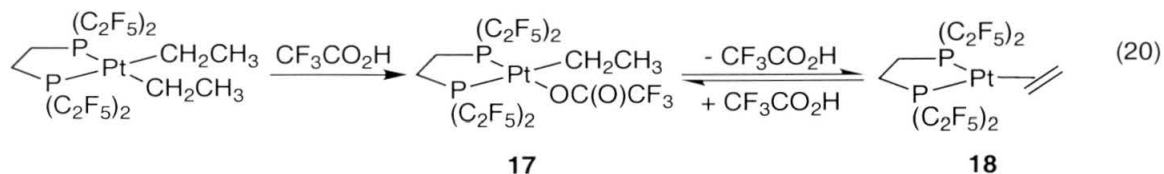
(eq. 17). Although only diphosphine ligands were used, there were striking differences in the observed behavior of the compounds. Protonation of (dppm)PtEt₂ (dppm = Ph₂CH₂PPh₂) resulted in the formation of binuclear species **13** followed by extrusion of ethylene to give hydride **14** (eq. 18).¹⁷ The authors were unable to distinguish between monomolecular and bimolecular



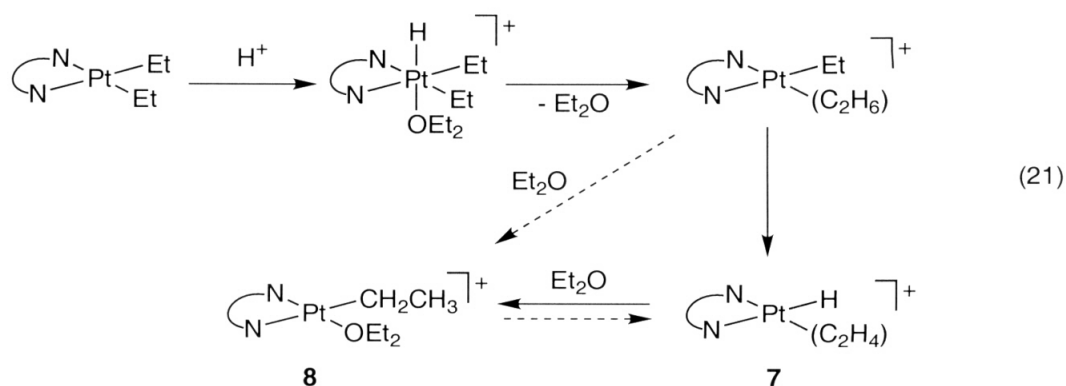
mechanisms for β-hydride elimination. With phosphines of a bigger bite angle, protonation of the diethyl compounds resulted in the formation of mononuclear olefin hydrides **15** or β-agostic alkyl species **16** (eq. 19).^{18,19} Interestingly, the preference for ethylene hydride *vs.* β-agostic ground states seems to be



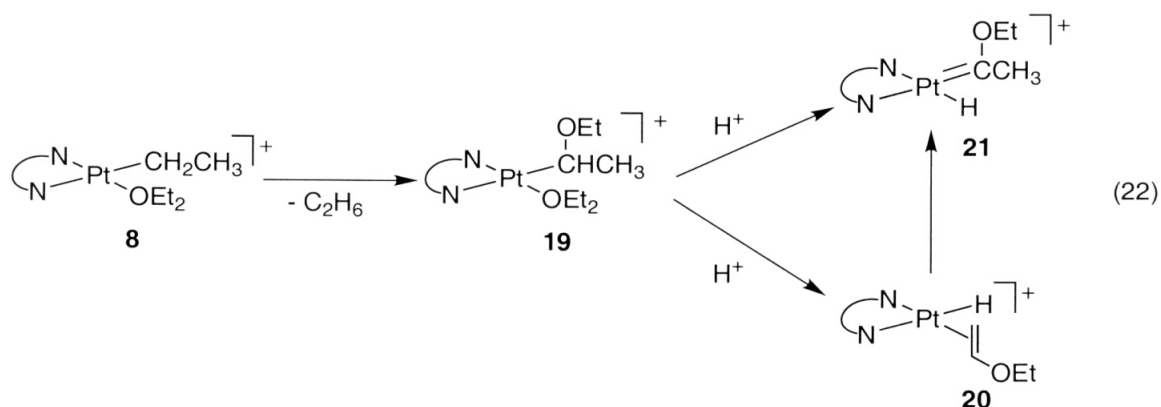
determined by the bite angle of the phosphine: smaller diphosphines (dbpe) favor the olefin hydride, whereas bulkier diphosphines (dbpp, dbpx) stabilize the β -agostic isomer. An exceptionally stable cationic platinum(II) complex **17** was prepared by Roddick and co-workers (eq. 20).²⁰ The complex can be prepared from both (dfepe)PtEt₂ and (dfepe)Pt(η^2 -C₂H₄) (**18**). In fact, the reaction of **18** with CF₃CO₂H is reversible and cationic **17** can be used as a catalyst for H/D exchange between ethylene and trifluoroacetic acid.



A mixture of olefin hydride **7** and ethyl cation **8** was formed when (phen)PtEt₂ was treated with [H(OEt₂)₂]BAr^f₄ at low temperatures in CD₂Cl₂. The relative ratio of **7** and **8** changes at different temperatures with **8** being favored at higher temperature. The olefin hydride **7** converts to the cationic ethyl complexes upon the addition of donor ligands (C₂H₄, CH₃CN, OEt₂). It is not clear whether the formation of **8** from **7** is reversible, since olefin hydride **7** can form directly from the ethane σ -complex. At present, we cannot distinguish between the two possibilities. At room temperature, the peaks corresponding to **7** and **8** broaden, most likely due to reversible insertion of ethylene in to the Pt-H bond and/or fast ether exchange (eq. 21). We see no evidence for the formation of a β -agostic ethyl complex – the ether complex appears to be a more stable compound. Apart from subtle and yet unidentified electronic effects, this preference may be largely due to sterics, with bulky di-*tert*-butylphosphino groups discouraging ether coordination in β -agostic structure **16**.



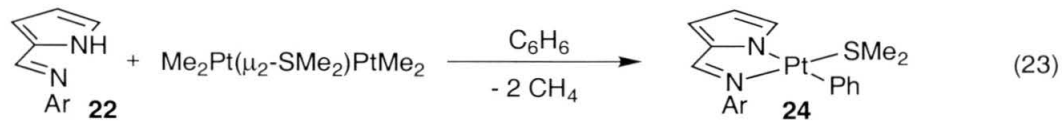
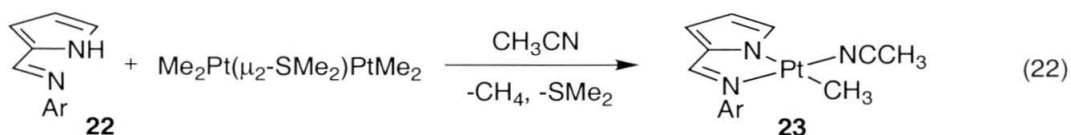
After several days at room temperature another C–H activation reaction at platinum(II) occurs as evidenced by the formation of another equivalent of ethane. We think that the cationic ethylplatinum(II) complex reacts with diethyl ether to form a carbene complex **21** (eq. 22). Peaks attributed to a vinyl ether platinum(II) complex **20** were also observed in ^1H NMR spectra. A similar reaction was reported for $[(\text{tmeda})\text{Pt}(\text{CH}_3)(\text{OEt}_2)]\text{BAr}_4^{\text{f}}$: intramolecular C–H activation first gives α -ethoxyethyl complex **19** which branches to the carbene hydride **21** and vinyl ether hydride **20**.⁸ For both phen and tmeda ligated systems, all intermediates eventually convert to the carbene hydride species.



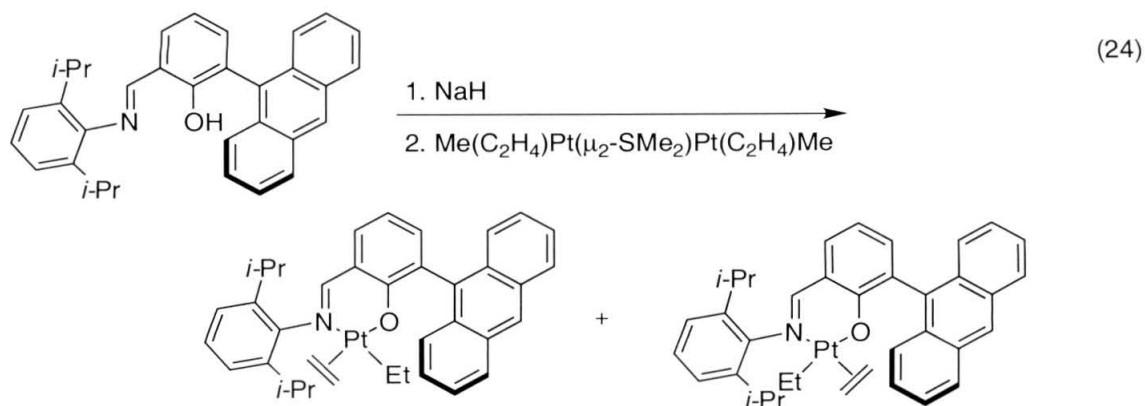
Chemistry of Neutral Complexes. The next step in our imaginary catalytic cycle (eq. 4) is oxidation of the olefin complex. Unfortunately, cationic ethylene

complex $[(\text{phen})\text{Pt}(\text{CH}_2\text{CH}_3)(\text{C}_2\text{H}_4)]\text{BAr}_4^f$ is stable to dioxygen or hydrogen peroxide in methanol. Based on our studies of the reaction of platinum(II) complexes with dioxygen, we anticipated that neutral complexes will be easier to oxidize than their cationic analogs.

A series of neutral platinum(II) complexes with monoanionic ligands was recently prepared in our group.²¹ The methyl compounds **23** were prepared in the reaction between $\text{Me}_2\text{Pt}(\mu_2\text{-SMe}_2)_2\text{PtMe}_2$ and pyrroles **22** in acetonitrile (eq. 22). However, the phenyl-substituted compounds **24** were isolated when reaction was carried out in benzene (eq. 23). This result implies that C–H activation occurs during the synthesis of the phenyl complexes, although the exact nature of reactive species is not yet clear.



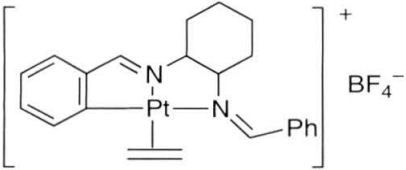
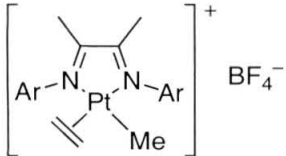
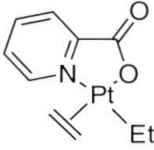
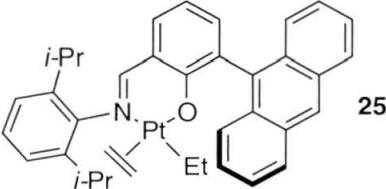
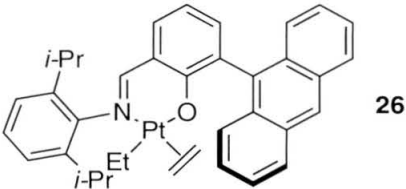
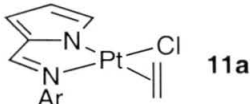
The neutral platinum(II) complexes of ethylene can be prepared starting with either Zeise's salt or $\text{Me}(\text{C}_2\text{H}_4)\text{Pt}(\mu_2\text{-Cl})_2\text{Pt}(\text{C}_2\text{H}_4)\text{Me}$ and deprotonated form of the pyrrole ligand (eqs. 13 and 14). Several other neutral olefin complexes have been prepared by analogous methods (eq. 24).²²



X-ray Structure Analysis. The olefin chloride **11a** was characterized by X-ray crystallography. The structural parameters of the coordinated ethylene in **11a** are compared with those of several analogous ethylene complexes of platinum(II) in Table 4. The length of the C=C bond ranges from 1.37 Å to 1.42 Å. It is evident that lengthening of the ethylene C=C bond is not determined solely by the overall charge of the olefin complex. It appears that comparisons can only be drawn for a series of closely related compounds as exemplified by **25** and **26**. In **26**, ethylene positioned trans to the strong σ -donor (imine) is farther away from platinum and, therefore, is not as stretched as when it is trans to a weaker ligand (alkoxide).

Table 4. Selected Bond Lengths of Platinum(II) Olefin Complexes. Ar is 1-(2,6-di-*iso*-propyl)phenyl, Pt-centroid distance is defined as the distance between the platinum atom and the midpoint between two olefinic carbons.

Compound	d(C=C), Å	d(Pt-centroid)*, Å	Ref.
K[PtCl ₃ (C ₂ H ₄)]	1.375	2.016	23
	1.376	2.063	24

	1.381	2.055	25
	1.27*	2.025*	26
	1.375 1.383 1.401 1.418		22
	1.40	2.09	22
	1.38	2.12	22
	1.373	2.028	this work

*This bond length is surprisingly short. Reexamination of the details of structure determination and refinement revealed that structure had a high degree of disorder and might not have been refined in the right space group. Although the chemical composition of the complex is sufficiently well-defined, the structural parameters are unreliable.

Rotation Barriers. Lewis and co-workers carried out an extensive study of the barriers of olefin rotation in platinum(II) complexes and proposed that those are mostly determined by steric effects.²⁷⁻³⁰ The authors pointed out, and Hoffman

and co-workers later confirmed computationally,³¹ that metal-based π -symmetry orbitals are available for bonding in both in-plane and out-of-plane orientation of ethylene. Thus, in both olefin and carbene complexes of platinum(II), the π -bonding ligands are perpendicular to the plane of platinum and are forced to use orthogonal d -orbitals for backbonding.

In some cases, the presence of strong σ -donors increases the barrier for olefin rotation. The rotation around Pt-(C₂H₄) bond in Me(C₂H₄)Pt(μ_2 -Cl)₂Pt(C₂H₄)Me freezes out at -65 °C, whereas the ¹H NMR spectrum of Cl(C₂H₄)Pt(μ_2 -Cl)₂Pt(C₂H₄)Cl is still fluxional even at -90 °C.³² The authors proposed that methyl group increases electron density on platinum and, therefore, π -backbonding leading to a higher barrier of rotation. Although purely σ -donating ligands do not directly change the energy of the $d\pi$ orbitals, the overall energy of the d -orbital set is raised during the ligand approach.

In this context, the higher barrier of ethylene rotation in **11a** compared to **12a** seemed counterintuitive. Taking computational results into consideration, it appears that steric effects are responsible for the observed trend. Our calculations suggest that the transition state for olefin rotation lies very close to the in-plane orientation of ethylene. Although the origin of this steric effect is not yet clear, we think that the higher *trans*-influence of the methyl group lengthens the Pt-N(imine) bond thus relaxing steric requirements around the olefin binding pocket (Table 2).

Conclusions

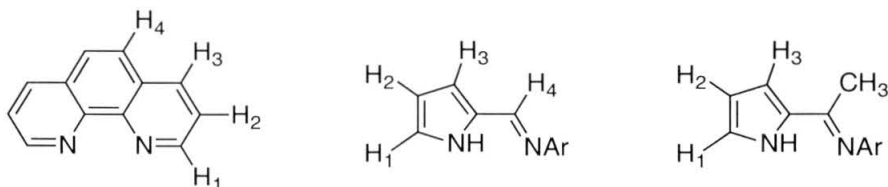
All of the chemistry described above relates to our attempts to develop a platinum(II)-catalyzed oxidative olefin dehydrogenation. It was previously

established in our group that C–H bond activation can be accomplished using cationic platinum(II) complexes. If alkanes with β -hydrogens are used, cationic olefin hydrides are formed. They can be prepared independently by treating (phen)PtEt₂ with [H(OEt₂)₂]BAr^f₄. Unfortunately, [(phen)Pt(C₂H₄)H]BF₄ is not very stable and eventually converts to carbene hydride [(phen)Pt(C(CH₃)OEt)H]BF₄. The formation of **7** is reversible and treatment with a good donor ligand results in the formation of ethyl complexes [(phen)Pt(C₂H₅)L]BF₄, L = C₂H₄, CH₃CN, or Et₂O. These compounds are air stable. [(phen)Pt(C₂H₅)(C₂H₄)]BF₄ does not react with dioxygen or hydrogen peroxide even at elevated temperatures. Since one of the steps of the proposed catalytic cycle is oxidation of a platinum(II) complex with dioxygen, we decided to prepare neutral olefin complexes hoping that neutral intermediates will be easier to oxidize. However, olefin complexes **11a** and **12b** do not react with dioxygen or hydrogen peroxide.

Putting well-studied individual steps of the proposed cycle together to form a working catalytic process is a formidable challenge. Electrophilic platinum(II) complexes, the very same compounds which are stable to oxidation with dioxygen, the most preferred stoichiometric oxidant, are needed to do C–H activation. Neutral complexes of platinum(II) with monoanionic ligands are more promising candidates. These complexes are capable of C–H activation,^{21,33} although the scope of this reaction remains to be studied. Despite early unsuccessful attempts to oxidize them, the complexes can be made more electron-rich through modifications of the ligand framework.

Experimental

General Considerations. All air and moisture sensitive compounds were manipulated using standard high-vacuum line, Schlenk or cannula techniques, or in a dry box under a nitrogen atmosphere, as described previously.³⁴ 1,10-phenanthroline (phen), 2-acetylpyrrole and Zeise's salt ($\text{K}[\text{PtCl}_3(\text{C}_2\text{H}_4)]$) were purchased from Aldrich. Ultra-high purity oxygen was purchased from Liquid Air Products and used without further purification. Solvents were purified by passage through solvent purification columns containing activated alumina.³⁵ The following compounds were prepared according to literature procedures: $(\text{C}_2\text{H}_4)(\text{CH}_3)\text{Pt}(\mu_2\text{-Cl})_2\text{Pt}(\text{C}_2\text{H}_4)(\text{CH}_3)$,³² $[\text{H}(\text{OEt}_2)_2][\text{BAr}^f_4]$.³⁶ Dimethylplatinum(II) complexes of α -diimines were prepared from $(\text{CH}_3)_2\text{Pt}(\mu_2\text{-(CH}_3)_2\text{S})_2\text{Pt}(\text{CH}_3)_2$ by the method published by Bercaw and co-workers.⁶ α -Diimines were prepared as described earlier. NMR spectra were acquired on Varian ^{UNITY}INOVA 500 (499.853 MHz for ^1H) and Varian *MERCURY-VX* 300 (300.08 MHz for ^1H). All ^1H NMR shifts are relative to the residual NMR solvent. The labeling is shown below. Elemental analyses were carried out by Midwest Microlab, Indianapolis, IN.



DFT Calculations. Density functional theory (DFT) calculations were carried out using the Jaguar software package.³⁷⁻⁴¹ Platinum was described using the LACVP Hay and Wadt effective core potential (ECP) to replace the core electrons

and using the standard double zeta contraction. In addition, all other atoms (C, Cl, N and H) were described using the 6-31G** basis.⁴² Collectively, this ECP basis is referred to as LACVP**. We used the generalized gradient approximate (GGA) but included exact exchange in the hybrid 3 parameter Becke scheme. The correlation density function was LYP. All structures in this study were optimized using this hybrid B3LYP method.

All geometries of stable intermediates and transition states were fully optimized with the above basis and methods. The geometries of the intermediates were optimized with no symmetry constraints.

Typical Procedure for Alkane Activation with 1. Cation **1** was prepared *in situ* by treating a slurry of **2** with 1 equiv. of aq. HBF₄. After substrate was added, the NMR tube was placed into a 45° oil bath for several hours. The progress of reaction was monitored by ¹H NMR spectroscopy. For more information see ref. 5.

(phen)Pt(CH₂CH₃)₂. (NBD)Pt(CH₂CH₃)₂ (450 mg, 1.14 mmol) and phenanthroline (205 mg, 1.14 mmol) were placed into a Schlenk flask. Toluene (5 ml) was added by syringe. The flask was placed into an oil bath at 75 °C. The reaction mixture was stirred for 9 hours. The color changed to red and deep red crystals started to form in the flask. The solution was cooled to room temperature and filtered. The crystals were washed with diethyl ether (3x15 mL) and dried *in vacuo*. Yield: (394 mg (79%). ¹H NMR (CD₂Cl₂, δ): 1.16 (t, 6H, ³J_{HH} = 8.0 Hz, ³J_{PtH} = 81.3 Hz, PtCH₂CH₃), 1.80 (q, 4H, ³J_{HH} = 8.0 Hz, ³J_{PtH} = 88.4 Hz, PtCH₂CH₃), 7.80 (dd, 2H, ³J_{HH} = 5.2 Hz, ³J_{HH} = 8.2 Hz, H₂ on phen), 7.87 (s, 2H, H₄ on phen), 8.57 (dd, 2H, ³J_{HH} = 1.3 Hz, ³J_{HH} = 8.2 Hz, H₃ on phen), 9.43 (dd, 2H, ³J_{HH} = 1.1 Hz, ³J_{HH} = 5.0 Hz, ³J_{PtH} = 23 Hz, H₁ on phen).

[(phen)Pt(C₂H₄)(CH₂CH₃)]BAr^f₄ (9). (phen)PtEt₂ was dissolved in 10 ml of CH₂Cl₂ at -40 °C under 1 atm of ethylene. Cold (-78 °C) solution of [H(OEt₂)₂]BAr^f₄ in CH₂Cl₂ was added by syringe. The reaction mixture turned yellow. The solution was warmed to room temperature and stirred for 1 hour. Volatiles were removed in *vacuo*. Yield (%). ¹H NMR (CD₂Cl₂, δ): 1.09 (t, 6H, ³J_{HH} = 7.7 Hz, ³J_{PtH} = 28.6 Hz, PtCH₂CH₃), 1.40 (q, 4H, ³J_{HH} = 7.5 Hz, ³J_{PtH} = 72.5 Hz, PtCH₂CH₃), 4.37 (s, 4H, ²J_{PtH} = 69.8 Hz, Pt(C₂H₄)), 7.54 (s, 4H, *p*-H in B(3,5-(CF₃)₂C₆H₃)₄), 7.73 (s, 8H, *o*-H in B(3,5-(CF₃)₂C₆H₃)₄), 8.03 (dd, 1H, ³J_{HH} = 5.5 Hz, ³J_{HH} = 8.0 Hz, H₂ on phen), 8.12 (s, 2H, H₄ on phen), 8.19 (dd, 1H, ³J_{HH} = 5.0 Hz, ³J_{HH} = 7.7 Hz, H₂ on phen), 8.47 (d, 1H, ³J_{HH} = 4.9 Hz, ³J_{PtH} = 15 Hz, H₁ on phen), 8.71 (d, 1H, ³J_{HH} = 7.7 Hz, H₃), 8.86 (d, 1H, ³J_{HH} = 7.7 Hz, H₃), 9.19 (d, 1H, ³J_{HH} = 5.5 Hz, ³J_{PtH} = 50 Hz, H₁ on phen).

[(phen)Pt(NCCH₃)(CH₂CH₃)]BAr^f₄ (10). (phen)PtEt₂ was dissolved in 10 ml of CH₃CN at -20 °C. Cold (-78 °C) solution of [H(OEt₂)₂]BAr^f₄ in CH₂Cl₂ was added by syringe. The reaction mixture turned yellow. The solution was warmed to room temperature and stirred for 1 hour. Volatiles were removed in *vacuo*. Yield (%). ¹H NMR (CD₂Cl₂, δ): 1.07 (t, 6H, ³J_{HH} = 7.5 Hz, ³J_{PtH} = 40 Hz, PtCH₂CH₃), 1.96 (q, 4H, ³J_{HH} = 7.5 Hz, ³J_{PtH} = 75 Hz, PtCH₂CH₃), 2.68 (s, 3H, ²J_{PtH} = 12 Hz, Pt(NCCH₃)), 7.54 (s, 4H, *p*-H in B(3,5-(CF₃)₂C₆H₃)₄), 7.71 (s, 8H, *o*-H in B(3,5-(CF₃)₂C₆H₃)₄), 7.99 (dd, 1H, ³J_{HH} = 5.5 Hz, ³J_{HH} = 7.5 Hz, H₂ on phen), 8.01 (dd, 1H, ³J_{HH} = 5.0 Hz, ³J_{HH} = 8 Hz, H₂ on phen), 8.07 (s, 1H, H₄ on phen), 8.08 (s, 1H, H₄ on phen), 8.71 (dd, 1H, ³J_{HH} = 8.5 Hz, ³J_{HH} = 1.5 Hz, H₃ on phen), 8.73 (dd, 1H, ³J_{HH} = 8.5 Hz, ³J_{HH} = 1 Hz, H₃ on phen), 9.03 (dd, 1H, ³J_{HH} = 5 Hz, ³J_{HH} = 1 Hz, H₁ on phen), 9.19 (d, 1H, ³J_{HH} = 5 Hz, ³J_{HH} = 1 Hz, ³J_{PtH} = 55 Hz, H₁ on phen).

$[(\text{phen})\text{Pt}(\text{OEt}_2)(\text{CH}_2\text{CH}_3)]\text{BAr}^f_4$ (8) and $[(\text{phen})\text{Pt}(\text{C}_2\text{H}_4)\text{H}]\text{BAr}^f_4$ (7). In a drybox, placed equimolar amounts of $(\text{phen})\text{PtEt}_2$ and $[\text{H}(\text{OEt}_2)_2][\text{BAr}^f_4]$. Methylene chloride- d_2 was added by vacuum transfer at $-78\text{ }^\circ\text{C}$. The solution was kept at $-78\text{ }^\circ\text{C}$ until it was placed into the cold NMR probe.

2-Acetylpyrrole-2,6-dimethylaniline imine. 2,6-Dimethylaniline (5ml, 0.04 mol) was placed into a 25 ml flask under air. Addition of methanol (5 ml) was followed by the addition of 2-acetylpyrrole (4.38 g, 0.04 mmol) and several drops of aq. HCOOH . The reaction was left to stir at room temperature for 1 day. Cooled the mixture to $0\text{ }^\circ\text{C}$ and filtered. Washed the precipitate with 10 ml of cold methanol. Dried *in vacuo*.

General Procedure for the Synthesis of 11. The pyrrole ligand (0.81 mmol) was dissolved in THF (15 ml) in a 50 ml Schlenk flask. The solution was cooled to $-20\text{ }^\circ\text{C}$ and $t\text{-BuLi}$ (0.6 ml of 1.6 M solution, 1.0 mmol, 1.2 equiv.) was added by syringe. The solution was stirred for 10 min before $\text{K}[\text{Pt}(\text{C}_2\text{H}_4)\text{Cl}_3]$ (300 mg, 0.81 mmol) was added. The reaction mixture was warmed up to room temperature and stirred for 45 min. All platinum starting material went into solution which changed the color to yellow. The reaction was quenched with water (10 ml). After diethyl ether (20 ml) was added and the aqueous layer washed twice with Et_2O (2x20ml), the combined organic layers were dried over MgSO_4 . Volatiles were removed *in vacuo*.

$(2\text{-C}_4\text{H}_3\text{N})\text{CH}=\text{N}(1\text{-}2,6\text{-}(i\text{-Pr})_2\text{-C}_6\text{H}_3)\text{Pt}(\text{C}_2\text{H}_4)\text{Cl}$ (11a). Yellow oil which gave dark yellow crystals after addition of petroleum ether. Yield 0.3 g (72%). ^1H NMR (CD_2Cl_2 , $23\text{ }^\circ\text{C}$, δ): 1.09 (d, 6H, $^3J_{\text{HH}} = 6.8\text{ Hz}$, $\text{CH}(\text{CH}_3)_2$), 1.37 (d, 6H, $^3J_{\text{HH}} = 6.8\text{ Hz}$, $\text{CH}(\text{CH}_3)_2$), 3.27 (sept, 2H, $^3J_{\text{HH}} = 6.8\text{ Hz}$, $\text{CH}(\text{CH}_3)_2$), 3.90 (s, 4H, $^2J_{\text{PH}} = 54.6$

Hz, Pt(C₂H₄)), 6.4 (dd, 1H, ³J_{HH} = 2.0 Hz, ³J_{HH} = 3.9 Hz, H₂), 6.89 (dd, 1H, ³J_{HH} = 3.9 Hz, ³J_{HH} = 1.0 Hz, H₃), 7.2-7.3 (m, 5H, H₁, H₄, -2,6-(*i*-Pr)₂C₆H₃).

(2-C₄H₃N)CH=N(1-2,6-(CH₃)₂-C₆H₃)Pt(C₂H₄)Cl (11b). Yellow solid. Yield 0.35 g (95%). ¹H NMR (CD₂Cl₂, 23 °C, δ): 2.19 (s, 6H, CH₃), 3.77 (s, 4H, ²J_{PH} = 54.3 Hz, Pt(C₂H₄)), 6.29 (dd, 1H, ³J_{HH} = 2.1 Hz, ³J_{HH} = 3.9 Hz, H₂), 6.83 (dd, 1H, ³J_{HH} = 3.9 Hz, ³J_{HH} = 1.0 Hz, H₃), 7.09 (s, 3H, 2,6-Me₂C₆H₃), 7.09 (s, 3H, 2,6-Me₂C₆H₃), 7.23, 7.28 (each s, each 1H, H₁, H₄).

(2-C₄H₃N)CH=N(1-3,5-(CH₃)₂-C₆H₃)Pt(C₂H₄)Cl (11c). Yellow solid. Crude yield 280 mg (75%). ¹H NMR (CD₂Cl₂, 23 °C, δ): 2.27 (s, 6H, CH₃), 3.96 (s, 4H, ²J_{PH} = 55.5 Hz, Pt(C₂H₄)), 6.26 (dd, 1H, ³J_{HH} = 2.1 Hz, ³J_{HH} = 4.2 Hz, H₂), 6.63 (s, 2H, *o*-H in 3,5-Me₂C₆H₃), 6.81 (dd, 1H, ³J_{HH} = 2.1 Hz, ³J_{HH} = 4.2 Hz, H₃), 6.93 (s, 1H, *p*-H in 3,5-Me₂C₆H₃), 7.24 (br s, 1H, ³J_{PH} = 24 Hz, H₁), 7.36 (s, 1H, ³J_{PH} = 86.4 Hz, H₄).

General Procedure for the Synthesis of 12. The pyrrole ligand (0.2 mmol) was dissolved in THF in a 50 ml Schlenk flask. The solution was cooled to -20 °C and *t*-BuLi (1.2 equiv.) was added by syringe. The solution was stirred for 10 min before (C₂H₄)(CH₃)Pt(μ₂-Cl)₂Pt(C₂H₄)(CH₃) (0.5 equiv.) was added. All platinum starting material went into solution which changed the color to yellow. The reaction mixture was stirred for 15 min at -20 °C. The reaction was quenched with water (5-10 ml). The organic phase was separated and washed with diethyl ether (2x15 ml). The combined organic layers were dried over MgSO₄. Volatiles were removed *in vacuo*.

(2-C₄H₃N)CH=N(1-2,6-(*i*-Pr)₂-C₆H₃)Pt(C₂H₄)Cl (12a). Yellow oil, solidified after a pentane wash. ¹H NMR (CD₂Cl₂, 23 °C, δ): 0.59 (s, 3H, ²J_{PH} = 76 Hz, PtCH₃), 0.97 (d, 6H, ³J_{HH} = 6.5 Hz, CH(CH₃)₂), 1.22 (d, 6H, ³J_{HH} = 6.5 Hz,

CH(CH₃)₂), 3.05 (sept, 2H, ³J_{HH} = 6.5 Hz, CH(CH₃)₂), 3.05 (s, 4H, ²J_{PtH} = 58.5 Hz, Pt(C₂H₄)), 6.02 (dd, 1H, ³J_{HH} = 2.0 Hz, ³J_{HH} = 3.5 Hz, H₂), 6.74 (dd, 1H, ³J_{HH} = 3.9 Hz, ⁴J_{HH} = 1.5 Hz, H₃), 7.0 (dd, 1H, ³J_{PtH} = 14 Hz, ³J_{HH} = 2.0 Hz, ⁴J_{HH} = 1.0 Hz, H₁), 7.13 (s, 3H, 2,6-(*i*-Pr)₂C₆H₃), 7.75 (s, ¹H, ³J_{PtH} = 30.5 Hz, H₄).

(2-C₄H₃N)CH=N(1-2,6-(CH₃)₂-C₆H₃)Pt(C₂H₄)Cl (12b). Yellow solid. ¹H NMR (C₆D₆, 23 °C, δ): 1.25 (s, 3H, ²J_{PtH} = 75.9 Hz, PtCH₃), 2.22 (s, 6H, CH₃), 3.25 (s, 4H, ²J_{PtH} = 59.1 Hz, Pt(C₂H₄)), 6.74 (dd, 1H, ³J_{PtH} = 19.8 Hz, ³J_{HH} = 2.1 Hz, ³J_{HH} = 3.9 Hz, H₂), 7.08 (dd, 1H, ³J_{HH} = 3.6 Hz, ³J_{HH} = 1.0 Hz, H₃), 7.15 (dd, 1H, both ³J_{HH} = 1.0 Hz, H₁), 7.16 (m, 3H, 2,6-Me₂C₆H₃), 7.72 (s, 1H, ³J_{PtH} = 18.3 Hz, H₄).

Structure Determination of 11a. X-ray quality crystals were obtained by slow evaporation of the solution of **11a** in CH₂Cl₂. All hydrogen atoms were refined as riding atoms because the thermal parameters of two hydrogen atoms (H2A and H6) refined to negative values and therefore prevented the least squares refinement from converging with a satisfactory shift/error value. The positional parameters of all the hydrogen atoms were satisfactory when unrestrained during least squares refinement.

Refinement of F² against ALL reflections. The weighted R-factor (*w*R) and goodness of fit (S) are based on F², conventional R-factors ® are based on F, with F set to zero for negative F². The threshold expression of F² > 2σ(F²) is used only for calculating R-factors(gt), *etc.*, and is not relevant to the choice of reflections for refinement. R-factors based on F² are statistically about twice as large as those based on F, and R-factors based on ALL data will be even larger.

All esds (except the esd in the dihedral angle between two l.s. planes) are estimated using the full covariance matrix. The cell esds are taken into account

individually in the estimation of esds in distances, angles and torsion angles; correlations between esds in cell parameters are only used when they are defined by crystal symmetry. An approximate (isotropic) treatment of cell esds is used for estimating esds involving l.s. planes.

Crystallographic data have been deposited at the CCDC, 12 Union Road, Cambridge CB2 1EZ, UK, and copies can be obtained on request, free of charge, by quoting the publication citation and the deposition number 162307.

References

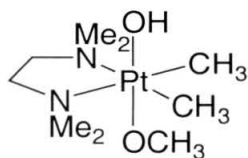
- (1) Arakawa, H.; Aresta, M.; Armor, J. N.; Barteau, M. A.; Beckman, E. J.; Bell, A. T.; Bercaw, J. E.; Creutz, C.; Dinjus, E.; Dixon, D. A.; Domen, K.; DuBois, D. L.; Eckert, J.; Fujita, E.; Gibson, D. H.; Goddard, W. A.; Goodman, D. W.; Keller, J.; Kubas, G. J.; Kung, H. H.; Lyons, J. E.; Manzer, L. E.; Marks, T. J.; Morokuma, K.; Nicholas, K. M.; Periana, R.; Que, L.; Rostrup-Nielsen, J.; Sachtler, W. M. H.; Schmidt, L. D.; Sen, A.; Somorjai, G. A.; Stair, P. C.; Stults, B. R.; Tumas, W. *Chem. Rev.* **2001**, *101*, 953-996.
- (2) Parshall, G. W.; Ittel, S. D. *Homogeneous Catalysis*; 2nd ed.; John Wiley & Sons, Inc.: New York, 1992.
- (3) Tullo, A. H. *Chem. Eng. News* **2001**, *79*, 18-24.
- (4) Jensen, C. M. *Chem. Commun. (Cambridge)* **1999**, 2443-2449.
- (5) Khodakov, A.; Olthof, B.; Bell, A. T.; Iglesia, E. *Journal of Catalysis* **1999**, *181*, 205-216.
- (6) Zhong, A. Z.; Labinger, J. A.; Bercaw, J. E. *J. Am. Chem. Soc.*, to be submitted.
- (7) Rosenblum, M. *Acc. Chem. Res.* **1974**, *7*, 122.
- (8) Holtcamp, M. W.; Labinger, J. A.; Bercaw, J. E.; Henling, L. M.; Day, M. W. *Inorg. Chim. Acta* **1998**, *270*, 467-478.
- (9) Chaudhury, N.; Puddephatt, R. C. *J. Organomet. Chem.* **1975**, *84*, 105-115.
- (10) James, B. R. *Homogeneous Hydrogenation*; Wiley: New York, 1973.
- (11) Vanleeuwen, P.; Roobeek, C. F.; Frijns, J. H. G.; Orpen, A. G. *Organometallics* **1990**, *9*, 1211-1222.

- (12) Stein, J.; Lewis, L. N.; Gao, Y.; Scott, R. A. *J. Am. Chem. Soc.* **1999**, *121*, 3693-3703.
- (13) Tagge, C. D.; Simpson, R. D.; Bergman, R. G.; Hostetler, M. J.; Girolami, G. S.; Nuzzo, R. G. *J. Am. Chem. Soc.* **1996**, *118*, 2634-2643.
- (14) Whitesides, G. M.; Gaasch, J. F.; Stedronsky, E. R. *J. Am. Chem. Soc.* **1972**, *94*, 5258-5270.
- (15) McCarthy, T. J.; Nuzzo, R. G.; Whitesides, G. M. *J. Am. Chem. Soc.* **1981**, *103*, 3396-3403.
- (16) Whitesides, G. M. *Pure Appl. Chem.* **1981**, *53*, 287-292.
- (17) Azam, K. A.; Brown, M. P.; Cooper, S. J.; Puddephatt, R. J. *Organometallics* **1982**, *1*, 1183-1188.
- (18) Carr, N.; Mole, L.; Orpen, A. G.; Spencer, J. L. *J. Chem. Soc., Dalton Trans.* **1992**, 2653-2662.
- (19) Mole, L.; Spencer, J. L.; Carr, N.; Orpen, A. G. *Organometallics* **1991**, *10*, 49-52.
- (20) White, S.; Bennett, B. L.; Roddick, D. M. *Organometallics* **1999**, *18*, 2536-2542.
- (21) Scollard, J. D.; Carter, C. A. G.; Bercaw, J. E.; Labinger, J. A.; Baker, R. T., manuscript in preparation.
- (22) Younkin, T. R., personal communication.
- (23) Kwick, A.; Koetzle, T. F.; Thomas, R. *J. Chem. Phys.* **1974**, *61*, 2711-2719.
- (24) Gervasio, G.; Mason, S. A.; Maresca, L.; Natile, G. *Inorg. Chem.* **1986**, *25*, 2207-2211.
- (25) Baar, C. R.; Jenkins, H. A.; Yap, G. P. A.; Puddephatt, R. J. *Organometallics* **1998**, *17*, 4329-4331.

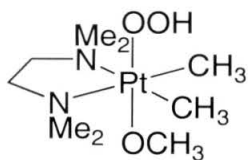
- (26) Fusto, M.; Giordano, F.; Orabona, I.; Ruffo, F.; Panunzi, A. *Organometallics* **1997**, *16*, 5981-5987.
- (27) Ashley-Smith, J.; Souek, Z.; Johnson, B. F. G.; Lewis, J. J. *Chem. Soc., Dalton Trans.* **1974**, 128-133.
- (28) Ashley-Smith, J.; Douek, I.; Johnson, B. F. G.; Lewis, J. J. *Chem. Soc., Dalton Trans.* **1972**, 1776-1780.
- (29) Holloway, C. E.; Hulley, G.; Johnson, B. F. G.; Lewis, J. J. *Chem. Soc. A* **1970**, 1653-1658.
- (30) Holloway, C. E.; Hulley, G.; Johnson, B. F. G.; Lewis, J. J. *Chem. Soc. A* **1969**, 53-57.
- (31) Albright, T. A.; Hoffmann, R.; Thibault, J. C.; Thorn, D. L. *J. Am. Chem. Soc.* **1979**, *101*, 3801-3812.
- (32) Scott, J. D.; Puddephatt, R. J. *Organometallics* **1986**, *5*, 1253-1257.
- (33) Wick, D. D.; Goldberg, K. I. *J. Am. Chem. Soc.* **1997**, *119*, 10235.
- (34) Shriver, D. F.; Drezdson, M. A. *The Manipulation of Air-Sensitive Compounds*; 2nd ed.; John Wiley & Sons: New York, 1986.
- (35) Pangborn, A. B.; Giardello, M. A.; Grubbs, R. H.; Rosen, R. K.; Timmers, F. *J. Organometallics* **1996**, *15*, 1518-1520.
- (36) Brookhart, M.; Grant, B.; Volpe, A. F. *Organometallics* **1992**, *11*, 3920-3922.
- (37) Ringnalda, M. N.; Langlois, J.; Murphy, R. B.; Greeley, B. H.; Cortis, C.; Russo, T. V.; Marten, B.; Donnely, R. E.; Pollard, W. T.; Cao, Y.; Muller, R. P.; Mainz, D. T.; Wright, J. R.; Miller, G. H.; Goddard, W. A. I.; Friesner, R. A., *Jaguar PS-GVB*, v. 2.3, Schrodinger, Inc., **1996**.
- (38) Hay, P. J.; Wadt, W. R. *J. Phys. Chem.* **1985**, *82*, 270.
- (39) Frisch, M. J.; Pople, J. A.; Binkley, J. S. *J. Phys. Chem.* **1984**, *80*.

- (40) Slater, J. C. *Quantum Theory of Molecules and Solids, vol. 4: The Self-Consistent Field for Molecules and Solids*; McGraw-Hill: New York, 1974.
- (41) Perdrew, J. P. *Electronic Structure Theory of Solids*; Akademie Verlag: Berlin, 1991.
- (42) Kaupp, M.; vR., S. P.; Dolg, M.; Stoll, H. J. *Am. Chem. Soc.* **1992**, *114*, 8202.

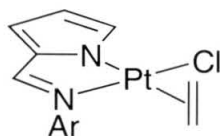
Compound Nomenclature for Appendices



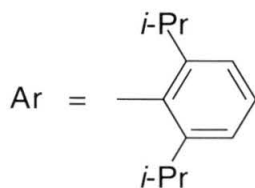
Structure 1



Structure 2



Structure 3



STRUCTURE DETERMINATION OF 1

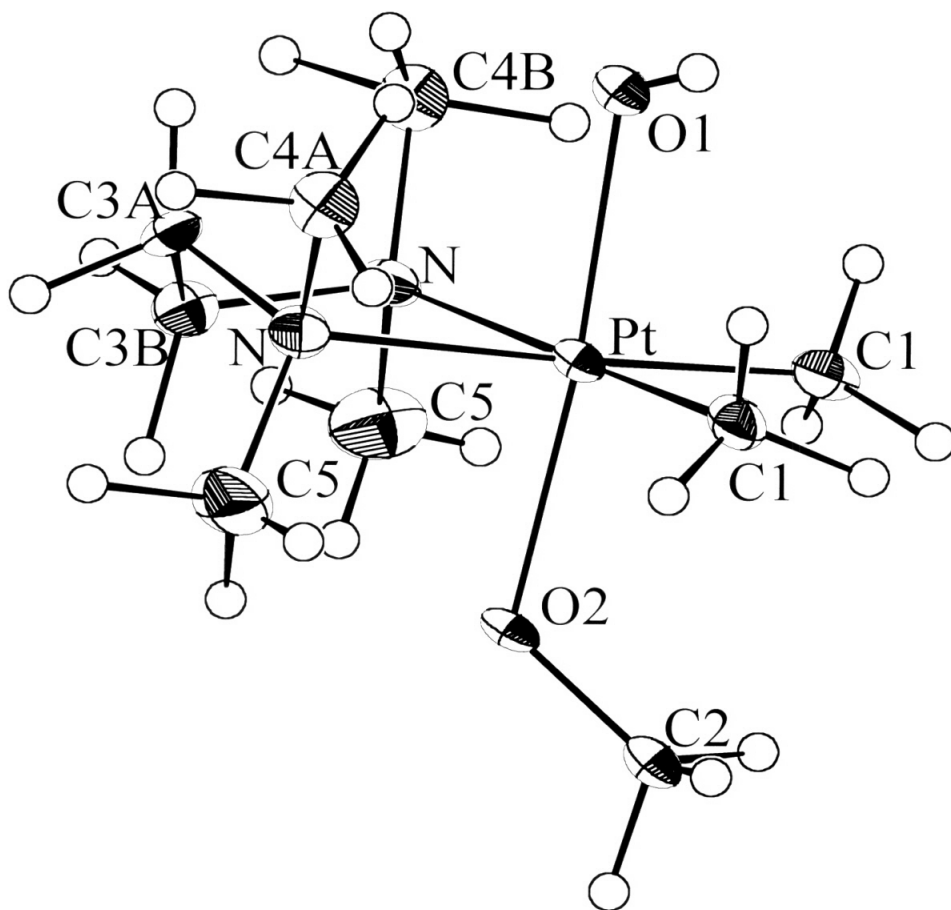


Figure 1. Labeled Diamond view of **1**, with 50% ellipsoids. Hydrogen atoms other than H0A have been omitted.

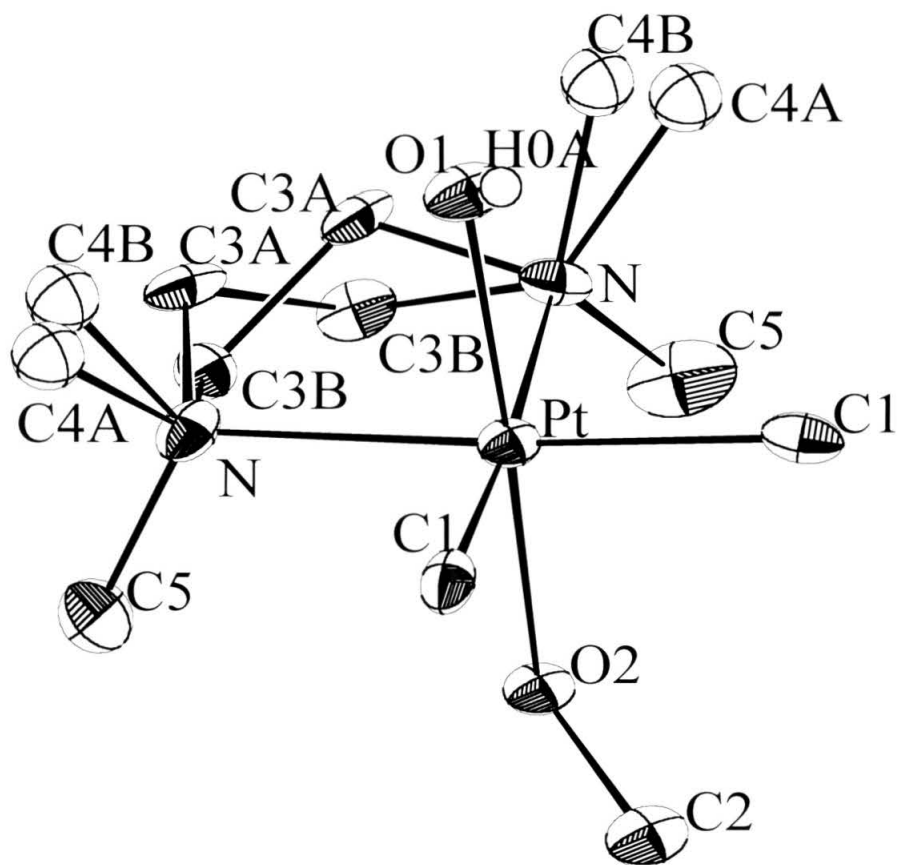
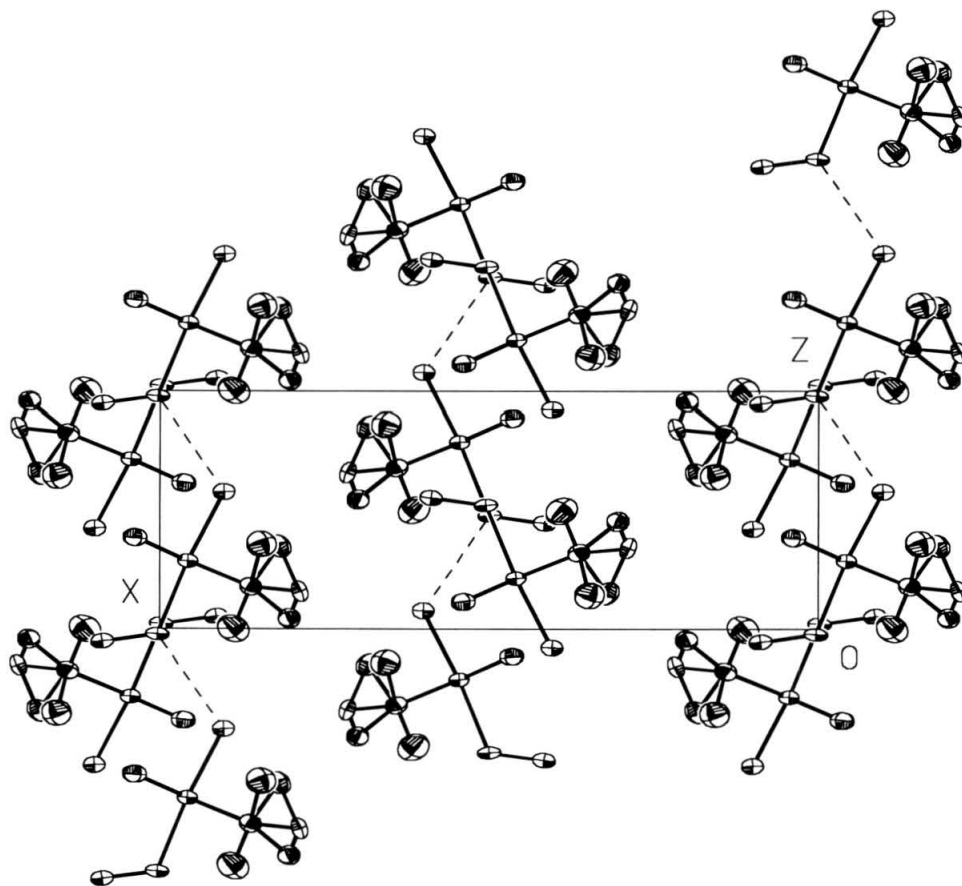


Figure 2. Crystal packing in **1** viewed along the *b* axis, showing the unit cell boundaries, with 50% ellipsoids. Hydrogen atoms have been omitted. Note intermolecular hydrogen bonds.



Crystal Data Details for 1

Empirical formula	C ₉ H ₂₆ N ₂ O ₂ Pt
Formula weight	389.41
Crystallization solvent	methanol
Crystal shape	prismatic
Crystal color	colorless
Crystal size	0.11 x 0.13 x 0.15 mm

Data Collection

Type of diffractometer	CAD-4
Wavelength	0.71073 Å MoK α
Data collection temperature	84 K
Theta range for 25 reflections used in lattice determination	13 to 14°
Unit cell dimensions	a = 16.101(5) Å $\alpha = 90^\circ$ b = 13.245(4) Å $\beta = 90^\circ$ c = 6.134(2) Å $\gamma = 90^\circ$
Volume	1308.1(7) Å ³
Z	4
Crystal system	orthorhombic
Space group	Pnma (# 62)
Density (calculated)	1.977 g/cm ³
F(000)	752
Theta range for data collection	1.5 to 25°
Completeness to theta = 25°	100.0%
Index ranges	-19 ≤ h ≤ 19, -15 ≤ k ≤ 0, -7 ≤ l ≤ 7
Data collection scan type	ω -scan
Reflections collected	5701
Independent reflections	1203 [R _{int} = 0.013]
Reflections > 2 σ (I)	1026
Average σ (I)/(net I)	0.0299

Absorption coefficient	10.71 mm ⁻¹
Absorption correction	ψ-scan (North, 1968)
Max. and min. transmission	1.10 and 0.89
Reflections monitored for decay	75
Decay of standards	0%

Structure Solution and Refinement

Primary solution method	direct methods
Secondary solution method	difference map
Hydrogen placement	calculated
Refinement method	full-matrix least-squares on F ²
Data / restraints / parameters	1203 / 0 / 133
Treatment of hydrogen atoms	coordinates refined, U _{iso} fixed at 120% U _{eq} of attached atom
Goodness-of-fit on F ²	1.828
Final R indices	
[I > 2σ(I), 1026 reflections]	R1 = 0.0297, wR2 = 0.0533
R indices (all data)	R1 = 0.0460, wR2 = 0.0593
Type of weighting scheme used	sigma
Weighting scheme used	w = 1 / σ ² (Fo ²)
Max shift/error	0.155
Average shift/error	0.011
Largest diff. peak and hole	1.62 and -2.31 e·Å ⁻³

Programs Used

Cell refinement	CAD-4 Software (Enraf-Nonius, 1989)
Data collection	CAD-4 Software (Enraf-Nonius, 1989)
Data reduction	CRYM (Duchamp, 1964)
Structure solution	SHELXS-97 (Sheldrick, 1990)
Structure refinement	SHELXL-97 (Sheldrick, 1997)
Graphics	Diamond, Bruker SHELXTL v5.1

References

- Diamond 2.1. (2000) Crystal Impact GbR, Bonn, Germany.
- Duchamp, D. J. (1964). Am. Crystallogr. Assoc. Meet., Bozeman, Montana., Paper B14, 29-30
- Nonius. (1989). CAD-4 Software. Version 5. Nonius, Delft, The Netherlands
- Spek, A.L. (1990). *Acta Cryst.*, A46, C-34.
- Sheldrick, G. M. (1990). *Acta Cryst.*, A46, 467-473.
- Sheldrick, G. M. (1997). SHELXL-97. Program for Structures Refinement. Univ. of Gottingen, Federal Republic of Germany

Special Refinement Details

Four crystals were examined on the diffractometer; data were only collected for the last. The first three crystals were discarded due to broad diffraction peaks and severe indexing problems. The crystals were mounted on a glass fiber with Paratone-N oil. Data were collected with 1.5° ω -scans because of the poor crystal quality.

The individual backgrounds were replaced by a background function of two theta derived from weak reflections with $I < 3\sigma(I)$. For point group *mmm*, the $\text{GOF}_{\text{merge}}$ was 1.08 (1203 multiples); R_{int} was 0.013 for 94 duplicates (there are only a few duplicates since four equivalent sets of reflections were collected). Y-scan data were used for the absorption correction. There was no decay. Weights were calculated as $1/s^2(F_o^2)$; variances ($s^2(F_o^2)$) were derived from counting statistics plus an additional term, $(0.014I)^2$; variances of the merged data were obtained by propagation of error plus another additional term, $(0.014\langle I \rangle)^2$.

No reflections were specifically omitted from the final processed dataset. Refinement of F^2 was against all reflections. The weighted R-factor (wR) and goodness of fit (S) are based on F^2 , conventional R-factors (R) are based on F , with F set to zero for negative F^2 . The threshold expression of $F^2 > 2\sigma(F^2)$ is used only for calculating R-factors(gt), etc., and is not relevant to the choice of reflections for refinement.

The molecule lies on a mirror plane, which contains the heavy atoms Pt, O1, O2, C2 and bisects the tmeda. The tmeda backbone carbon C3 and one of the

methyl groups, C4, are each disordered over two sites (C3A, C3B and C4A, C4B) with occupancy $\frac{1}{2}$ since C3A is bonded to the mirror image of C3B. The coordinates of all hydrogen atoms including the half-populated sites were refined with U_{iso} 's fixed at 120% of the U_{eq} of the attached atom. All bonds involving the hydrogen atoms are reasonable given the large esd's. There is a hydrogen bond between O1 and the O2 at $x, y, z-1$ ($\text{O1}\cdots\text{O2}$ is $2.946(9)\text{\AA}$ and the O1-H1A-O2 angle is $172(18)^\circ$), which forms a linear chain of molecules along the c axis.

The largest shift/esd of 0.155 is for the x coordinate of the half-hydrogen H3AA which oscillates approximately 0.05\AA from cycle to cycle. Seventeen peaks in the final difference map have intensities $\geq |1| \text{ e}\cdot\text{\AA}^{-3}$; the two largest are $-2.31 \text{ e}\cdot\text{\AA}^{-3}$ (0.92\AA from Pt) and $1.62 \text{ e}\cdot\text{\AA}^{-3}$ (0.89\AA from Pt). Nine of these peaks, with intensities up to $1.45 \text{ e}\cdot\text{\AA}^{-3}$ and $-1.53 \text{ e}\cdot\text{\AA}^{-3}$, are in the vicinity of the disordered region. There are several close intermolecular contacts between both H0A and H5A (C5 was not split into two sites) and the hydrogens in the disordered region. Clearly, there are some subtleties to the disorder/packing that are not readily modeled.

Table 1. Atomic coordinates ($\times 10^4$) and equivalent isotropic displacement parameters ($\text{\AA}^2 \times 10^3$) for **1**. $U(\text{eq})$ is defined as one third of the trace of the orthogonalized U_{ij} tensor.

	x	y	z	U_{eq}
Pt	4569(1)	7500	2137(1)	24(1)
O1	4018(5)	7500	-776(11)	38(2)
O2	5027(5)	7500	5218(10)	29(2)
N	3613(3)	6391(5)	3215(8)	31(1)
C1	5369(5)	6432(6)	1148(11)	32(2)
C2	5864(7)	7500	5534(17)	37(3)
C3A ^a	2863(12)	6983(16)	3420(30)	36(5)
C4A ^a	3439(15)	5580(20)	1410(30)	40(5) ^b
C3B ^a	3022(12)	7046(14)	4540(40)	34(5)
C4B ^a	3169(15)	5886(19)	1500(30)	41(5) ^b
C5	3875(7)	5729(9)	4983(17)	60(3)

^a Population: 1/2

^b U_{iso}

Table 2. Bond lengths [Å] and angles [°] for **1**.

Pt-O1	1.995(7)	C4B-N-C5	114.2(11)
Pt-C1	2.007(8)	C3A-N-C5	120.3(10)
Pt-O2	2.028(6)	C4B-N-C3B	110.1(14)
Pt-N	2.229(6)	C5-N-C3B	97.3(10)
O1-H0A	0.55(12)	C3A-N-C4A	106.5(14)
O2-C2	1.362(13)	C5-N-C4A	99.4(12)
N-C4B	1.436(19)	C4B-N-Pt	115.7(9)
N-C3A	1.445(19)	C3A-N-Pt	104.2(9)
N-C5	1.457(11)	C5-N-Pt	114.6(5)
N-C3B	1.52(2)	C3B-N-Pt	102.4(8)
N-C4A	1.57(2)	C4A-N-Pt	111.5(8)
C1-H1A	1.00(7)	Pt-C1-H1A	113(4)
C1-H1B	0.91(8)	Pt-C1-H1B	112(5)
C1-H1C	0.89(8)	H1A-C1-H1B	111(6)
C2-H2A	1.00(11)	Pt-C1-H1C	112(5)
C2-H2B	0.94(7)	H1A-C1-H1C	112(6)
C3A-C3B ⁱ	1.48(2)	H1B-C1-H1C	96(6)
C3A-H3AA	1.0(3)	O2-C2-H2A	115(6)
C3A-H3AB	0.91(14)	O2-C2-H2B	116(5)
C4A-H4AA	1.13(16)	H2A-C2-H2B	100(6)
C4A-H4AB	0.94(17)	N-C3A-H3AA	120(10)
C4A-H4AC	1.0(2)	N-C3A-H3AB	123(9)
C3B-H3BA	0.9(3)	H3AA-C3A-H3AB	95(10)
C3B-H3BB	1.09(13)	N-C4A-H4AA	108(8)
C4B-H4BA	1.19(16)	N-C4A-H4AB	103(10)
C4B-H4BB	1.1(2)	H4AA-C4A-H4AB	94(10)
C4B-H4BC	0.86(18)	N-C4A-H4AC	94(10)
C5-H5A	1.08(10)	H4AA-C4A-H4AC	126(10)
C5-H5B	0.83(10)	H4AB-C4A-H4AC	130(10)
C5-H5C	0.95(10)	N-C3B-H3BA	106(10)
C4A...C4B	0.60(3)	N-C3B-H3BB	111(7)
C3A...C3B	0.74(2)	H3BA-C3B-H3BB	104(10)
O1-Pt-C1	90.8(3)	N-C4B-H4BA	111(8)
C1 ⁱ -Pt-C1	89.6(5)	N-C4B-H4BB	93(10)
O1-Pt-O2	174.9(3)	N-C4B-H4BC	102(10)
C1-Pt-O2	92.8(3)	H4BA-C4B-H4BC	102(10)
O1-Pt-N	87.6(2)	H4BB-C4B-H4BC	120(10)
C1 ⁱ -Pt-N	176.1(3)	N-C5-H5A	111(5)
C1-Pt-N	93.9(3)	N-C5-H5B	116(7)
O2-Pt-N	88.6(2)	H5A-C5-H5B	106(8)
N-Pt-N ⁱ	82.5(3)	N-C5-H5C	110(6)
Pt-O1-H0A	113(10)	H5A-C5-H5C	108(7)
C2-O2-Pt	119.5(6)	H5B-C5-H5C	104(9)

Appendix B

STRUCTURE DETERMINATION OF 2

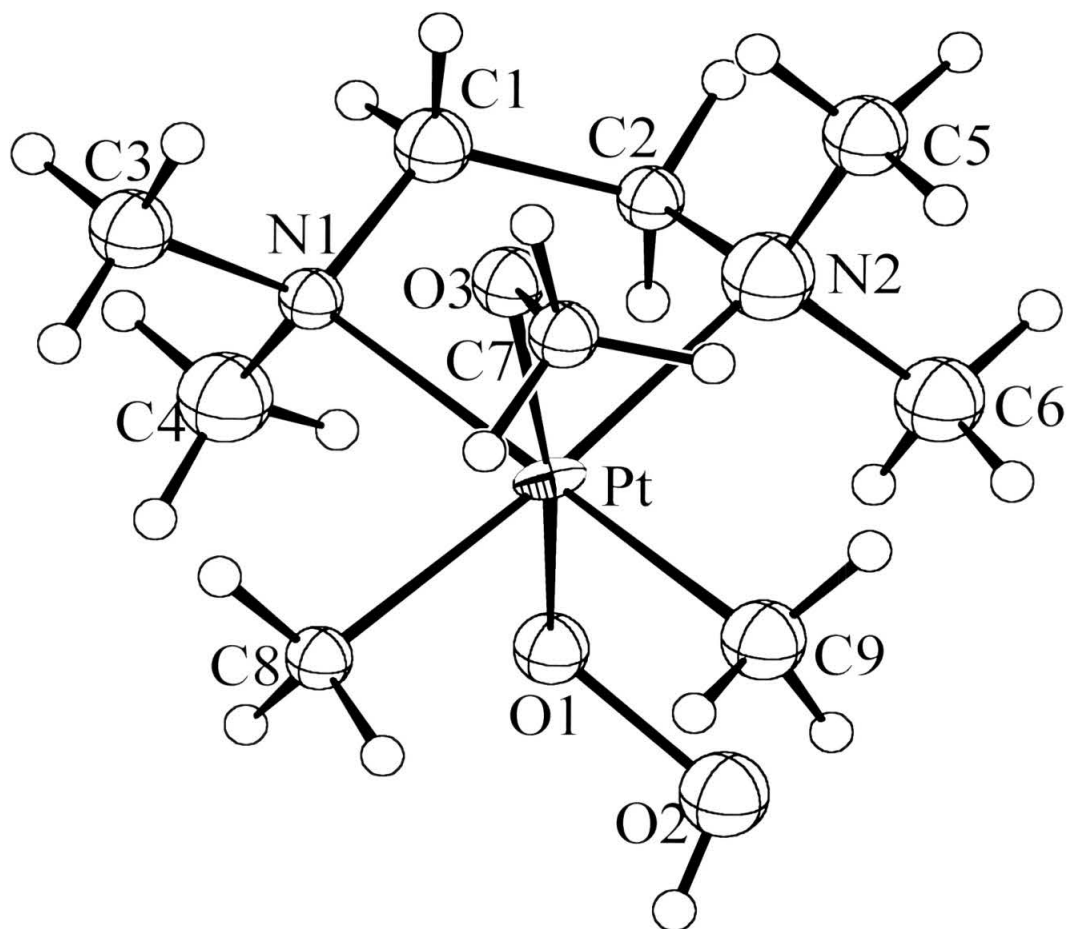


Figure 1. Unlabeled Diamond view of the molecule, with 50% ellipsoids (only Pt is anisotropic). Orientation A is in black and orientation B in dark grey. Hydrogen atoms are at arbitrary scale.

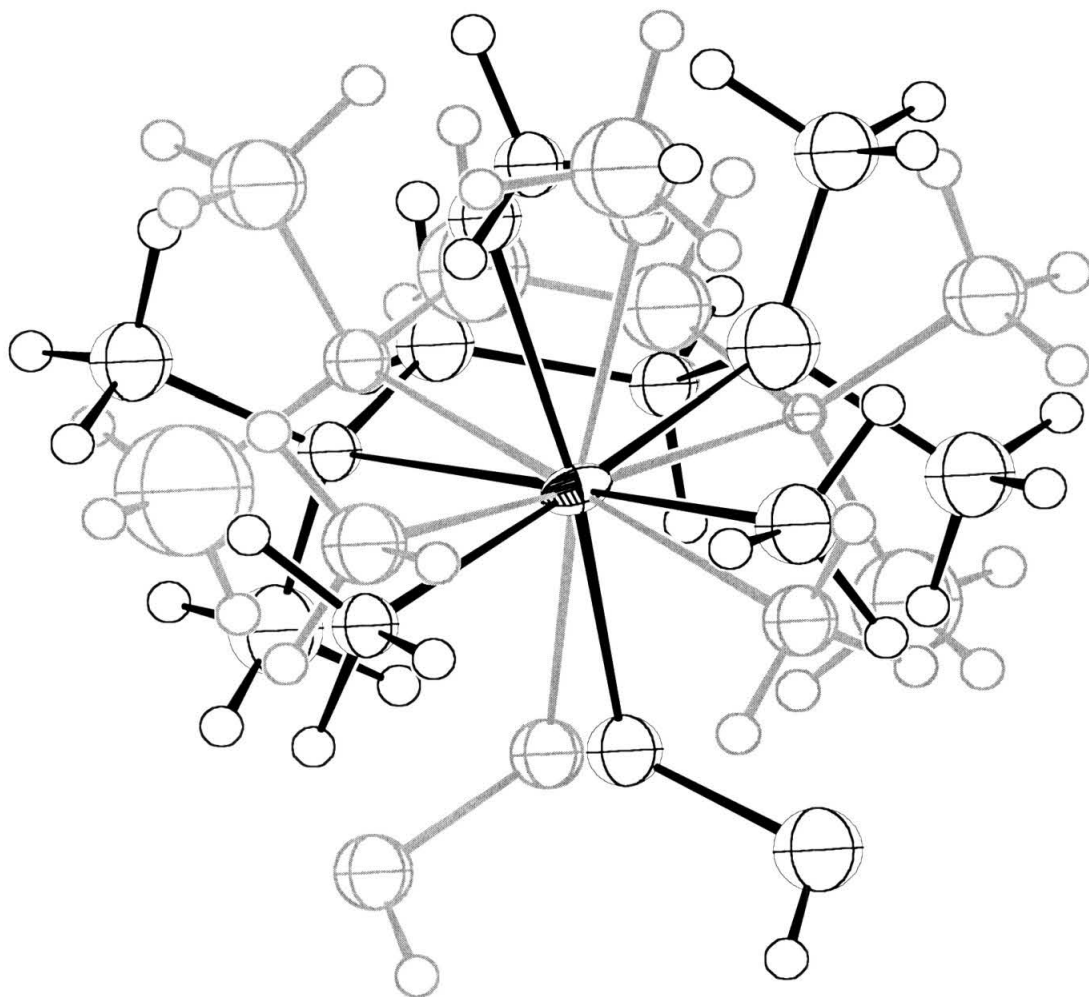
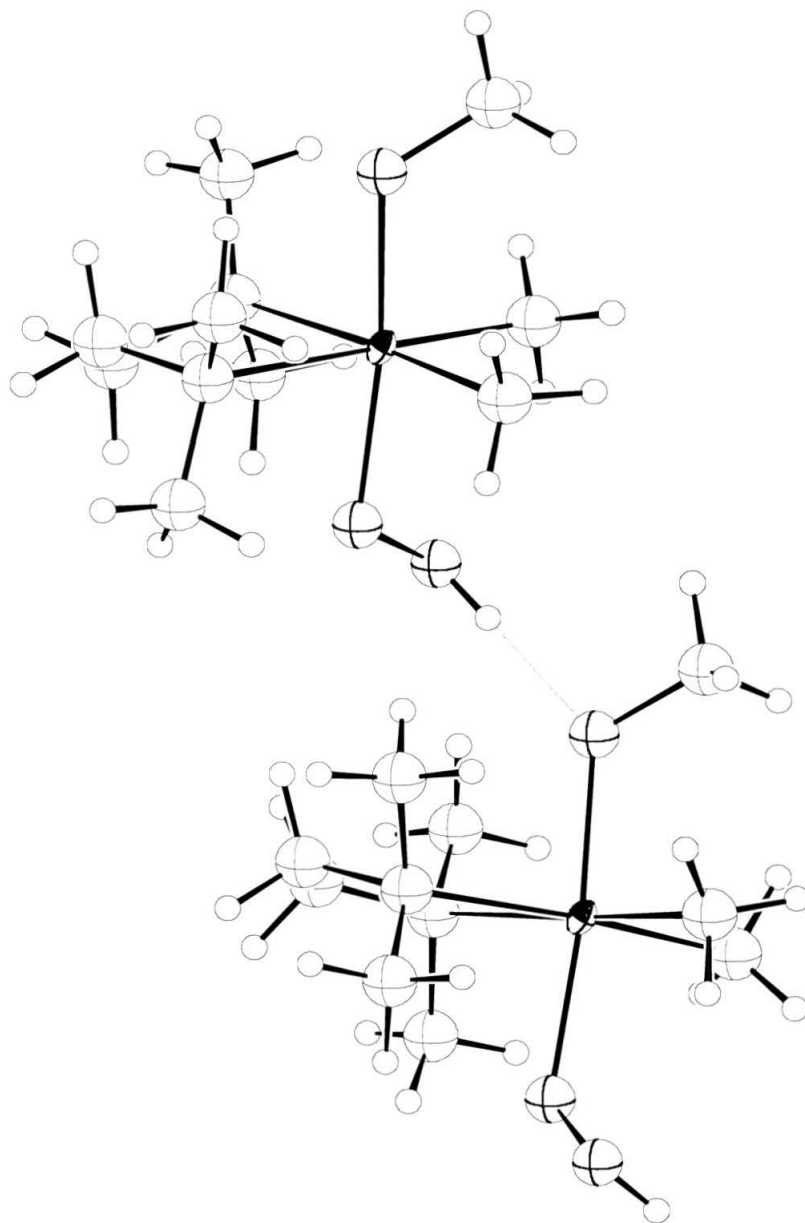


Figure 2. Unlabeled Diamond view of an $A(x+1,y,z, \text{top})$, $B(x,y,z, \text{bottom})$ pair of molecules showing the hydroperoxy-methoxy hydrogen bonding.



Crystal Data Details for 2

Empirical formula	C ₉ H ₂₆ N ₂ O ₃ Pt
Formula weight	405.41
Crystallization solvent	acetone
Crystal shape	irregular thin wedge
Crystal color	colorless
Crystal size	0.07 x 0.21 x 0.22 mm

Data Collection

Preliminary photograph(s)	rotation
Type of diffractometer	Bruker SMART 1000 ccd
Wavelength	0.71073 Å MoK α
Data collection temperature	98 K
Theta range for 8290 reflections used in lattice determination	2.7 to 28.4°
Unit cell dimensions	a = 6.5985(8) Å α = 90° b = 13.5019(16) Å β = 93.408(2)° c = 14.9187(18) Å γ = 90°
Volume	1326.8(3) Å ³
Z	4
Crystal system	monoclinic
Space group	P 2 ₁ /n (# 14)
Density (calculated)	2.030 g/cm ³
F(000)	784
Theta range for data collection	2.0 to 25.0°
Completeness to theta = 25.00°	100.0%
Index ranges	-7 ≤ h ≤ 7, -16 ≤ k ≤ 16, -17 ≤ l ≤ 17
Data collection scan type	ω scans at 5 fixed ϕ values
Reflections collected	16295
Independent reflections	2335 [R _{int} = 0.0741]
Reflections > 2 σ (I)	2096

Average $\sigma(I)/(\text{net } I)$	0.0424
Absorption coefficient	10.57 mm^{-1}
Absorption correction	empirical
Max. and min. transmission	1.000 and 0.471
Reflections monitored for decay	first 75 scans recollected at end of runs
Decay of standards	0%

Structure Solution and Refinement

Primary solution method	direct methods
Secondary solution method	difference map
Hydrogen placement	calculated
Refinement method	full-matrix least-squares on F^2
Data / restraints / parameters	2335 / 0 / 123
Treatment of hydrogen atoms	not refined, U_{iso} fixed at 120% U_{eq} of attached atom
Goodness-of-fit on F^2	2.20
Final R indices	
[$I > 2\sigma(I)$, 2096 reflections]	$R1 = 0.0458$, $wR2 = 0.0990$
R indices (all data)	$R1 = 0.0516$, $wR2 = 0.1001$
Type of weighting scheme used	sigma
Weighting scheme used	$w = 1/s^2(F_o^2)$
Max shift/error	0.020
Average shift/error	0.001
Largest diff. peak and hole	2.98 and $-2.73 \text{ e} \cdot \text{\AA}^{-3}$

Programs Used

Cell refinement	Bruker SMART v5.606, Bruker SAINT v6.02
Data collection	Bruker SMART v5.060
Data reduction	Bruker SAINT v6.02
Structure solution	SHELX-97 (Sheldrick, 1997)
Structure refinement	SHELX-97 (Sheldrick, 1997)
Graphics	Diamond, Bruker SHELXTL v5.1

References

- Bruker (1999) SMART (v5.060), SMART (v5.606), SAINT (v6.02) and SHELXTL (v5.1). Bruker AXS Inc., Madison, Wisconsin, USA.
- Diamond 2.1. (2000) Crystal Impact GbR, Bonn, Germany.
- Spek, A.L. (1990). *Acta Cryst.*, **A46**, C-34.
- Sheldrick, G. M. (1997). SHELXL-97. Program for Structures Refinement. Univ. of Gottingen, Federal Republic of Germany.

Special Refinement Details

A semi-opaque, rounded thin wedge was selected from a batch of freshly grown crystals and mounted on a glass fiber with Paratone-N oil. This sample was the best of many chosen from a number of crystallizations; data collected at room temperature were no better than low-temperature data. Five runs of data were collected with 15 second long, -0.3° wide ω -scans at five values of χ (0, 120, 240, 180, and 300°) with the detector 5 cm (nominal) distant at a θ of -28° . The spots were broad and sometimes split. The initial cell for data reduction was calculated from 999 centered reflections chosen from throughout the data frames. A total of 41 reflections was discarded in the triclinic least-squares with a reciprocal lattice vector tolerance of 0.008 (0.005 is customary). Of the rejects, 20 had substantially non-integral indices and presumably are from a small fragment with a different orientation. There was no evidence of a larger cell. For data processing with SAINT v6.02, all defaults were used, except: a fixed box size of $2.0 \times 2.0 \times 1.2$ was used, periodic orientation matrix updating was disabled, the instrument error was set to zero, no Laue class integration restraints were used, and for the post-integration global least squares refinement, no constraints were applied. The profiles exhibited an apparently considerable truncation of many reflections, especially in the z -direction. A number of both larger and smaller box sizes were tried but gave worse refinements of the structure. Both the initial cell refinement and the global cell refinement gave an ω zero $\sim 0.4^\circ$ too negative. No decay correction was needed. The crystal boundaries were rudely indexed as faces; these were not good enough for a face-indexed absorption correction. A SADABS v2.03 beta correction was applied (relative correction factors: 1.000 to

0.471) with $g = 0.113$, 100 refinement cycles, and defaults for the remaining parameters. Again, a number of other options such as discarding portions of the data and using different orders of Bessel functions did not lead to a better model refinement.

No reflections were specifically omitted from the final processed dataset but the data were truncated at a 2θ of 50° as the high angle spots seemed fuzzier; 3469 reflections were rejected, with 20 space group-absence violations, 0 inconsistent equivalents, and no reflections suppressed. Refinement of F^2 was against all reflections. The weighted R-factor (wR) and goodness of fit (Σ) are based on F^2 , conventional R-factors (R) are based on F , with F set to zero for negative F^2 . The threshold expression of $F^2 > 2\sigma(F^2)$ is used only for calculating R-factors(gt), *etc.*, and is not relevant to the choice of reflections for refinement.

The asymmetric unit consists of one molecule of $\text{Pt}(\text{tmeda})(\text{CH}_3)_2(\text{OOH})(\text{OCH}_3)$, which is disordered $\sim 1:1$ over two orientations. All atoms except the platinum were split and modeled with two sites. The major difference between the two orientations is the position of the terminal hydroperoxy oxygen atom; it can lie under either of the two methyl groups. The rest of the molecule tilts to accommodate these two positions, as can be seen above. Orientation A has a slightly more reasonable structure than orientation B, which has a carbon atom (C1B of the tmeda backbone) with distorted geometry. This distortion is most likely due to additional disorder of the tmeda, a failing to which this ligand is all too prone; see, e.g., structure **1**, $\text{Pt}(\text{tmeda})(\text{CH}_3)_2(\text{OH})(\text{OCH}_3)$. Atom N2B has a small U_{iso} and tmeda methyl carbon C4B has a large U_{iso} . The distances and angles seem reasonable, given the large e.s.d's.

The location of the platinum atom could easily be determined by direct methods or from a Patterson map. The remaining non-hydrogen atoms were laboriously determined from successive structure factor - Fourier calculations. [Early refinement tended to hamper the subsequent location of missing atoms.] When several of the ligand atoms were initially refined anisotropically with one fully occupied site, SHELXL did not suggest splitting them. However, these individual sites were manually divided into two and refined successfully with

isotropic displacement parameters. The separation between the two positions for the nine pairs of close atoms (see Table 4) range from 0.50(2) Å to 1.10(1) Å. The platinum atom was refined anisotropically, all other non-hydrogen atoms isotropically. All hydrogen atoms were placed at calculated positions with U_{iso} 's fixed at 120% of the U_{iso} 's of the attached atoms. No restraints or constraints were used. Since the molecule is small and disordered, some chemical assumptions were obviously used in the interpretation of this structure. As a test, both the methoxy carbon and the terminal hydroperoxy oxygen were independently refined as a C/O mixture. The results were a somewhat disappointing ~60% of the appropriate atom. Of the 20 largest peaks in the final difference map, 6 are greater than $|2| \text{ e}\cdot\text{\AA}^{-3}$ and another 12 are greater than $|1| \text{ e}\cdot\text{\AA}^{-3}$. Seven of these 18 peaks are near the platinum atom, including the largest positive peak of $2.98 \text{ e}\cdot\text{\AA}^{-3}$ at a distance of 0.89 Å. The largest negative peak of $-2.73 \text{ e}\cdot\text{\AA}^{-3}$ is 0.75 Å from N2B (anomalously small U_{iso}); the other big excursions not near the platinum are $2.29 \text{ e}\cdot\text{\AA}^{-3}$ at 0.88 Å from C8B, $1.79 \text{ e}\cdot\text{\AA}^{-3}$ at 0.67 Å from C6B, $-1.66 \text{ e}\cdot\text{\AA}^{-3}$ at 1.45 Å from O2B, $1.63 \text{ e}\cdot\text{\AA}^{-3}$ at 0.68 Å from N2B, $-1.23 \text{ e}\cdot\text{\AA}^{-3}$ at 0.99 Å from H8BC, $-1.21 \text{ e}\cdot\text{\AA}^{-3}$ at 1.07 Å from O2A, $1.13 \text{ e}\cdot\text{\AA}^{-3}$ at 0.76 Å from C4B, and $1.06 \text{ e}\cdot\text{\AA}^{-3}$ at 0.80 Å from O1B. The 6 most disagreeable reflections all have $k = 5$ as well as F_{calc} weak and less than F_{obs} . This suggests twinning. The 20 reflections discarded in the initial unit cell determination could not be indexed by themselves. No other effort was made to investigate this fairly minor problem.

A Platon analysis of intermolecular contacts suggests two potential hydrogen bonds, each between a donor hydroperoxy OH and an acceptor methoxy O. One bond is between two molecules of orientation A translated one unit along the a -axis; the other between two molecules of orientation B similarly related.

D-H	d(D-H)	d(H...A)	<DHA	d(D...A)	A
O2A-H0A	0.840	2.344	151.94	3.111	O3A_a [x+1, y, z]
O2B-H0B	0.840	2.449	151.66	3.213	O3B_b [x+1, y, z]

However, the intermolecular distances also reveal some impossibly short contacts, such as 2.08 Å between O2A (x,y,z) and C5A ($x+1,y,z$). Therefore, two molecules of orientation A cannot be adjacent along the a -axis and thus

molecules of orientation A must comprise no more than 50% of the total molecules in the crystal. The population parameter for orientation A refined to 0.508(9), or essentially 1:1. Thus orientations A and B must alternate along the *a*-axis. This alternation must be occasionally broken since no evidence of a larger cell is seen. There are no appreciable intermolecular platinum – hydroperoxy or hydroperoxy – hydroperoxy interactions. As shown in the hydrogen bond table, there is a good hydrogen bond between the hydroperoxy group of one orientation and the methoxy oxygen of the other orientation.

Table 1. Atomic coordinates ($\times 10^4$) and equivalent isotropic displacement parameters ($\text{\AA}^2 \times 10^3$) for **2**. $U(\text{eq})$ is defined as one-third of the trace of the orthogonalized U_{ij} tensor.

	x	y	z	U_{eq} or U_{iso}
Pt	230.8(0.5)	3025.1(0.2)	1570.9(0.2)	16.2(0.2)*
O1A ^a	2970(20)	2404(12)	1818(11)	25(4)
O2A ^a	3980(20)	2151(9)	985(9)	34(4)
O3A ^a	-2603(19)	3652(9)	1546(8)	23(3)
N1A ^a	-70(30)	2781(11)	3066(11)	18(4)
N2A ^a	-1130(40)	1560(16)	1475(13)	36(6)
C1A ^a	-1100(40)	1842(15)	3110(15)	26(5)
C2A ^a	-670(40)	1084(14)	2410(12)	19(5)
C3A ^a	-1040(30)	3635(15)	3524(13)	30(5)
C4A ^a	1800(40)	2569(17)	3563(15)	39(6)
C5A ^a	-3150(30)	1518(15)	1104(13)	31(5)
C6A ^a	230(30)	896(16)	916(14)	35(5)
C7A ^a	-3240(30)	4289(14)	846(13)	21(5)
C8A ^a	1540(30)	4401(14)	1805(13)	19(5)
C9A ^a	530(40)	3224(15)	251(14)	30(5)
O1B ^b	2990(20)	2621(12)	2092(11)	23(4)
O2B ^b	4180(20)	3387(9)	2543(8)	26(4)
O3B ^b	-2630(20)	3196(9)	1009(8)	18(3)
N1B ^b	-1020(30)	2787(11)	2888(11)	19(4)
N2B ^b	-420(30)	1369(12)	1462(10)	7(4)
C1B ^b	-1890(50)	1810(20)	2900(20)	53(9)
C2B ^b	-1470(40)	1196(18)	2301(16)	36(7)
C3B ^b	-2860(40)	3276(16)	3024(15)	39(6)
C4B ^b	330(60)	3120(30)	3640(20)	83(11)
C5B ^b	-1640(30)	1035(15)	683(13)	30(5)
C6B ^b	1550(40)	790(19)	1372(17)	52(7)
C7B ^b	-3200(50)	4030(20)	509(18)	49(7)
C8B ^b	690(40)	4516(17)	1706(15)	30(6)
C9B ^b	1520(40)	3096(15)	354(13)	23(5)

^a Population: 0.508(9)

^b Population: 0.492(9)

* U_{eq}

Table 2. Bond lengths [Å] and angles [°] for **2**.

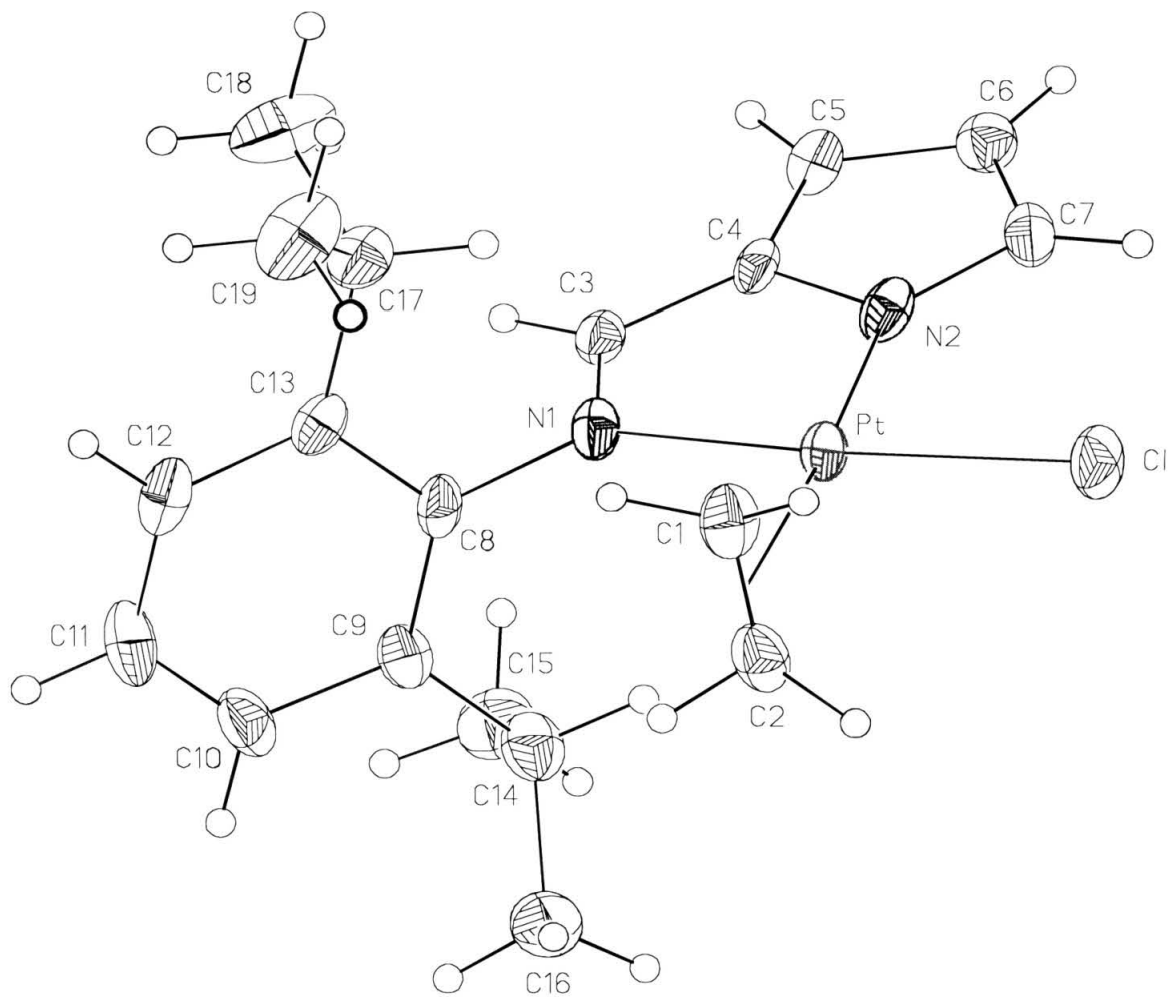
Pt-O1A	2.006(16)	N1B-C1B	1.43(3)
Pt-O3A	2.051(13)	N1B-C4B	1.46(4)
Pt-C8A	2.069(18)	N2B-C5B	1.44(2)
Pt-C9A	2.01(2)	N2B-C2B	1.48(3)
Pt-N1A	2.276(16)	N2B-C6B	1.53(3)
Pt-N2A	2.17(2)	C1B-C2B	1.26(3)
Pt-O1B	2.015(16)	C1B-H1BA	0.9900
Pt-O3B	2.033(13)	C1B-H1BB	0.9900
Pt-C8B	2.04(2)	C2B-H2BA	0.9900
Pt-C9B	2.05(2)	C2B-H2BB	0.9900
Pt-N1B	2.200(16)	C3B-H3BA	0.9800
Pt-N2B	2.281(16)	C3B-H3BB	0.9800
O1A-O2A	1.48(2)	C3B-H3BC	0.9800
O2A-H0A	0.8400	C4B-H4BA	0.9800
O3A-C7A	1.40(2)	C4B-H4BB	0.9800
N1A-C4A	1.43(3)	C4B-H4BC	0.9800
N1A-C1A	1.44(3)	C5B-H5BA	0.9800
N1A-C3A	1.50(3)	C5B-H5BB	0.9800
N2A-C5A	1.41(3)	C5B-H5BC	0.9800
N2A-C6A	1.55(3)	C6B-H6BA	0.9800
N2A-C2A	1.55(3)	C6B-H6BB	0.9800
C1A-C2A	1.50(3)	C6B-H6BC	0.9800
C1A-H1AA	0.9900	C7B-H7BA	0.9800
C1A-H1AB	0.9900	C7B-H7BB	0.9800
C2A-H2AA	0.9900	C7B-H7BC	0.9800
C2A-H2AB	0.9900	C8B-H8BA	0.9800
C3A-H3AA	0.9800	C8B-H8BB	0.9800
C3A-H3AB	0.9800	C8B-H8BC	0.9800
C3A-H3AC	0.9800	C9B-H9BA	0.9800
C4A-H4AA	0.9800	C9B-H9BB	0.9800
C4A-H4AB	0.9800	C9B-H9BC	0.9800
C4A-H4AC	0.9800	O1A...O1B	0.50(2)
C5A-H5AA	0.9800	O3A...O3B	1.01(1)
C5A-H5AB	0.9800	N1A...N1B	0.67(2)
C5A-H5AC	0.9800	N2A...N2B	0.54(2)
C6A-H6AA	0.9800	C1A...C1B	0.59(4)
C6A-H6AB	0.9800	C2A...C2B	0.57(3)
C6A-H6AC	0.9800	C7A...C7B	0.61(3)
C7A-H7AA	0.9800	C8A...C8B	0.59(3)
C7A-H7AB	0.9800	C9A...C9B	0.69(3)
C7A-H7AC	0.9800		
C8A-H8AA	0.9800	O1A-Pt-C9A	95.6(9)
C8A-H8AB	0.9800	O1A-Pt-O3A	170.5(6)
C8A-H8AC	0.9800	C9A-Pt-O3A	93.9(8)
C9A-H9AA	0.9800	O1A-Pt-C8A	89.0(8)
C9A-H9AB	0.9800	C9A-Pt-C8A	89.0(8)
C9A-H9AC	0.9800	O3A-Pt-C8A	90.1(7)
O1B-O2B	1.44(2)	O1A-Pt-N2A	89.8(7)
O2B-H0B	0.8400	C9A-Pt-N2A	97.0(8)
O3B-C7B	1.39(3)	O3A-Pt-N2A	90.0(7)
N1B-C3B	1.41(3)	C8A-Pt-N2A	174.1(7)

O1A-Pt-N1A	83.7(6)	N1A-C4A-H4AB	109.5
C9A-Pt-N1A	179.2(8)	H4AA-C4A-H4AB	109.5
O3A-Pt-N1A	86.8(6)	N1A-C4A-H4AC	109.5
C8A-Pt-N1A	91.4(7)	H4AA-C4A-H4AC	109.5
N2A-Pt-N1A	82.7(7)	H4AB-C4A-H4AC	109.5
O1B-Pt-O3B	170.8(5)	N2A-C5A-H5AA	109.5
O1B-Pt-C8B	96.0(8)	N2A-C5A-H5AB	109.5
O3B-Pt-C8B	93.2(8)	H5AA-C5A-H5AB	109.5
O1B-Pt-N2B	85.7(6)	N2A-C5A-H5AC	109.5
O3B-Pt-N2B	85.1(6)	H5AA-C5A-H5AC	109.5
O1B-Pt-C9B	86.6(8)	H5AB-C5A-H5AC	109.5
O3B-Pt-C9B	93.1(7)	N2A-C6A-H6AA	109.5
O1B-Pt-N1B	89.7(7)	N2A-C6A-H6AB	109.5
O3B-Pt-N1B	89.8(6)	H6AA-C6A-H6AB	109.5
C8B-Pt-N1B	96.7(7)	N2A-C6A-H6AC	109.5
C9B-Pt-N1B	173.9(7)	H6AA-C6A-H6AC	109.5
C8B-Pt-C9B	88.6(8)	H6AB-C6A-H6AC	109.5
C8B-Pt-N2B	177.0(8)	O3A-C7A-H7AA	109.5
C9B-Pt-N2B	94.0(7)	O3A-C7A-H7AB	109.5
N1B-Pt-N2B	80.8(6)	H7AA-C7A-H7AB	109.5
O2A-O1A-Pt	112.7(10)	O3A-C7A-H7AC	109.5
O1A-O2A-H0A	109.5	H7AA-C7A-H7AC	109.5
C7A-O3A-Pt	120.0(12)	H7AB-C7A-H7AC	109.5
C4A-N1A-C1A	101.3(16)	Pt-C8A-H8AA	109.5
C4A-N1A-C3A	107.3(17)	Pt-C8A-H8AB	109.5
C1A-N1A-C3A	116.1(17)	H8AA-C8A-H8AB	109.5
C4A-N1A-Pt	114.4(13)	Pt-C8A-H8AC	109.5
C1A-N1A-Pt	103.9(12)	H8AA-C8A-H8AC	109.5
C3A-N1A-Pt	113.5(11)	H8AB-C8A-H8AC	109.5
C5A-N2A-C6A	109.2(17)	Pt-C9A-H9AA	109.5
C5A-N2A-C2A	118.0(19)	Pt-C9A-H9AB	109.5
C6A-N2A-C2A	98.8(17)	H9AA-C9A-H9AB	109.5
C5A-N2A-Pt	116.0(15)	Pt-C9A-H9AC	109.5
C6A-N2A-Pt	108.2(14)	H9AA-C9A-H9AC	109.5
C2A-N2A-Pt	105.0(13)	H9AB-C9A-H9AC	109.5
N1A-C1A-C2A	117.2(18)	O2B-O1B-Pt	116.0(11)
N1A-C1A-H1AA	108.0	O1B-O2B-H0B	109.5
C2A-C1A-H1AA	108.0	C7B-O3B-Pt	121.9(15)
N1A-C1A-H1AB	108.0	C3B-N1B-C1B	95(2)
C2A-C1A-H1AB	108.0	C3B-N1B-C4B	104(2)
H1AA-C1A-H1AB	107.2	C1B-N1B-C4B	120(2)
C1A-C2A-N2A	107.8(17)	C3B-N1B-Pt	115.7(14)
C1A-C2A-H2AA	110.1	C1B-N1B-Pt	108.5(15)
N2A-C2A-H2AA	110.1	C4B-N1B-Pt	113(2)
C1A-C2A-H2AB	110.1	C5B-N2B-C2B	111.4(18)
N2A-C2A-H2AB	110.1	C5B-N2B-C6B	101.8(16)
H2AA-C2A-H2AB	108.5	C2B-N2B-C6B	115.8(18)
N1A-C3A-H3AA	109.5	C5B-N2B-Pt	117.3(12)
N1A-C3A-H3AB	109.5	C2B-N2B-Pt	101.0(12)
H3AA-C3A-H3AB	109.5	C6B-N2B-Pt	110.4(13)
N1A-C3A-H3AC	109.5	C2B-C1B-N1B	120(3)
H3AA-C3A-H3AC	109.5	C2B-C1B-H1BA	107.4
H3AB-C3A-H3AC	109.5	N1B-C1B-H1BA	107.4
N1A-C4A-H4AA	109.5	C2B-C1B-H1BB	107.4

N1B-C1B-H1BB	107.4	H5BB-C5B-H5BC	109.5
H1BA-C1B-H1BB	107.0	N2B-C6B-H6BA	109.5
C1B-C2B-N2B	129(2)	N2B-C6B-H6BB	109.5
C1B-C2B-H2BA	105.2	H6BA-C6B-H6BB	109.5
N2B-C2B-H2BA	105.2	N2B-C6B-H6BC	109.5
C1B-C2B-H2BB	105.2	H6BA-C6B-H6BC	109.5
N2B-C2B-H2BB	105.2	H6BB-C6B-H6BC	109.5
H2BA-C2B-H2BB	105.9	O3B-C7B-H7BA	109.5
N1B-C3B-H3BA	109.5	O3B-C7B-H7BB	109.5
N1B-C3B-H3BB	109.5	H7BA-C7B-H7BB	109.5
H3BA-C3B-H3BB	109.5	O3B-C7B-H7BC	109.5
N1B-C3B-H3BC	109.5	H7BA-C7B-H7BC	109.5
H3BA-C3B-H3BC	109.5	H7BB-C7B-H7BC	109.5
H3BB-C3B-H3BC	109.5	Pt-C8B-H8BA	109.5
N1B-C4B-H4BA	109.5	Pt-C8B-H8BB	109.5
N1B-C4B-H4BB	109.5	H8BA-C8B-H8BB	109.5
H4BA-C4B-H4BB	109.5	Pt-C8B-H8BC	109.5
N1B-C4B-H4BC	109.5	H8BA-C8B-H8BC	109.5
H4BA-C4B-H4BC	109.5	H8BB-C8B-H8BC	109.5
H4BB-C4B-H4BC	109.5	Pt-C9B-H9BA	109.5
N2B-C5B-H5BA	109.5	Pt-C9B-H9BB	109.5
N2B-C5B-H5BB	109.5	H9BA-C9B-H9BB	109.5
H5BA-C5B-H5BB	109.5	Pt-C9B-H9BC	109.5
N2B-C5B-H5BC	109.5	H9BA-C9B-H9BC	109.5
H5BA-C5B-H5BC	109.5	H9BB-C9B-H9BC	109.5

Appendix C

STRUCTURE DETERMINATION OF 3



Data Collection

Preliminary Photos	Rotation	
Type of diffractometer	CCD area detector	
Wavelength	0.71073 Å MoK α	
Data Collection Temperature	98(2) K	
θ range for 9081 reflections used in lattice determination	2.64 to 27.52°	
Unit cell dimensions	a = 8.4760(7) Å	β = 94.9960(10)°
	b = 14.4638(11) Å	
	c = 15.4387(12) Å	
Volume	1885.5(3) Å ³	
Z	4	
Crystal system	Monoclinic	
Space group	P2 ₁ /n	
Density (calculated)	1.803 Mg/m ³	
F(000)	992	
Data collection program	Bruker SMART	
θ range for data collection	1.93 to 28.66°	
Completeness to θ = 28.66°	94.1 %	
Index ranges	-11 \leq h \leq 11, -19 \leq k \leq 18, -20 \leq l \leq 20	
Data collection scan type	ω scans at 7 ϕ settings	
Data reduction program	Bruker SAINT v6.2	
Reflections collected	38615	
Independent reflections	4581 [R _{int} = 0.0855]	
Absorption coefficient	7.584 mm ⁻¹	
Absorption correction	SADABS	
Max. and min. transmission	1.000000 and 0.633973	

Structure Solution and Refinement

Structure solution program	SHELXS-97
Primary solution method	Direct methods

Secondary solution method	Direct methods
Hydrogen placement	Geometric positions
Structure refinement program	SHELXL-97
Refinement method	Full matrix least-squares on F^2
Data / restraints / parameters	4581 / 0 / 212
Treatment of hydrogen atoms	Riding
Goodness-of-fit on F^2	1.182
Final R indices	
[$I > 2\sigma(I)$, 3121 reflections]	$R1 = 0.0332$, $wR2 = 0.0479$
R indices (all data)	$R1 = 0.0670$, $wR2 = 0.0515$
Type of weighting scheme used	Sigma
Weighting scheme used	$w = 1/\sigma^2(F_o^2)$
Max shift/error	0.000
Average shift/error	0.000
Largest diff. peak and hole	1.692 and -0.874 e.Å ⁻³

Special Refinement Details

All hydrogen atoms were refined as riding atoms because the thermal parameters of two hydrogen atoms (H2A and H6) refined to negative values and therefore prevented the least squares refinement from converging with a satisfactory shift/error value. The positional parameters of all the hydrogen atoms were satisfactory when unrestrained during least squares refinement.

Refinement of F^2 against ALL reflections. The weighted R-factor (wR) and goodness of fit (S) are based on F^2 , conventional R-factors (R) are based on F , with F set to zero for negative F^2 . The threshold expression of $F^2 > 2\sigma(F^2)$ is used only for calculating R-factors(gt), *etc.*, and is not relevant to the choice of reflections for refinement. R-factors based on F^2 are statistically about twice as large as those based on F , and R-factors based on ALL data will be even larger.

All esds (except the esd in the dihedral angle between two l.s. planes) are estimated using the full covariance matrix. The cell esds are taken into account individually in the estimation of esds in distances, angles and torsion angles; correlations between esds in cell parameters are only used when they are defined by crystal symmetry. An approximate (isotropic) treatment of cell esds is used for estimating esds involving l.s. planes.

Table 1. Atomic coordinates ($\times 10^4$) and equivalent isotropic displacement parameters ($\text{\AA}^2 \times 10^3$) for **3** (CCDC 162307). $U(\text{eq})$ is defined as the trace of the orthogonalized U^{ij} tensor.

	x	y	z	U_{eq}
Pt	1453(1)	1925(1)	2127(1)	20(1)
Cl	-1227(2)	1698(1)	1872(1)	32(1)
N(1)	3856(5)	2014(3)	2243(2)	22(1)
N(2)	2006(5)	875(3)	1379(3)	23(1)
C(1)	1059(6)	2670(4)	3278(4)	28(1)
C(2)	999(6)	3291(4)	2603(3)	29(1)
C(3)	4551(6)	1370(3)	1818(3)	20(1)
C(4)	3581(6)	720(4)	1350(3)	19(1)
C(5)	3809(6)	-52(4)	845(3)	24(1)
C(6)	2327(6)	-372(4)	559(3)	25(1)
C(7)	1228(7)	205(4)	892(3)	26(1)
C(8)	4832(6)	2699(4)	2699(3)	22(1)
C(9)	5171(6)	3515(4)	2280(3)	24(1)
C(10)	6212(6)	4137(4)	2720(4)	31(1)
C(11)	6860(6)	3961(4)	3533(4)	34(2)
C(12)	6509(6)	3163(4)	3952(3)	30(1)
C(13)	5482(6)	2517(4)	3566(3)	23(1)
C(14)	4460(7)	3727(4)	1371(4)	30(1)
C(15)	5626(7)	3475(4)	705(4)	40(2)
C(16)	3898(7)	4724(4)	1243(4)	38(2)
C(17)	5107(7)	1605(4)	4007(4)	29(1)
C(18)	6445(8)	896(4)	3915(4)	49(2)
C(19)	4842(7)	1751(5)	4961(3)	45(2)

Table 2. Bond lengths [Å] and angles [°] for **3** (CCDC 162307).

Pt-N(2)	1.988(4)	C(19)-H(19A)	0.9800
Pt-N(1)	2.034(4)	C(19)-H(19B)	0.9800
Pt-C(1)	2.129(5)	C(19)-H(19C)	0.9800
Pt-C(2)	2.154(5)	N(2)-Pt-N(1)	79.30(17)
Pt-Cl	2.2951(13)	N(2)-Pt-C(1)	158.97(18)
N(1)-C(3)	1.307(6)	N(1)-Pt-C(1)	97.09(19)
N(1)-C(8)	1.435(6)	N(2)-Pt-C(2)	163.06(18)
N(2)-C(4)	1.358(6)	N(1)-Pt-C(2)	96.86(19)
N(2)-C(7)	1.361(6)	C(1)-Pt-C(2)	37.38(18)
C(1)-C(2)	1.373(7)	N(2)-Pt-Cl	94.08(12)
C(1)-H(1A)	0.9900	N(1)-Pt-Cl	173.30(13)
C(1)-H(1B)	0.9900	C(1)-Pt-Cl	89.46(15)
C(2)-H(2A)	0.9900	C(2)-Pt-Cl	89.21(15)
C(2)-H(2B)	0.9900	C(3)-N(1)-C(8)	118.1(4)
C(3)-C(4)	1.408(6)	C(3)-N(1)-Pt	113.7(3)
C(3)-H(3)	0.9500	C(8)-N(1)-Pt	128.1(3)
C(4)-C(5)	1.385(7)	C(4)-N(2)-C(7)	107.1(4)
C(5)-C(6)	1.375(7)	C(4)-N(2)-Pt	115.3(3)
C(5)-H(5)	0.9500	C(7)-N(2)-Pt	137.5(4)
C(6)-C(7)	1.383(7)	C(2)-C(1)-Pt	72.3(3)
C(6)-H(6)	0.9500	C(2)-C(1)-H(1A)	116.3
C(7)-H(7)	0.9500	Pt-C(1)-H(1A)	116.3
C(8)-C(9)	1.388(7)	C(2)-C(1)-H(1B)	116.3
C(8)-C(13)	1.427(7)	Pt-C(1)-H(1B)	116.3
C(9)-C(10)	1.394(7)	H(1A)-C(1)-H(1B)	113.3
C(9)-C(14)	1.509(7)	C(1)-C(2)-Pt	70.3(3)
C(10)-C(11)	1.350(7)	C(1)-C(2)-H(2A)	116.6
C(10)-H(10)	0.9500	Pt-C(2)-H(2A)	116.6
C(11)-C(12)	1.369(8)	C(1)-C(2)-H(2B)	116.6
C(11)-H(11)	0.9500	Pt-C(2)-H(2B)	116.6
C(12)-C(13)	1.377(7)	H(2A)-C(2)-H(2B)	113.6
C(12)-H(12)	0.9500	N(1)-C(3)-C(4)	117.7(5)
C(13)-C(17)	1.531(7)	N(1)-C(3)-H(3)	121.1
C(14)-C(16)	1.526(7)	C(4)-C(3)-H(3)	121.1
C(14)-C(15)	1.531(7)	N(2)-C(4)-C(5)	109.8(5)
C(14)-H(14)	1.0000	N(2)-C(4)-C(3)	113.8(5)
C(15)-H(15A)	0.9800	C(5)-C(4)-C(3)	136.4(5)
C(15)-H(15B)	0.9800	C(6)-C(5)-C(4)	106.5(5)
C(15)-H(15C)	0.9800	C(6)-C(5)-H(5)	126.8
C(16)-H(16A)	0.9800	C(4)-C(5)-H(5)	126.8
C(16)-H(16B)	0.9800	C(5)-C(6)-C(7)	107.7(5)
C(16)-H(16C)	0.9800	C(5)-C(6)-H(6)	126.2
C(17)-C(19)	1.524(7)	C(7)-C(6)-H(6)	126.2
C(17)-C(18)	1.545(7)	N(2)-C(7)-C(6)	109.0(5)
C(17)-H(17)	1.0000	N(2)-C(7)-H(7)	125.5
C(18)-H(18A)	0.9800	C(6)-C(7)-H(7)	125.5
C(18)-H(18B)	0.9800	C(9)-C(8)-C(13)	121.0(5)
C(18)-H(18C)	0.9800	C(9)-C(8)-N(1)	119.5(5)

C(13)-C(8)-N(1)	119.5(5)	H(15A)-C(15)-H(15C)	109.5
C(8)-C(9)-C(10)	118.0(5)	H(15B)-C(15)-H(15C)	109.5
C(8)-C(9)-C(14)	121.6(5)	C(14)-C(16)-H(16A)	109.5
C(10)-C(9)-C(14)	120.4(5)	C(14)-C(16)-H(16B)	109.5
C(11)-C(10)-C(9)	121.4(6)	H(16A)-C(16)-H(16B)	109.5
C(11)-C(10)-H(10)	119.3	C(14)-C(16)-H(16C)	109.5
C(9)-C(10)-H(10)	119.3	H(16A)-C(16)-H(16C)	109.5
C(10)-C(11)-C(12)	120.7(5)	H(16B)-C(16)-H(16C)	109.5
C(10)-C(11)-H(11)	119.6	C(19)-C(17)-C(13)	111.4(5)
C(12)-C(11)-H(11)	119.6	C(19)-C(17)-C(18)	110.6(5)
C(11)-C(12)-C(13)	121.4(5)	C(13)-C(17)-C(18)	110.4(5)
C(11)-C(12)-H(12)	119.3	C(19)-C(17)-H(17)	108.1
C(13)-C(12)-H(12)	119.3	C(13)-C(17)-H(17)	108.1
C(12)-C(13)-C(8)	117.4(5)	C(18)-C(17)-H(17)	108.1
C(12)-C(13)-C(17)	122.6(5)	C(17)-C(18)-H(18A)	109.5
C(8)-C(13)-C(17)	119.9(5)	C(17)-C(18)-H(18B)	109.5
C(9)-C(14)-C(16)	114.0(5)	H(18A)-C(18)-H(18B)	109.5
C(9)-C(14)-C(15)	110.3(5)	C(17)-C(18)-H(18C)	109.5
C(16)-C(14)-C(15)	110.5(5)	H(18A)-C(18)-H(18C)	109.5
C(9)-C(14)-H(14)	107.2	H(18B)-C(18)-H(18C)	109.5
C(16)-C(14)-H(14)	107.2	C(17)-C(19)-H(19A)	109.5
C(15)-C(14)-H(14)	107.2	C(17)-C(19)-H(19B)	109.5
C(14)-C(15)-H(15A)	109.5	H(19A)-C(19)-H(19B)	109.5
C(14)-C(15)-H(15B)	109.5	C(17)-C(19)-H(19C)	109.5
H(15A)-C(15)-H(15B)	109.5	H(19A)-C(19)-H(19C)	109.5
C(14)-C(15)-H(15C)	109.5	H(19B)-C(19)-H(19C)	109.5
